Cancer Hallmark

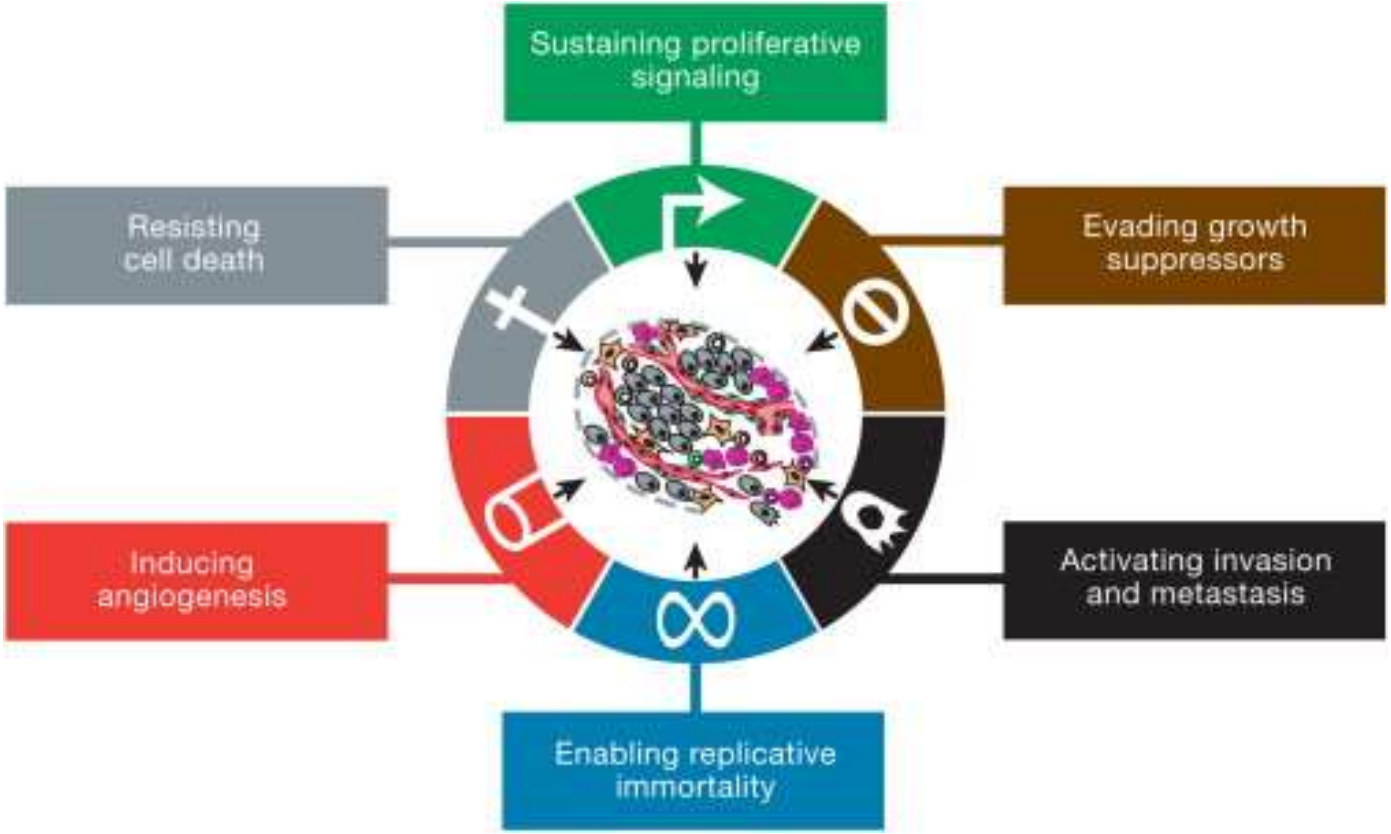

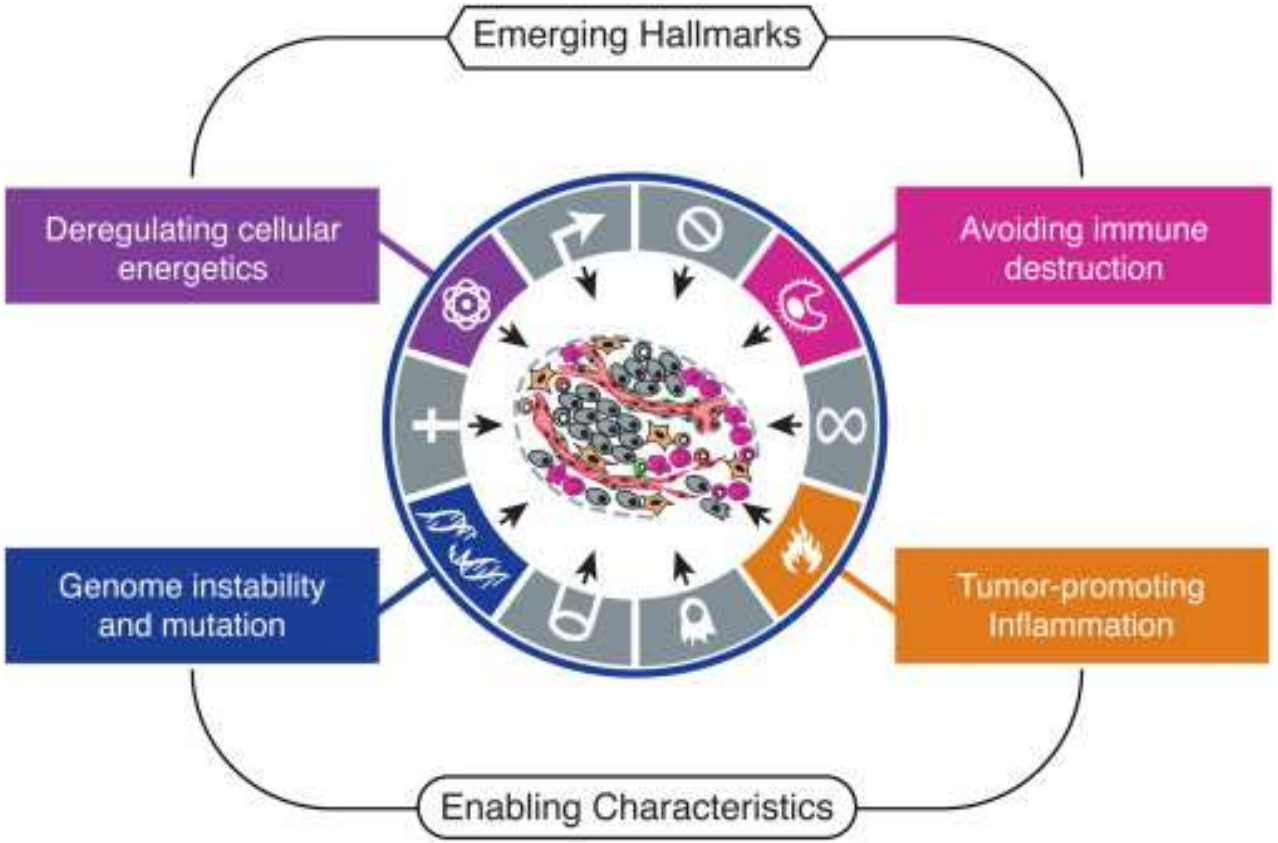

An increasing body of research suggests that two additional hallmarks of cancer are involved in the pathogenesis of some and perhaps all cancers. One involves the capability to modify, or reprogram, cellular metabolism in order to most effectively support neoplastic proliferation. The second allows cancer cells to evade immunological destruction, in particular by T and B lymphocytes, macrophages, and natural killer cells. Because neither capability is yet generalized and fully validated, they are labeled as emerging hallmarks. Additionally, two consequential characteristics of neoplasia facilitate acquisition of both core and emerging hallmarks. Genomic instability and thus mutability endow cancer cells with genetic alterations that drive tumor progression. Inflammation by innate immune cells designed to fight infections and heal wounds can instead result in their inadvertent support of multiple hallmark capabilities, thereby manifesting the now widely appreciated tumor-promoting consequences of inflammatory responses.

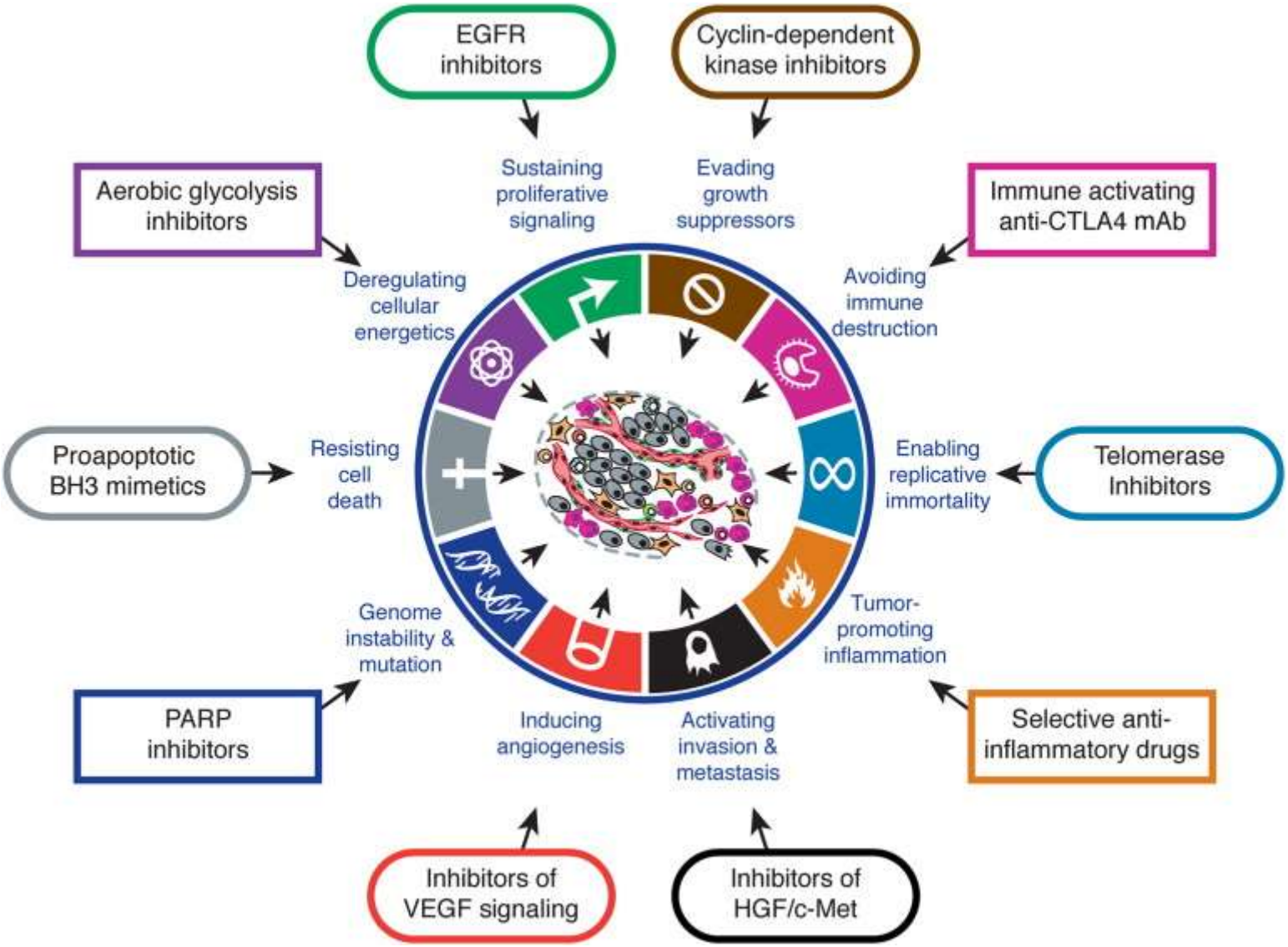
EGFR inhibitors
Cyclin-dependent kinase inhibitors
Sustaining proliferative signaling
Evading growth suppressors
Aerobic glycolysis inhibitors
Immune activating anti-CTLA4 mAb
Deregulating cellular energetics
Avoiding immune destruction
Proapoptotic BH3 mimetics
Resisting cell death
Enabling replicative immortality
Telomerase Inhibitors
Genome instability & mutation
Tumor-promoting inflammation
PARP inhibitors
Inducing angiogenesis
Activating invasion & metastasis
Selective anti-inflammatory drugs
Inhibitors of VEGF signaling
Inhibitors of HGF/c-Met

CANCER NANOTECHNOLOGY: OPPORTUNITIES AND CHALLENGES

NATURE REVIEWS | CANCER VOLUME 5 | MARCH 2005 | 161

Summary

- Nanotechnology concerns the study of devices that are themselves or have essential components in the 1–1,000 nm dimensional range (that is, from a few atoms to subcellular size).
- Two main subfields of nanotechnology are nanovectors — for the administration of targeted therapeutic and imaging moieties — and the precise patterning of surfaces.
- Nanotechnology is no stranger to oncology: liposomes are early examples of cancer nanotherapeutics, and nanoscale-targeted magnetic resonance imaging contrast agents illustrate the application of nanotechnology to diagnostics.
- Photolithography is a light-directed surface-patterning method, which is the technological foundation of microarrays and the surface-enhanced laser desorption/ionization time-of-flight approach to proteomics. Nanoscale resolution is now possible with photolithography, and will give rise to instruments that can pack a much greater density of information than current biochips.
- The ability of nanotechnology to yield advances in early detection, diagnostics, prognostics and the selection of therapeutic strategies is predicated based on its ability to 'multiplex' — that is, to detect a broad multiplicity of molecular signals and biomarkers in real time. Prime examples of multiplexing detection nanotechnologies are arrays of nanocantilevers, nanowires and nanotubes.
- Multifunctionality is the fundamental advantage of nanovectors for the cancer-specific delivery of therapeutic and imaging agents. Primary functionalities include the avoidance of biobarriers and biomarker-based targeting, and the reporting of therapeutic efficacy.
- Thousands of nanovectors are currently under study. By systematically combining them with preferred therapeutic and biological targeting moieties it might be possible to obtain a very large number of novel, personalized therapeutic agents.
- Novel mathematical models are needed, in order to secure the full import of nanotechnology into oncology.

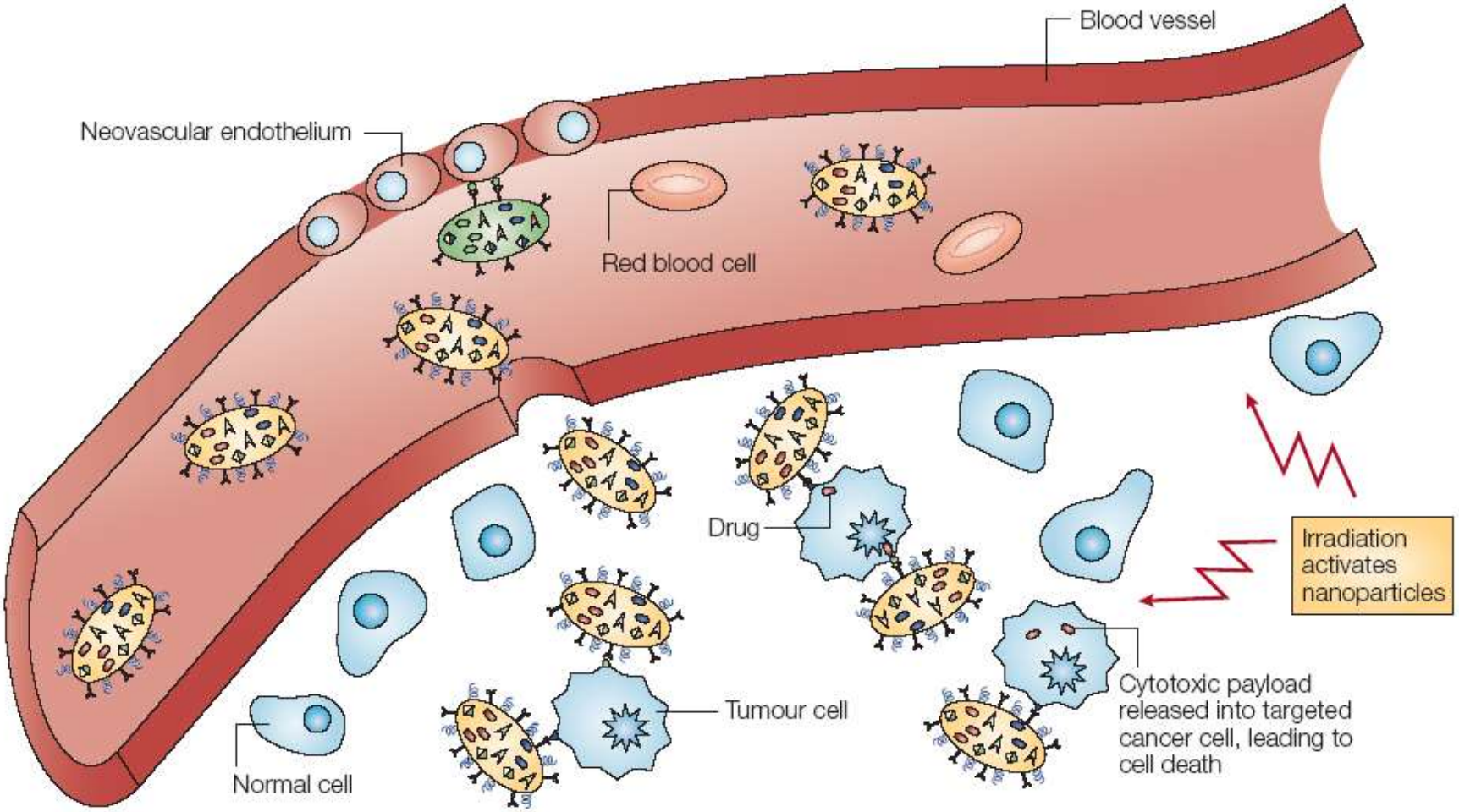

Figure 4 | **Multicomponent targeting strategies.** Nanoparticles extravasate into the tumour stroma through the fenestrations of the angiogenic vasculature, demonstrating targeting by enhanced permeation and retention. The particles carry multiple antibodies, which further target them to epitopes on cancer cells, and direct antitumour action. Nanoparticles are activated and release their cytotoxic action when irradiated by external energy. Not shown: nanoparticles might preferentially adhere to cancer neovasculature and cause it to collapse, providing anti-angiogenic therapy. The red blood cells are not shown to scale; the volume occupied by a red blood cell would suffice to host 1–10 million nanoparticles of 10 nm diameter.

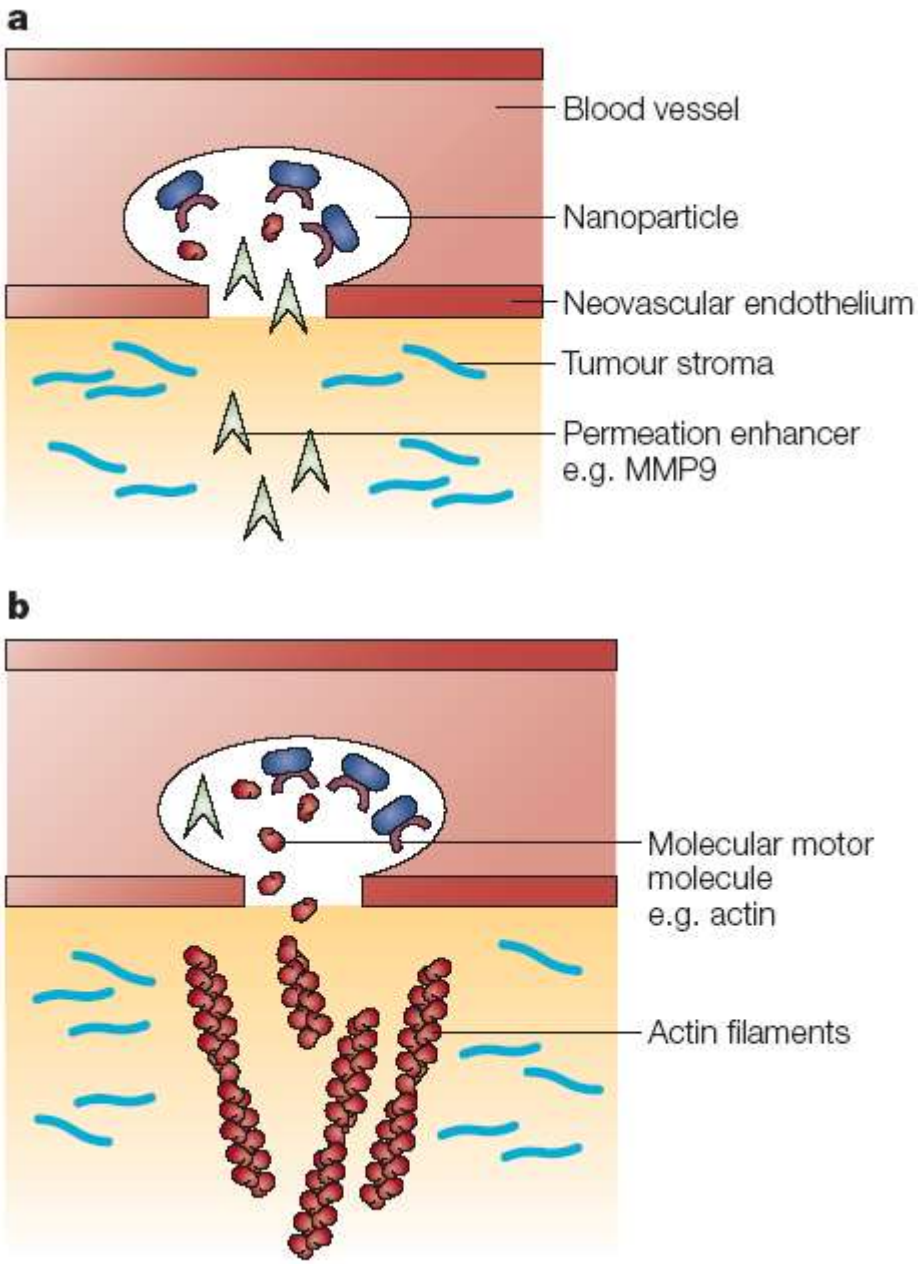

Figure 5 | **A vision for a future multistage nanodevice with multiple-barrier-avoidance capability**. A nanovector selectively binds to the cancer neovascular endothelium, releases a penetration enhancer, generates a fenestration, and deploys through it a track of molecular motor molecules such as actin. Therapeutic agents bound to a conjugate molecule such as myosin are then released by the nanovector, and travel along the 'molecular track' to reach deeply into the cancer lesion, despite the opposing oncotic osmotic pressure.

How Many Nanoparticle-based Drugs Reach Tumor?

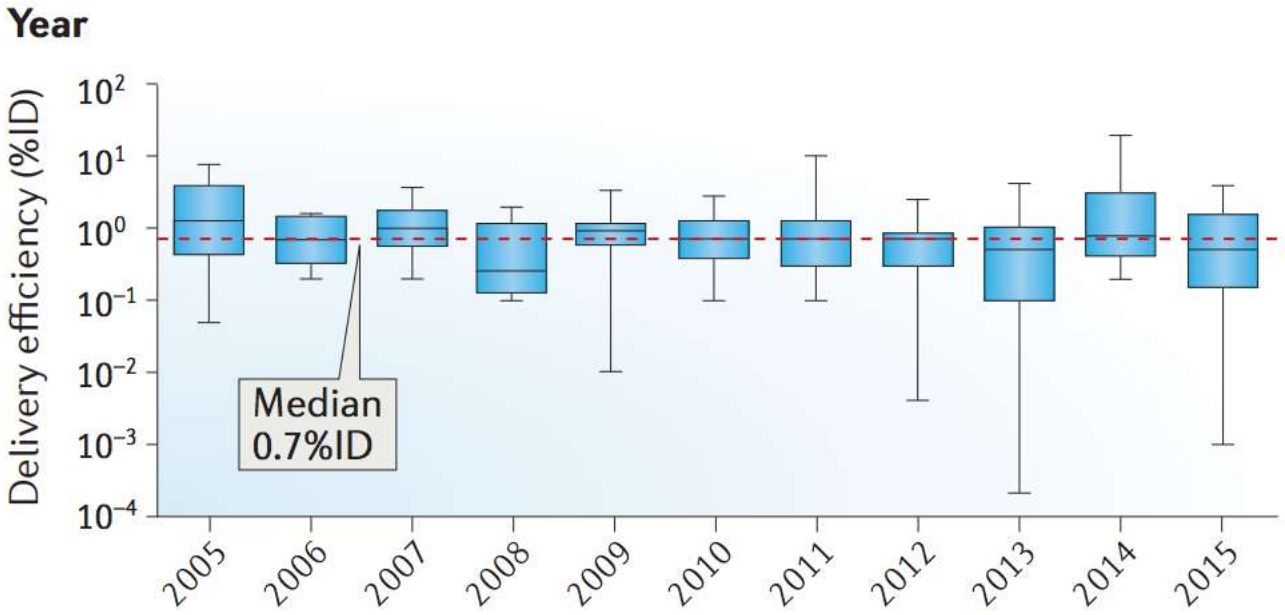

- Less than **one percent**!

Nat. Rev. Mater. **2016**, 1, 16014

nature nanotechnology

LETTERS

PUBLISHED ONLINE: 20 JANUARY 2013 | DOI: 10.1038/NNANO.2012.237

Transferrin-functionalized nanoparticles lose their targeting capabilities when a biomolecule corona adsorbs on the surface

Anna Salvati, Andrzej S. Pitek, Marco P. Monopoli, Kanlaya Prapainop, Francesca Baldelli Bombelli, Delyan R. Hristov, Philip M. Kelly, Christoffer Åberg, Eugene Mahon* and Kenneth A. Dawson*

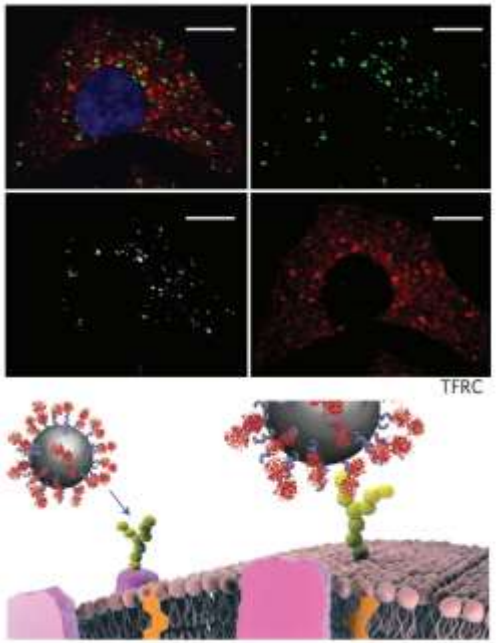

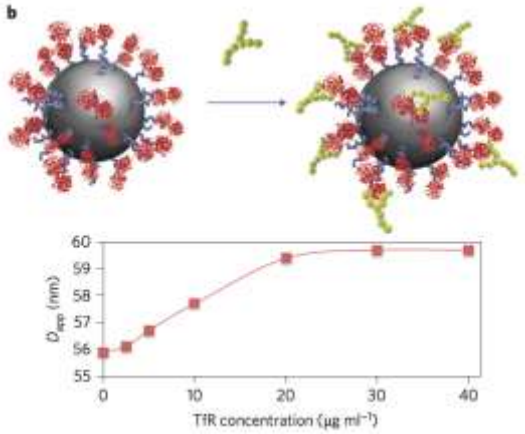

Desired situations

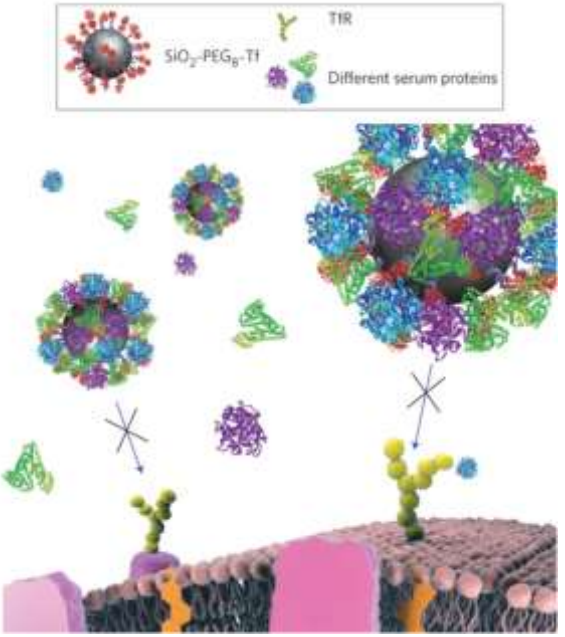

Actual situations

Nature Nanotechnology **2013**, *8*, 137-143.

Obstacles Hindering Efficacious, Site-specific Delivery to Tumor

NP Biological Fate

1. Mononuclear phagocyte system (MPS)
2. Renal clearance (D_h < 5.5 nm)
3. Biliary tract
4. EPR effect

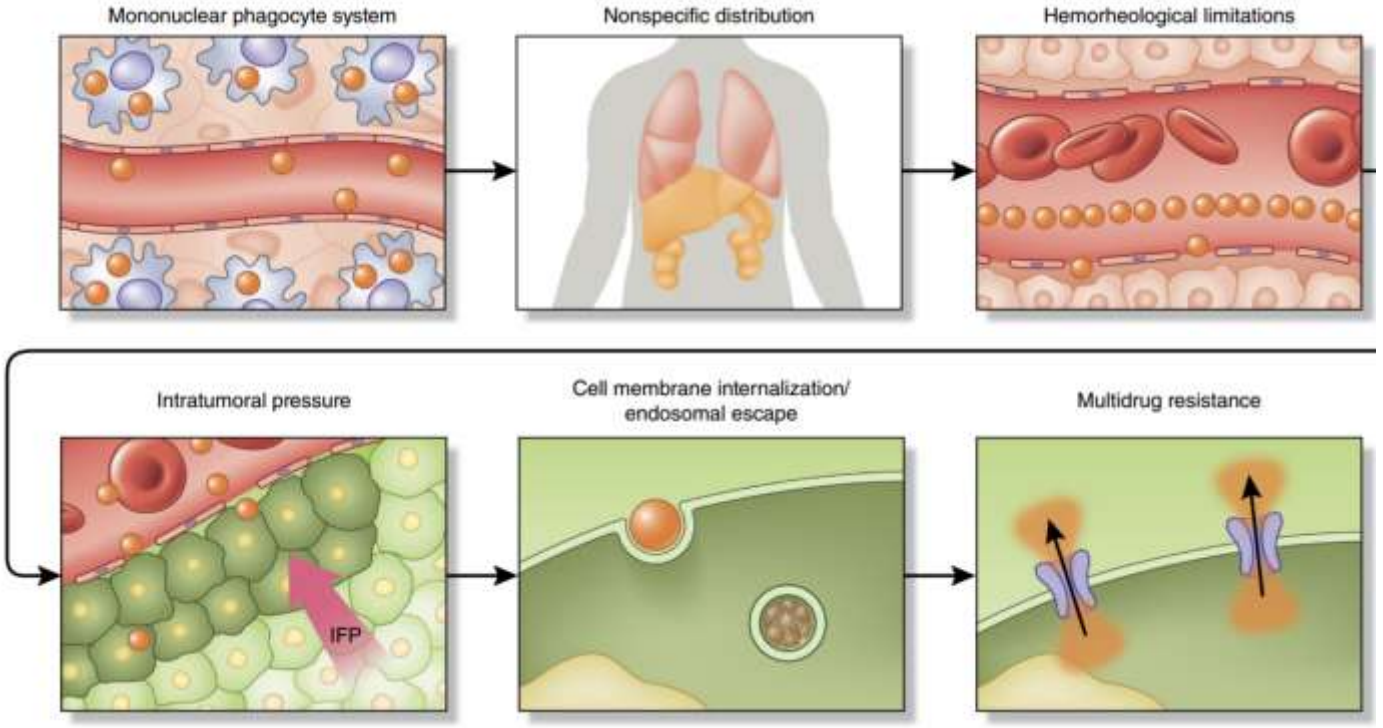

Nat Biotechnol **2015**, *33*, 941-951.

EPR Effect

(Enhanced Permeability and Retention)

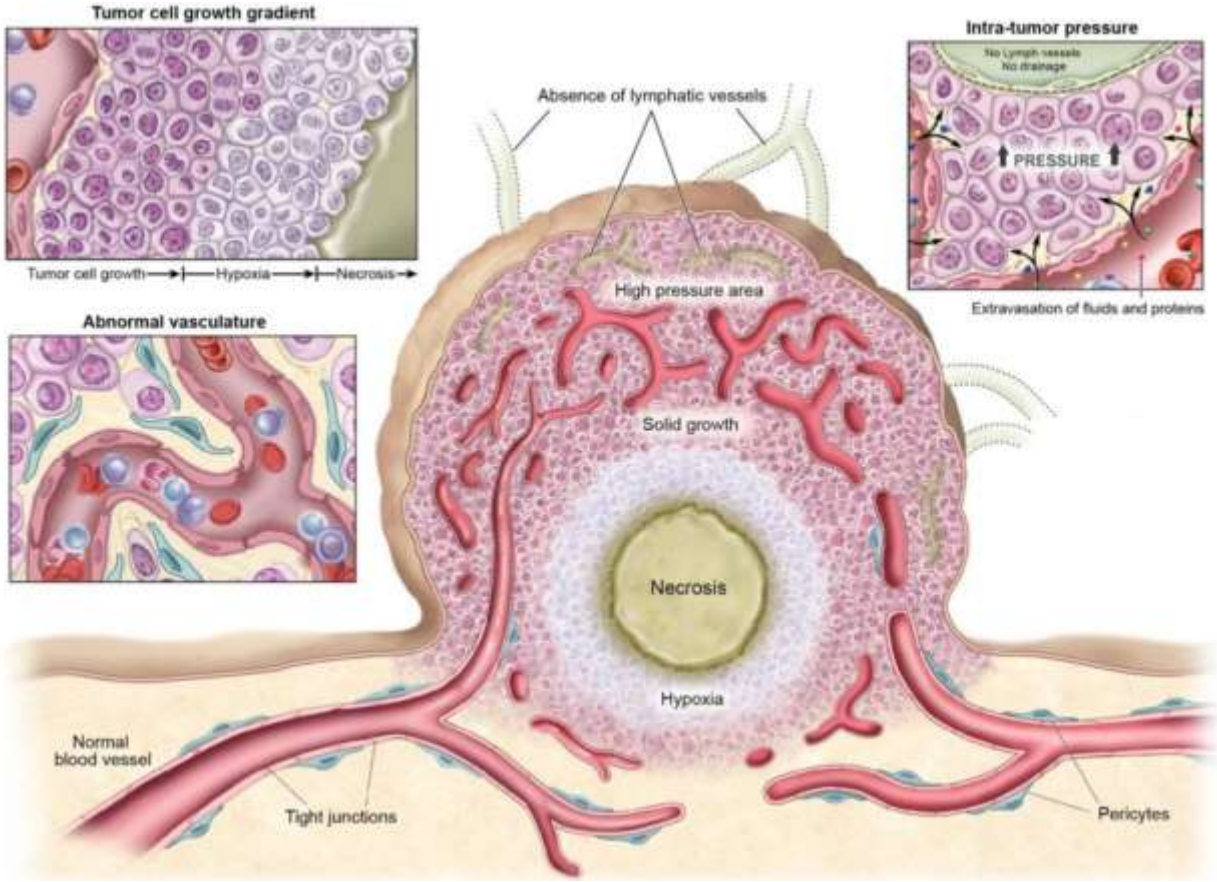

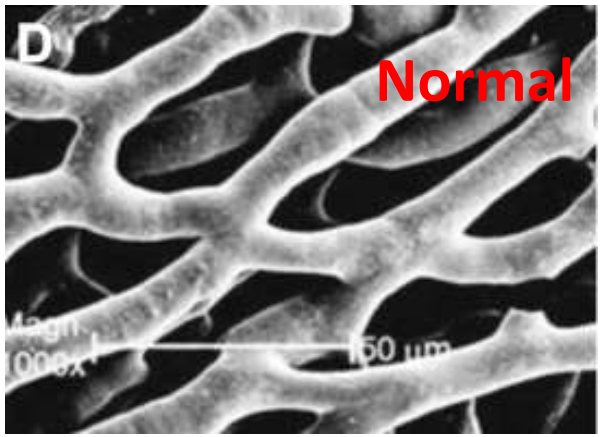

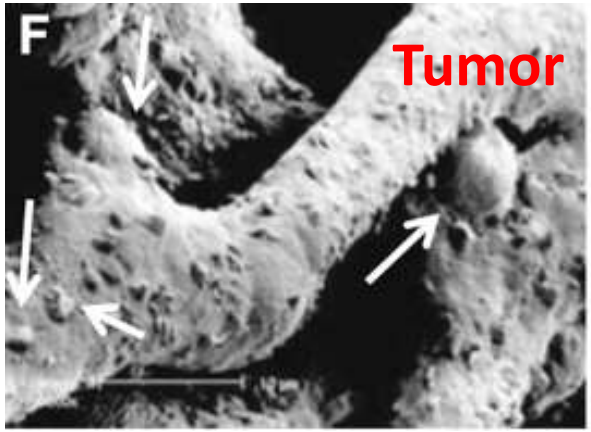

Theranostics **2014**, *4*, 81-89.

https://goo.gl/hCNlJp

Mesoporous Silica

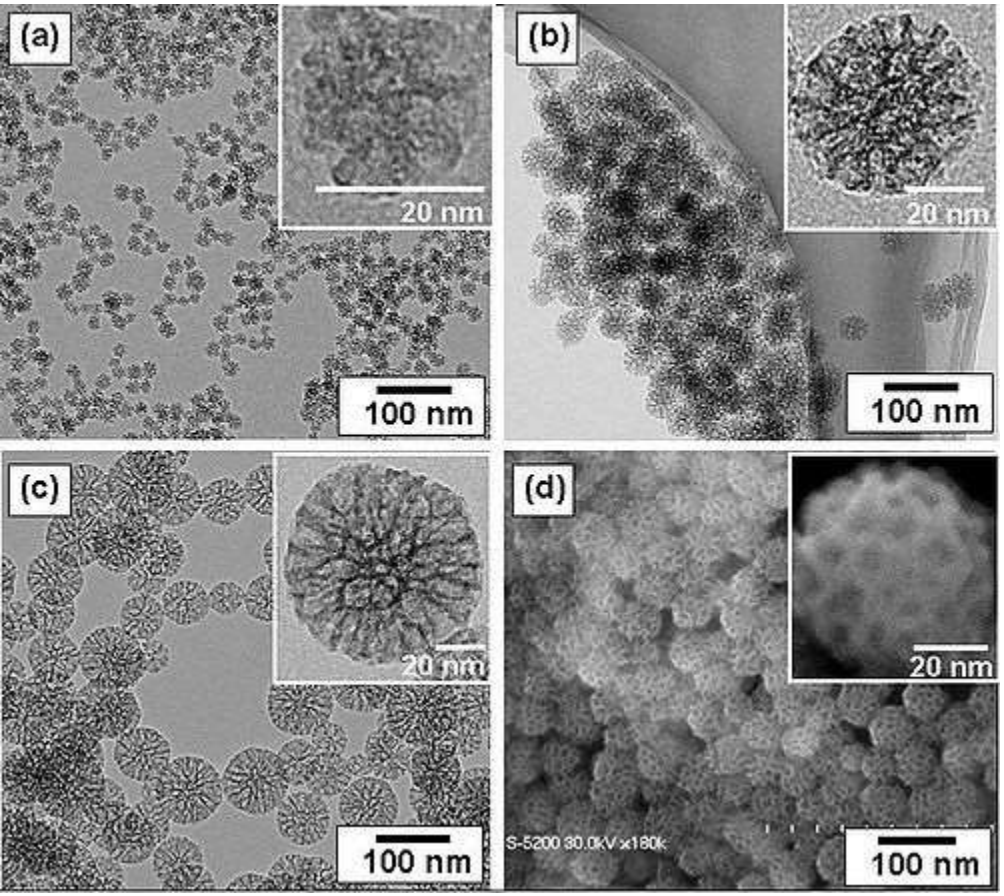

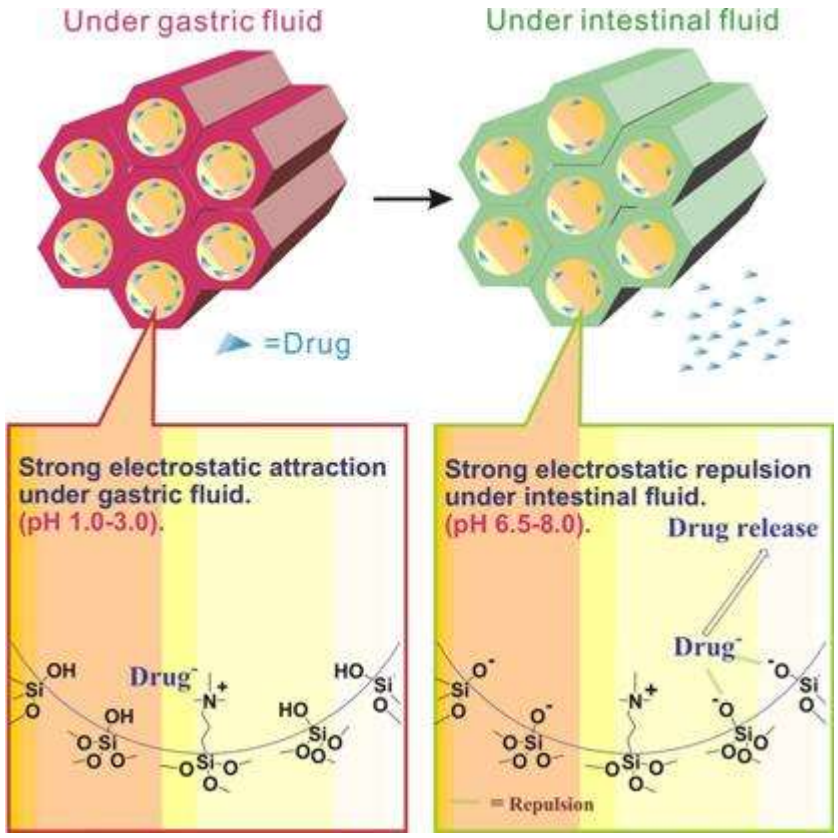

What can a Porous Silica Platform Do in BioMed?

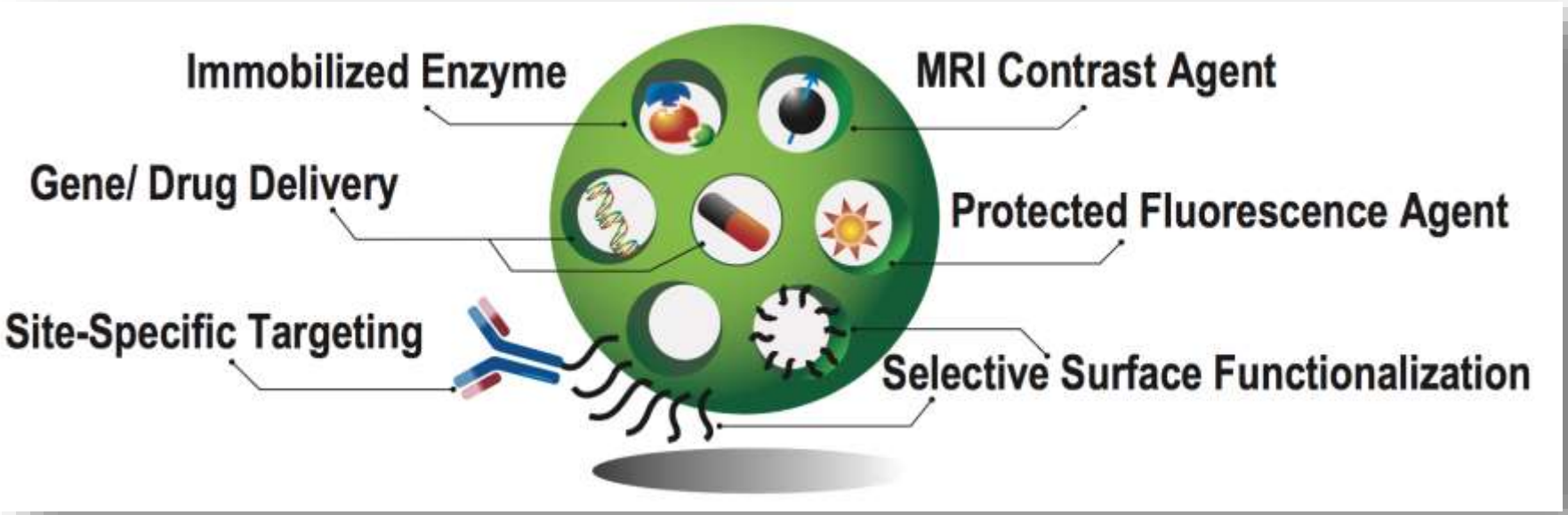

- High surface area
- Tunable pore size
- Thermal & chemical stability
- Non/Low toxicity
- Large pore volume
- Easy functionalization
- Controllable degradation rate
- Biocompatibility

State of the Art in Silica Nanoparticle Synthesis

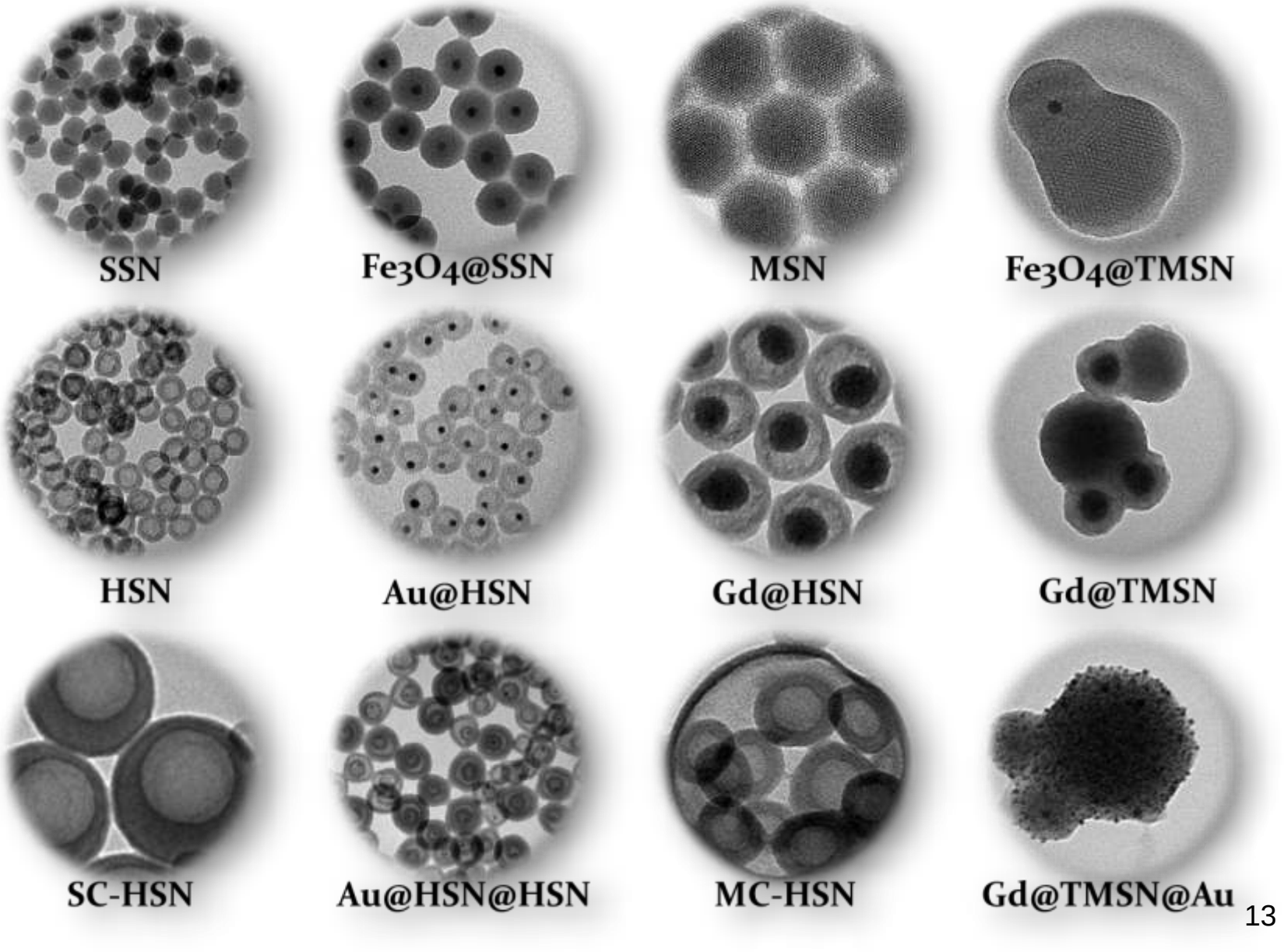

Synthesis and Selective Functionalization of MSNs

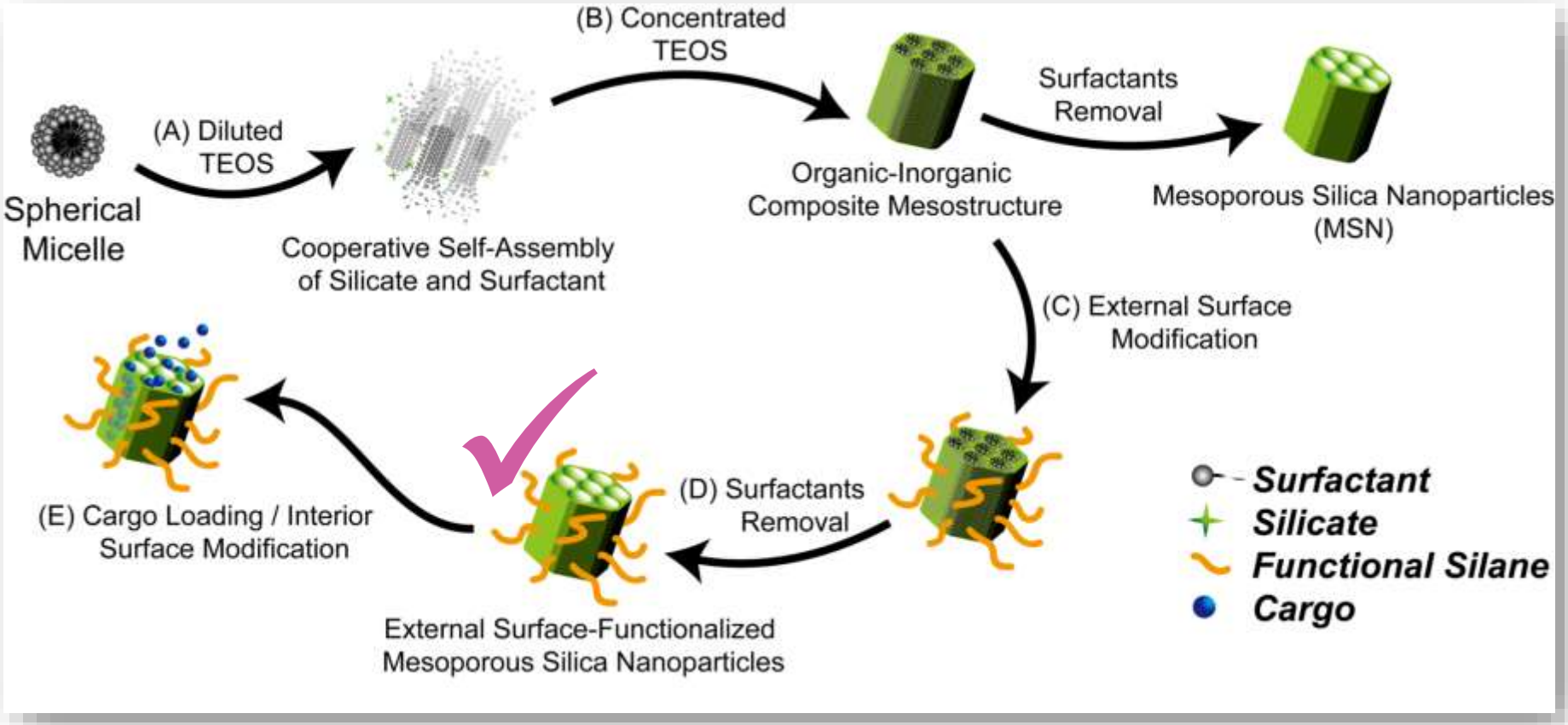

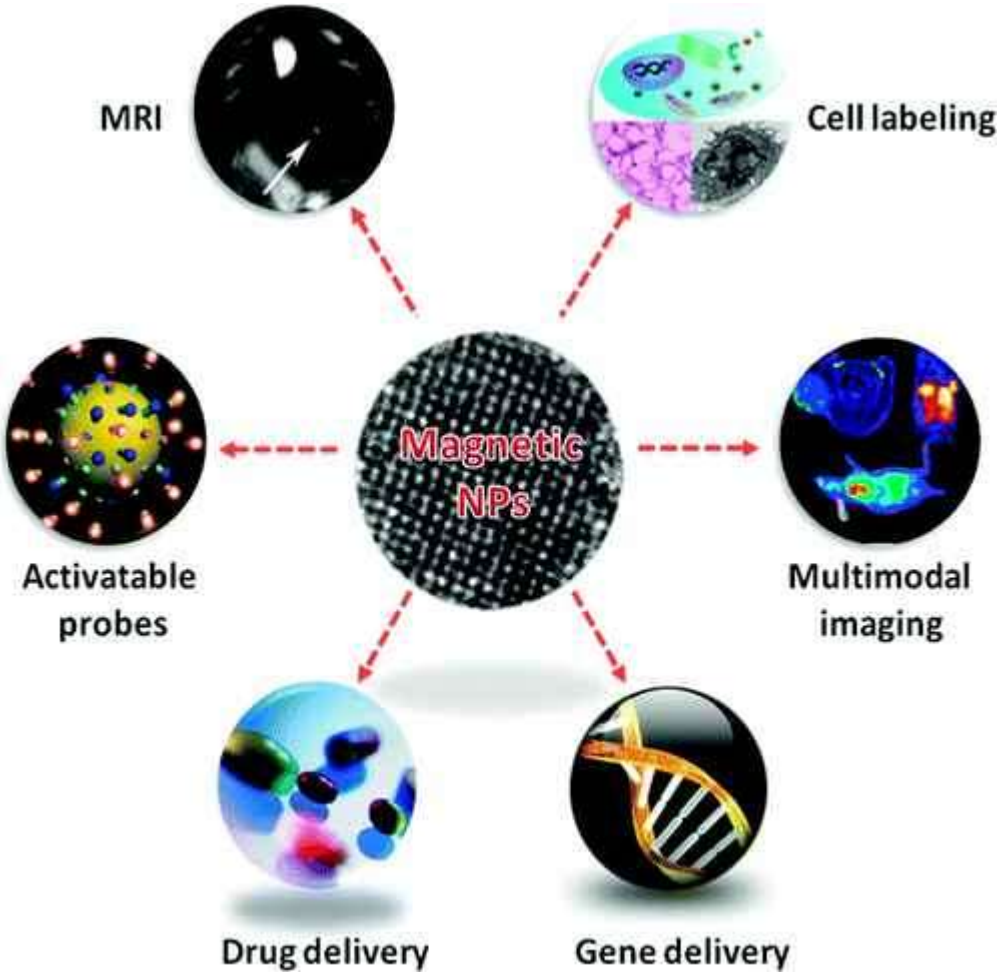
MRI
Cell labeling
Magnetic NPs
Activatable probes
Multimodal imaging
Drug delivery
Gene delivery

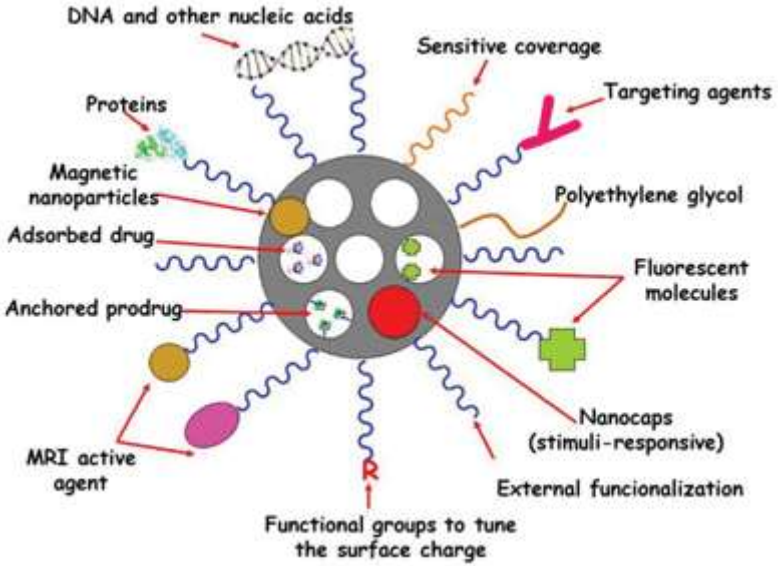
DNA and other nucleic acids
Sensitive coverage
Targeting agents
Proteins
Magnetic nanoparticles
Polyethylene glycol
Adsorbed drug
Fluorescent molecules
Anchored prodrug
Nanocaps (stimuli-responsive)
MRI active agent
External funcionalization
Functional groups to tune the surface charge

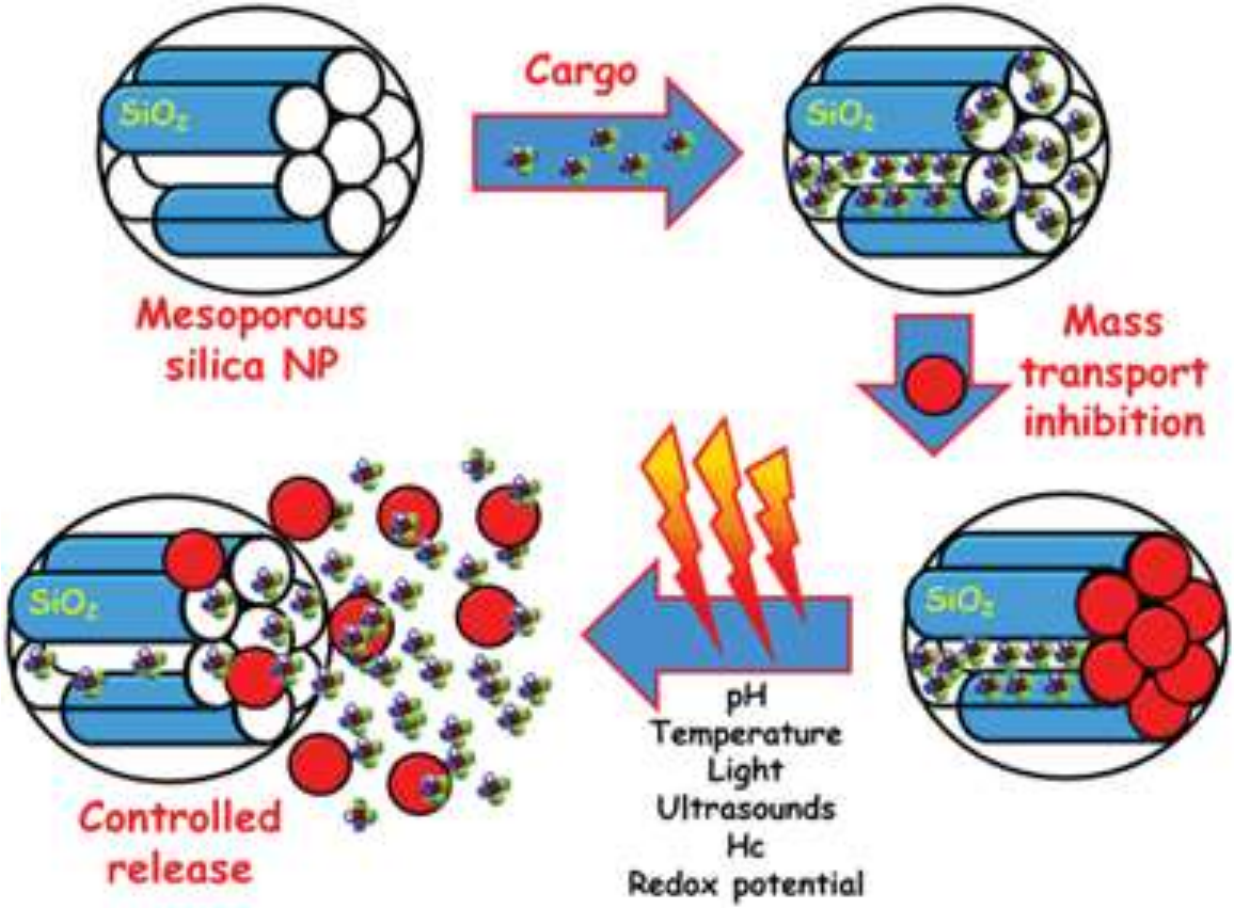
Cargo
SiO_2
SiO_2
Mesoporous silica NP
Mass transport inhibition
SiO_2
SiO_2
Controlled release
pH
Temperature
Light
Ultrasounds
Hc
Redox potential

How Much Does the Surface/Size of NP Matter in Their Own Biological Fate?

Surface Functionalization of MSNs

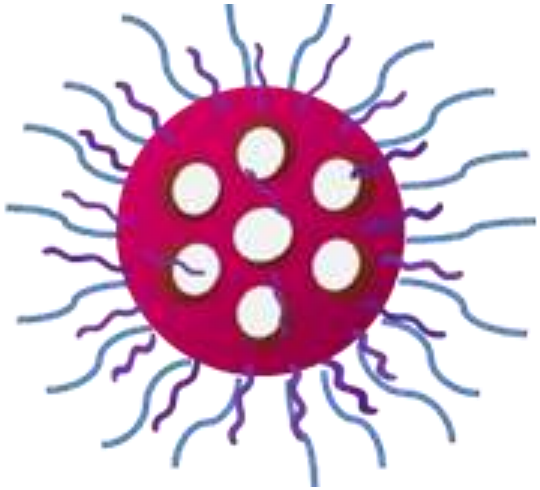

VS.

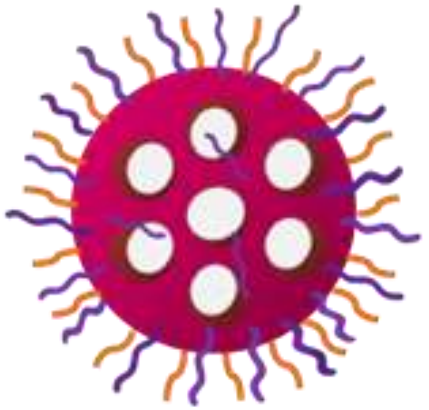

R-MSN@PEG-PEI

R-MSN@PEG-TA

Length:

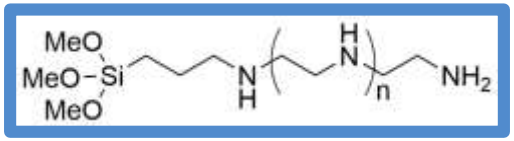

>

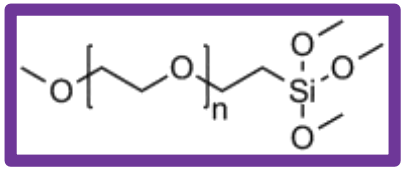

>

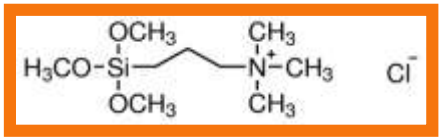

Characterization of MSNs

R-MSN@PEG-PEI R-MSN@PEG-TA

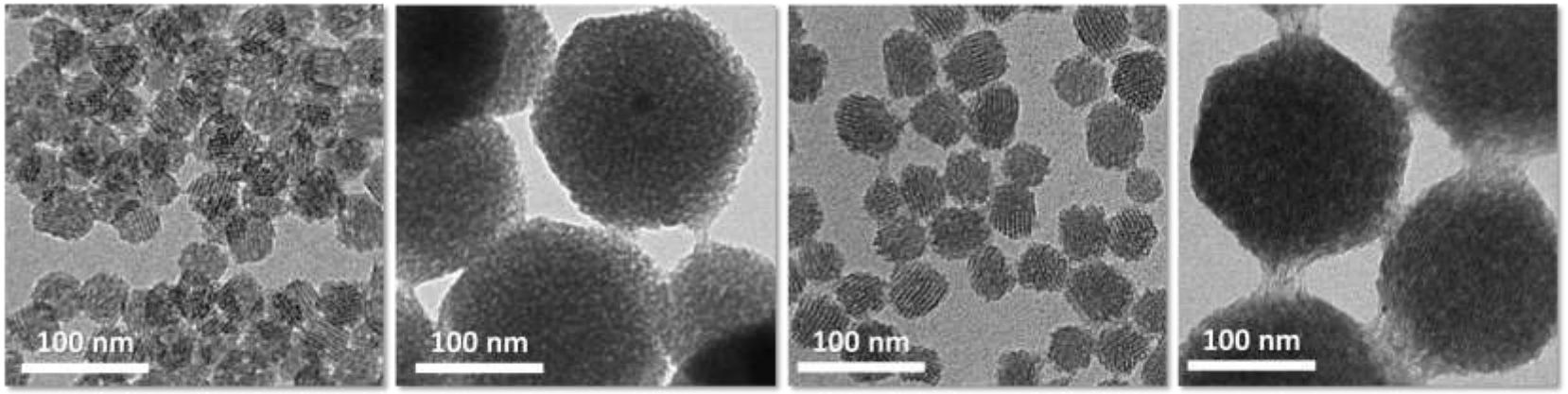

	Solvent	R-MSN@ PEG-PEI (50 nm)	R-MSN@ PEG-TA (50 nm)	R-MSN@ PEG-PEI (200 nm)	R-MSN@ PEG-TA (200 nm)
Zeta (mV)	H_2O	+41	+35.9	+34.7	+37.6
Hydrodynamic Diameter (nm)	H_2O (Z-average)	53.7	60.2	202.5	202.4
	10% FBS+DMEM (Peak)	79.1	61.1	239.3	220.3

Data not published

In Vitro

1. Cell and Nanoparticle interaction
2. Cell response and cellular signalling regulation
3. Cell cycle progression
4. Nanoparticle induced ROS generation and RBC hemolysis

- Cytotoxicity assay
- Cell uptake
- Western blot
- ROS detection
- Gene transfection
- Cell cycle
- Hemolysis assay

In Vivo

1. Biodistribution
2. Circulation
3. Pharmacokinetics (PK)
4. pharmacodynamics (PD)

- Two-photon fluorescence microscopy
- IVIS
- Blood Chemistry Report
- Complete Blood Count Report

Blood Circulation of NP in Mice

(Intravital two-photon imaging)

R-MSN@PEG-PEI (50 nm)

Dose: 200mg NP/kg BW

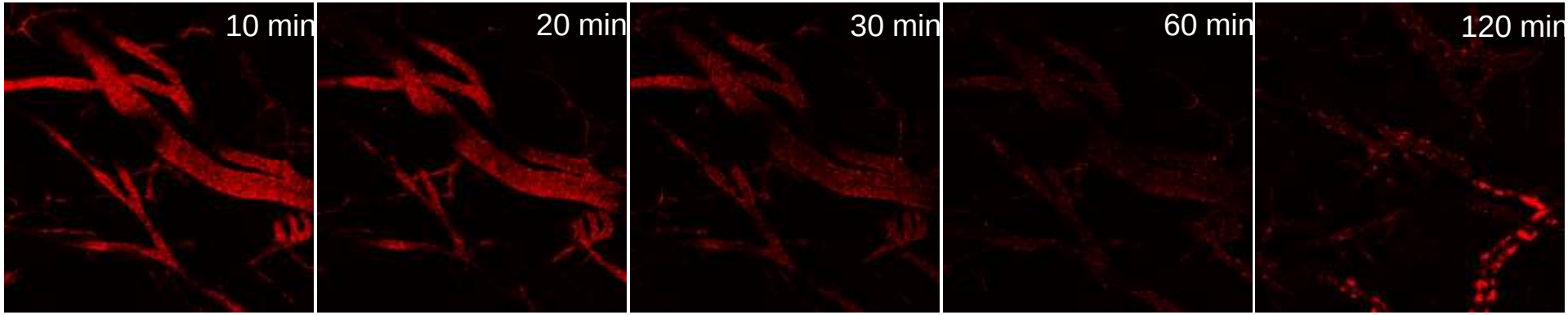

R-MSN@PEG-PEI (200 nm)

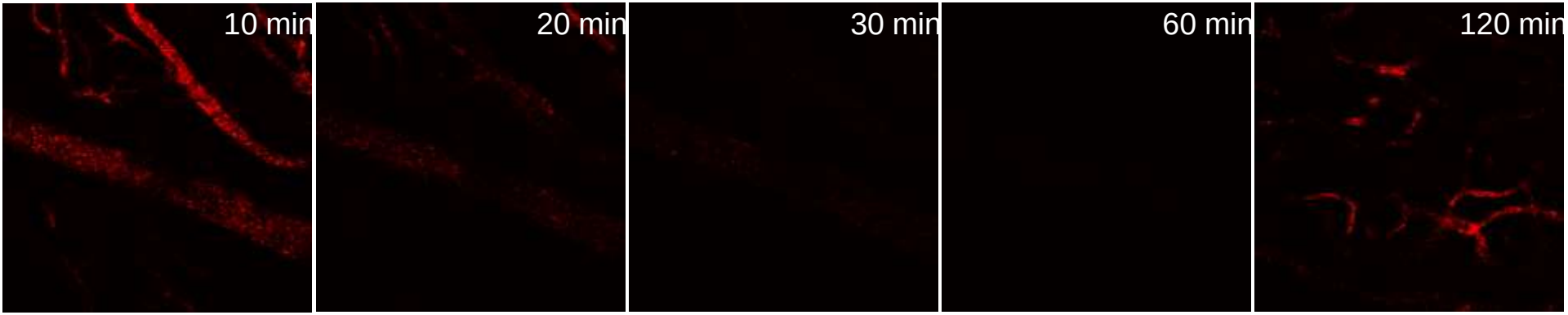

Data not published

Blood Circulation of NP

(Intravital two-photon imaging)

R-MSN@PEG-TA (50 nm)

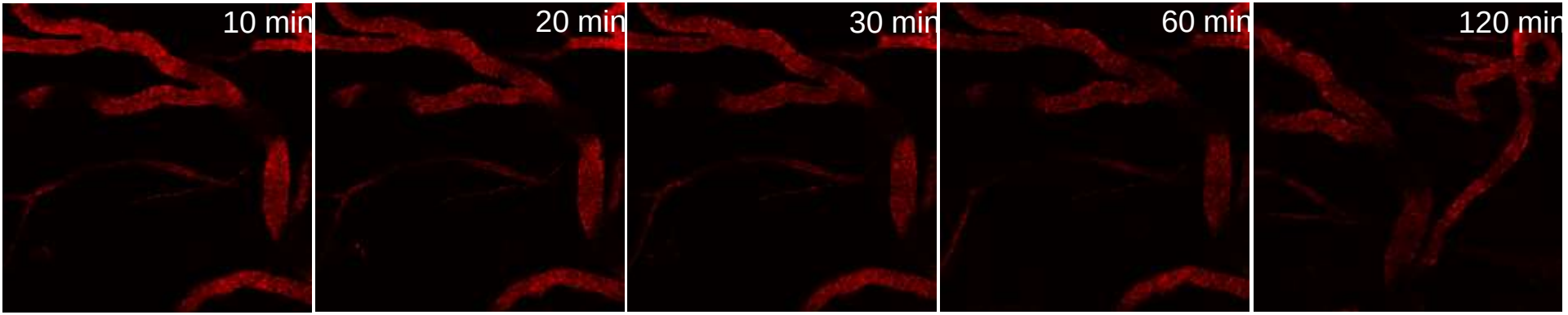

R-MSN@PEG-TA (200 nm)

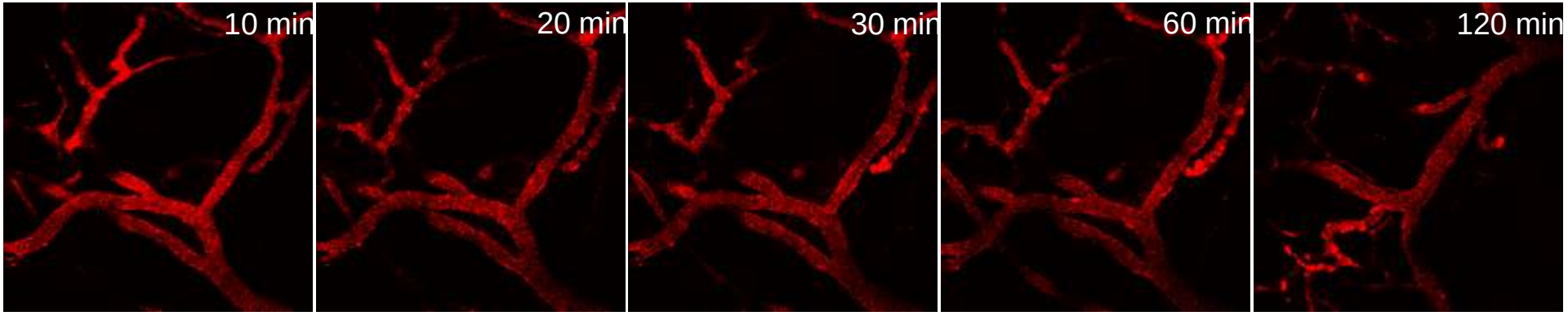

Ex vivo IVIS Images (4h)

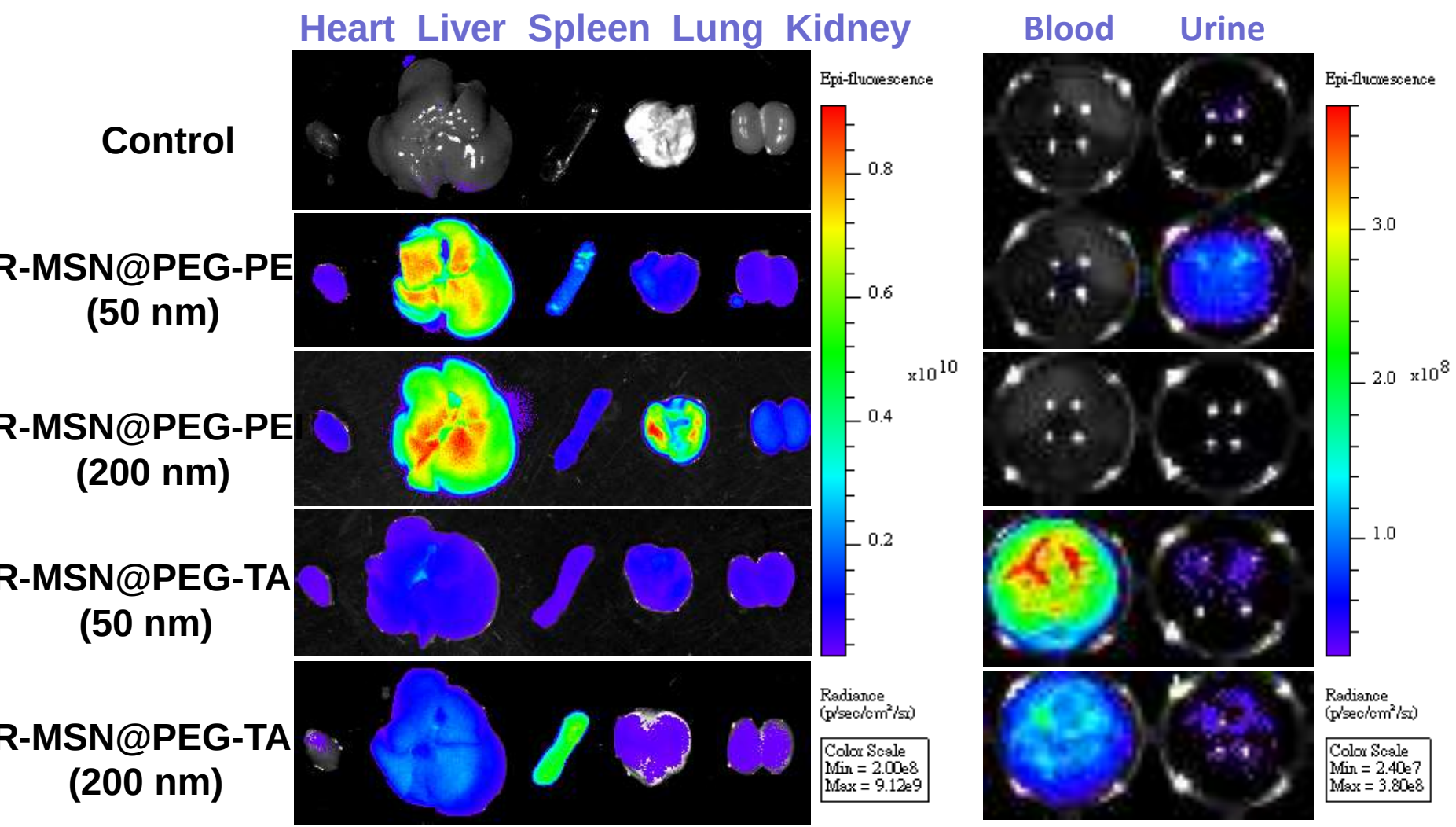

What if we inject these NPs into tumor-bearing mice?

In vivo IVIS Images (4h and 24h)
(NOD/SCID mice)

50 nm **200 nm**

R-MSN@ PEG-PEI **R-MSN@ PEG-TA** **R-MSN@ PEG-PEI** **R-MSN@ PEG-TA**

24h

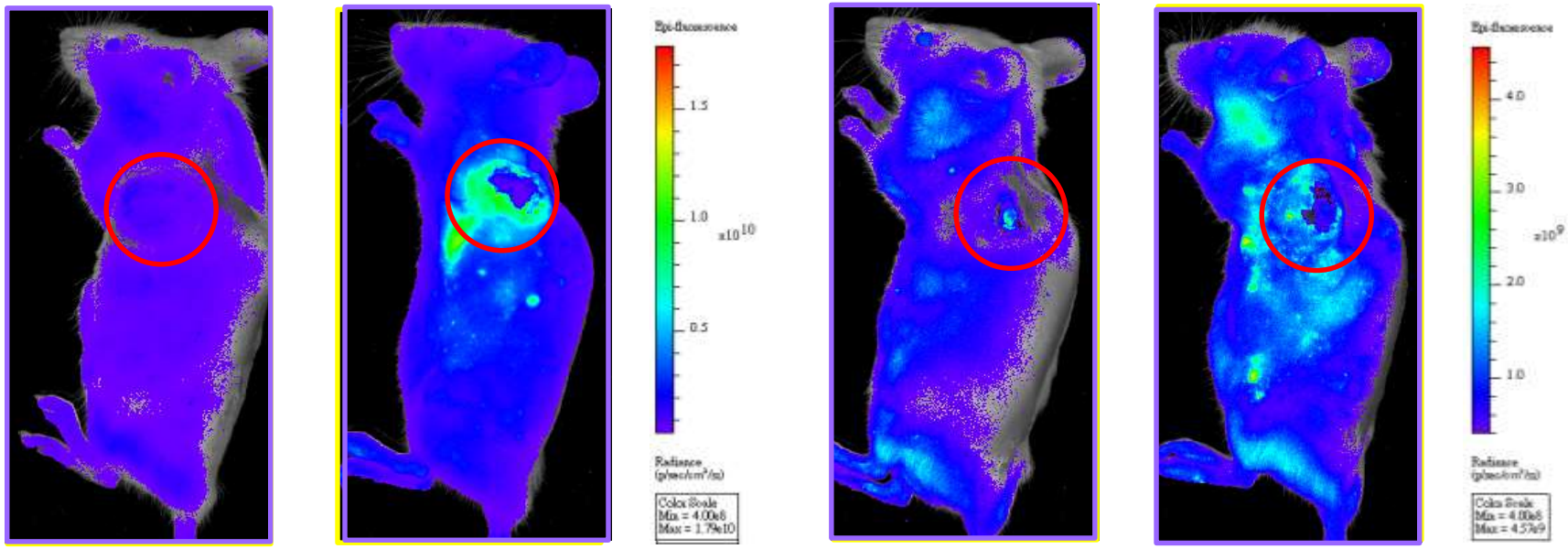

In vivo real-time distribution of NP in tumours (4h)

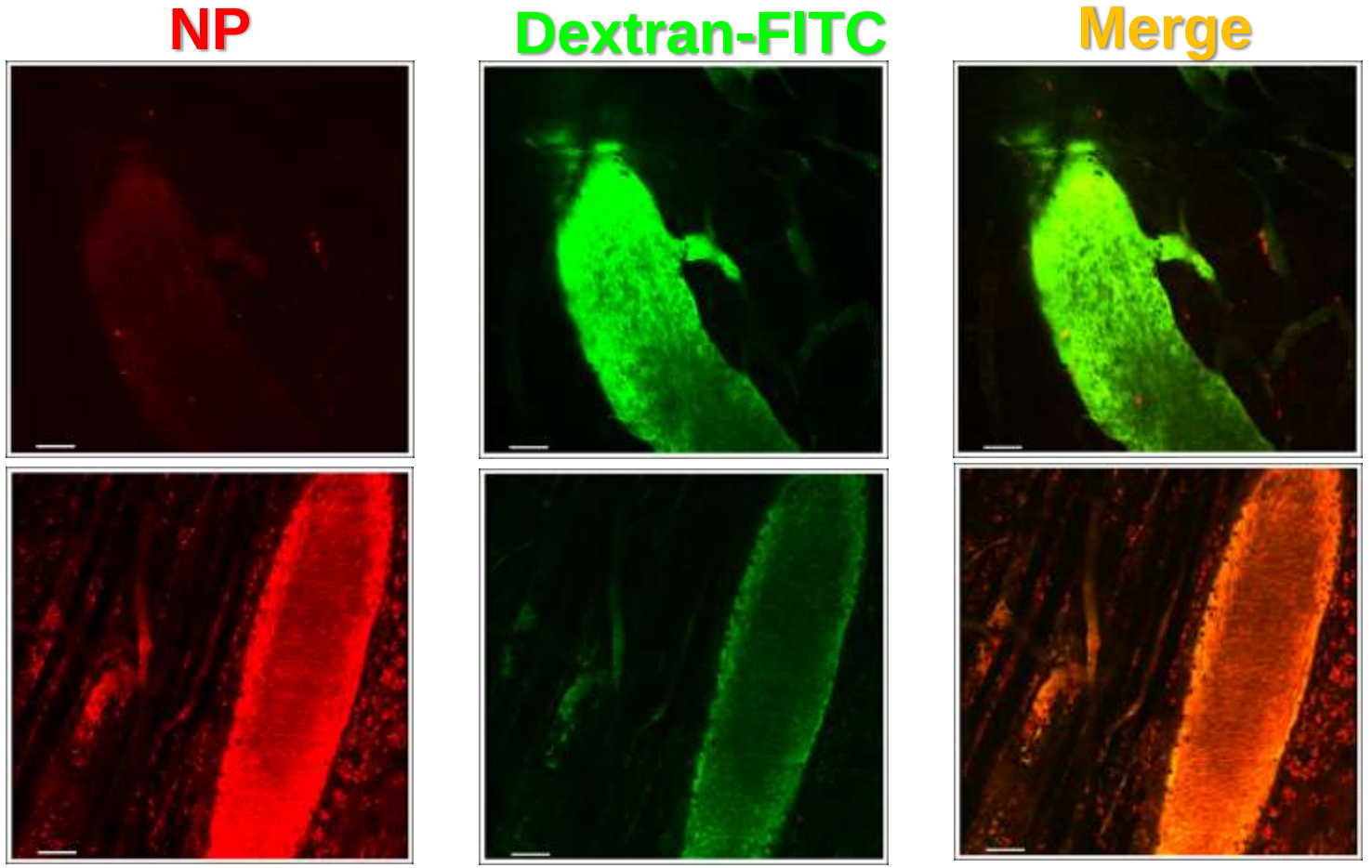

Scale bar: 50um

In vivo real-time distribution of NP in tumours (4h)

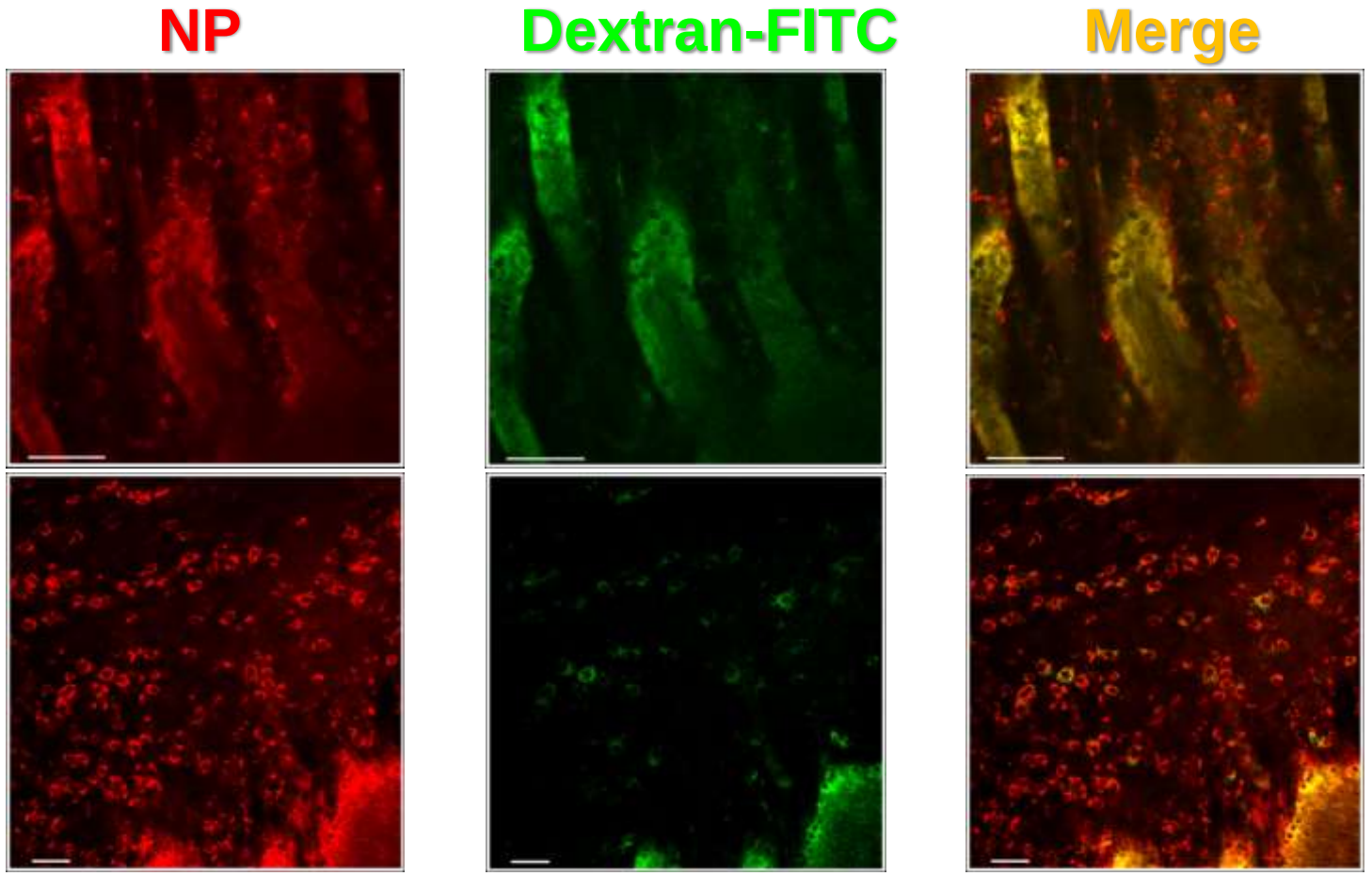

Scale bar: 50um

Ex vivo IVIS Images (24h)

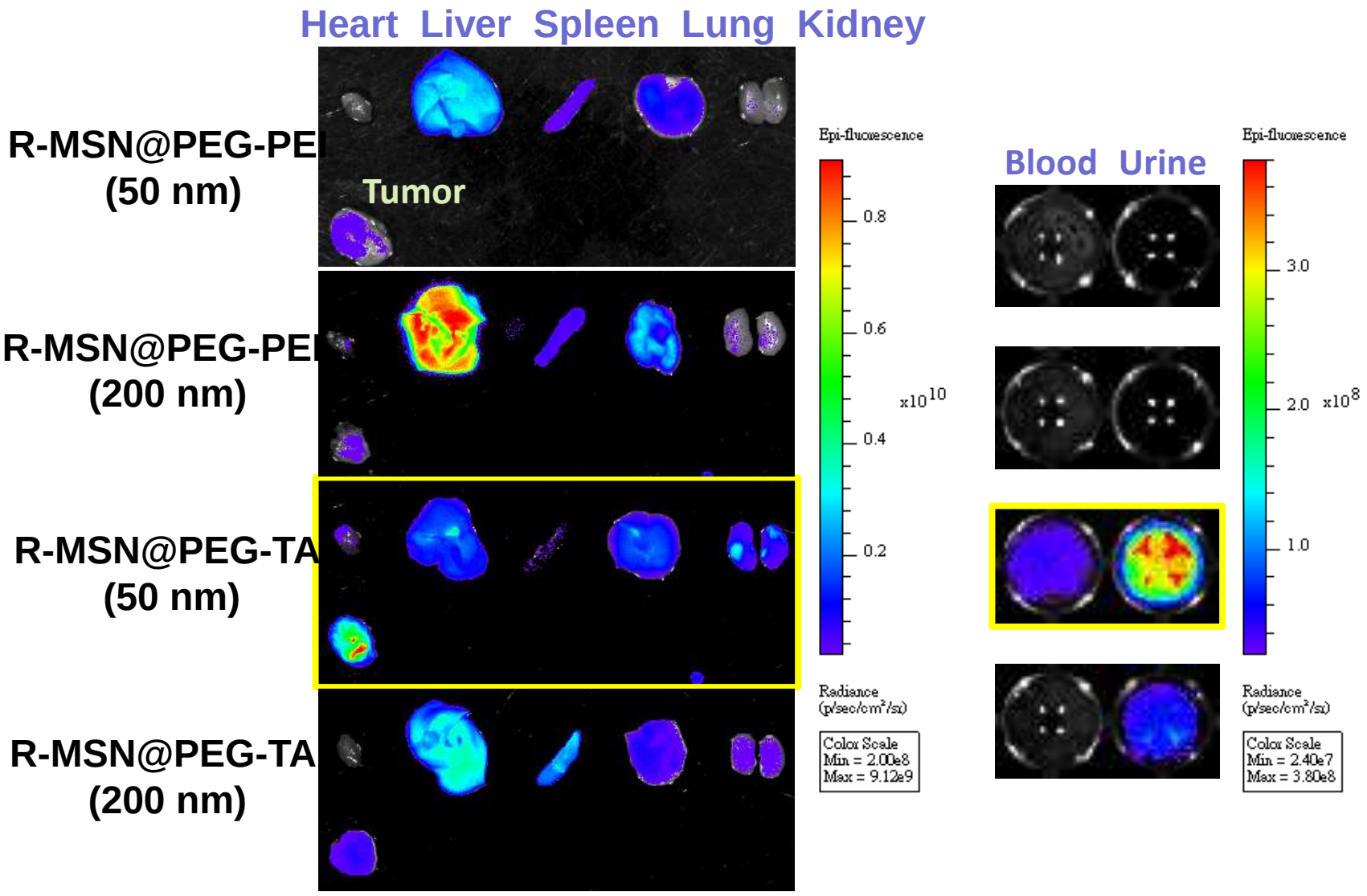

However, the targeting efficiency is dependent on mouse models

(NOD/SCID vs. BALB/c Nude)

- ✓ **Making much smaller NP (25 nm) can overcome this problem!**

A

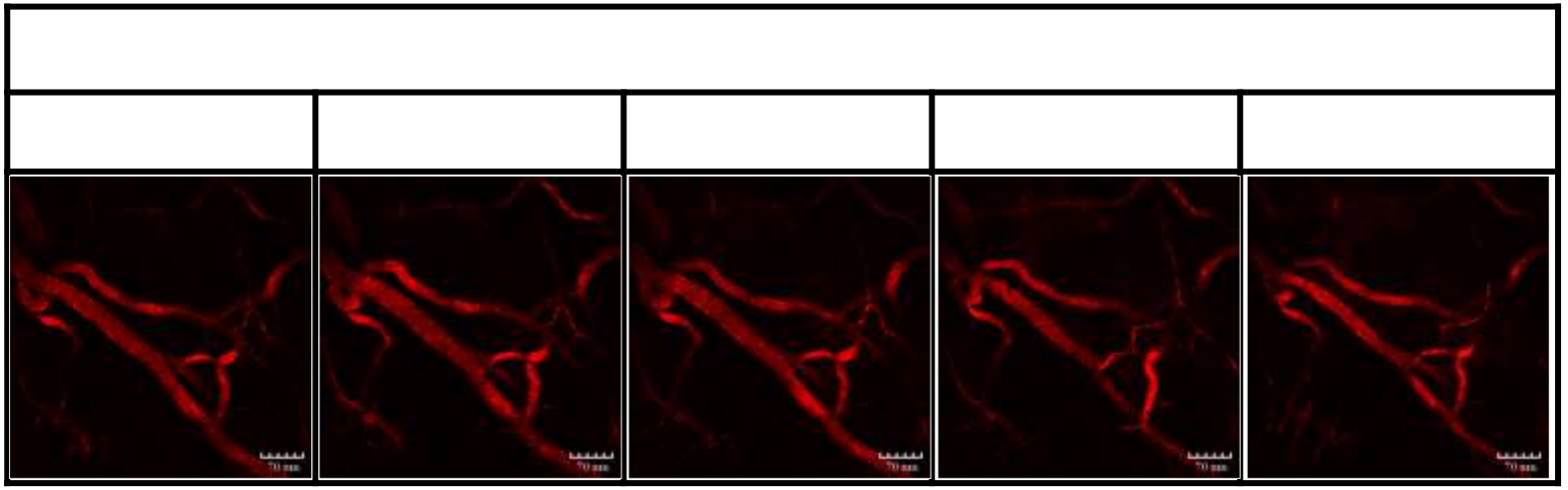

B

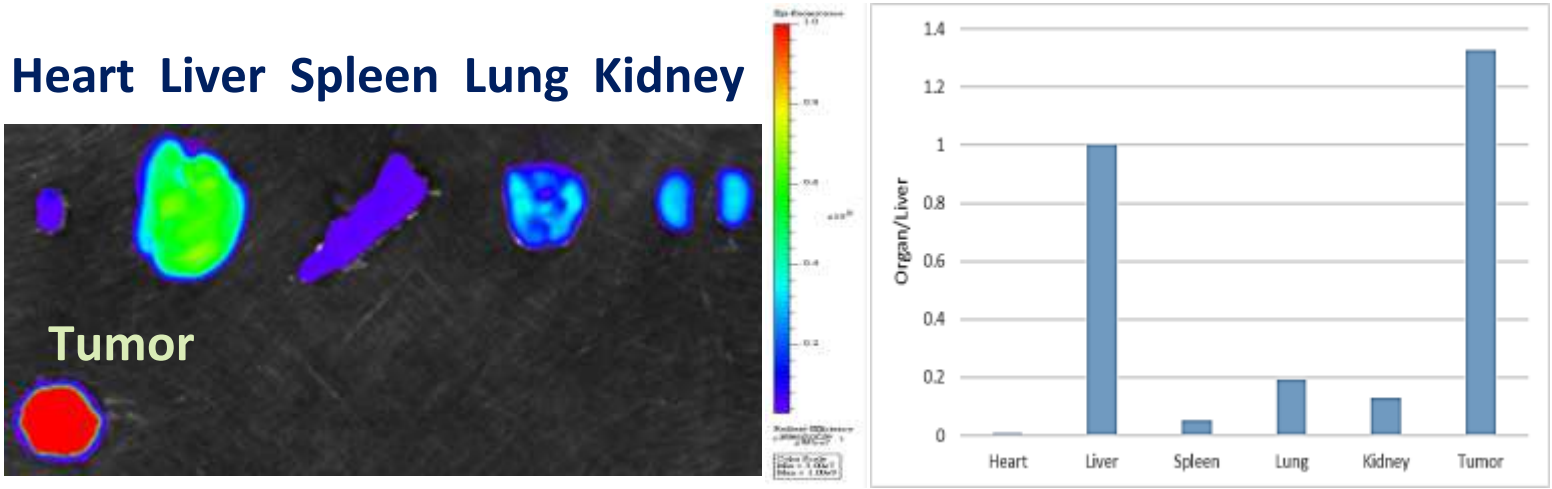

Data not published

In vivo real-time distribution of NP in tumours (4h)

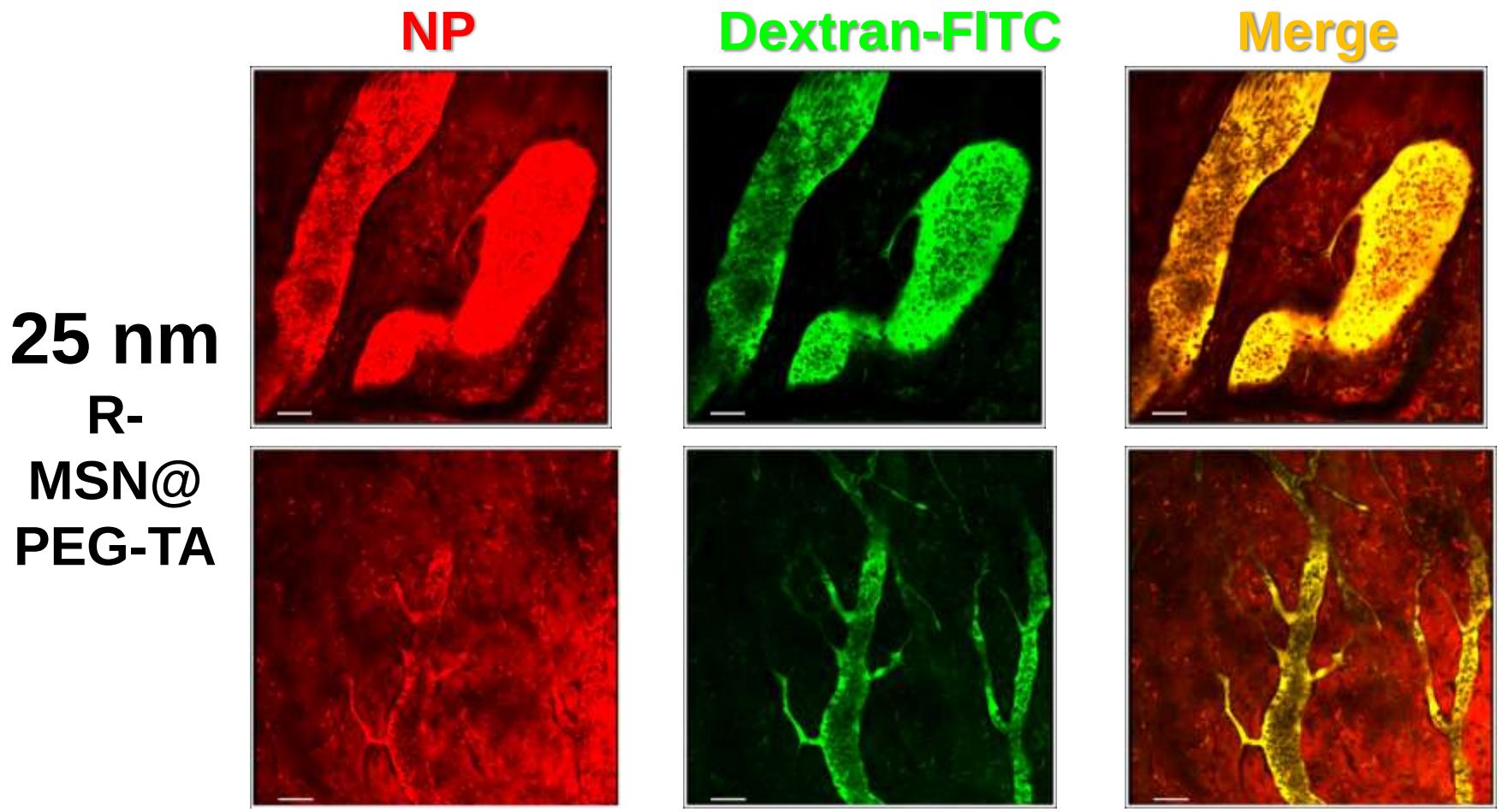

Scale bar: 50um

In vivo real-time distribution of NP in tumours (24h)

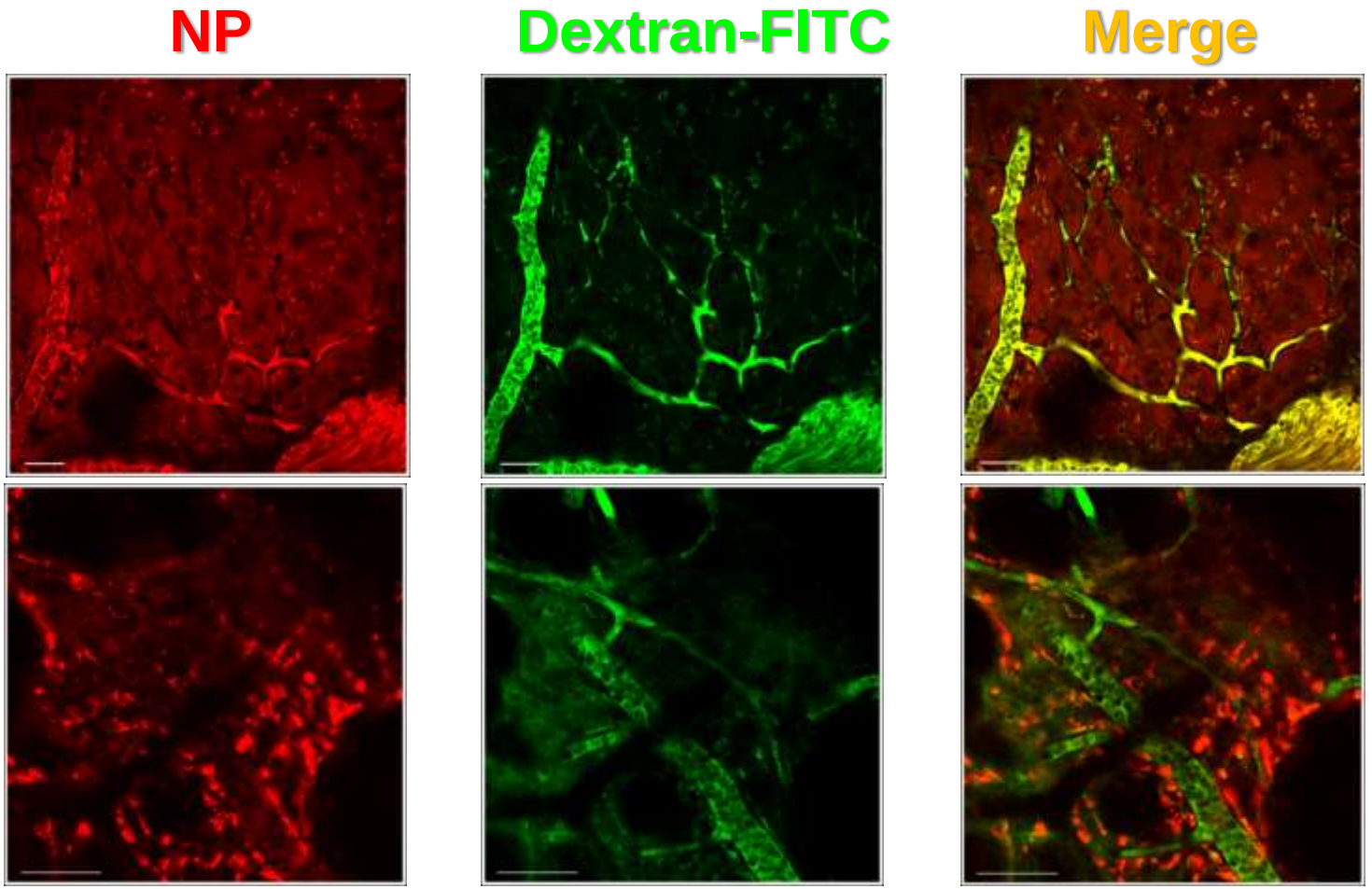

Scale bar: 50um

In vivo real-time distribution of NP in tumours (24h)

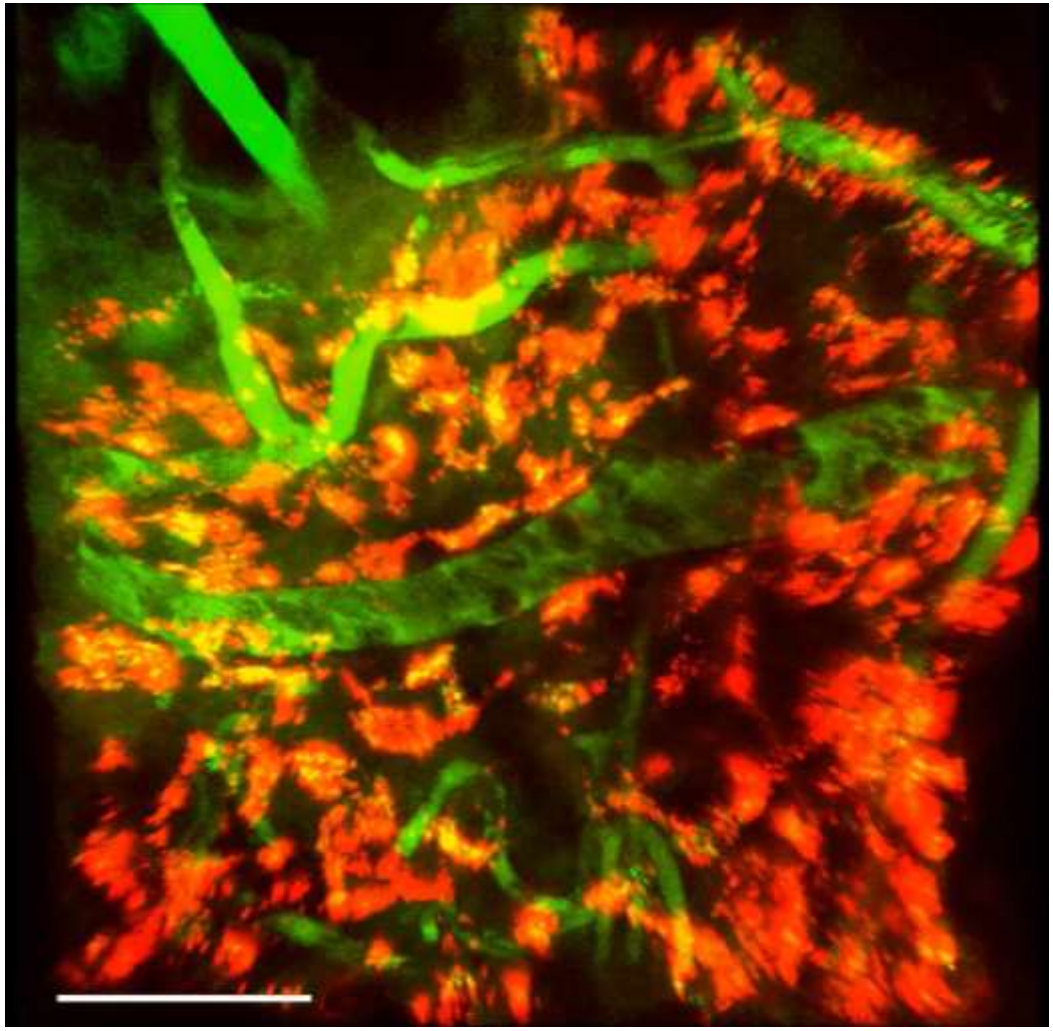

Scale bar: 50um

Renal clearance of quantum dots

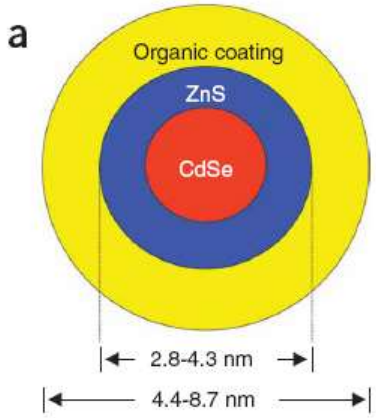

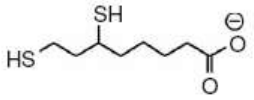

DHLA (MW 207)

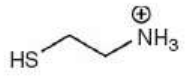

Cysteamine (MW 78)

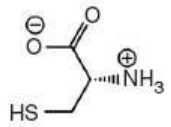

Cysteine (MW 121)

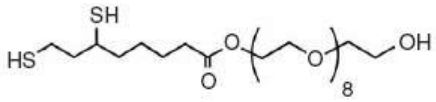

DHLA-PEG (MW 605)

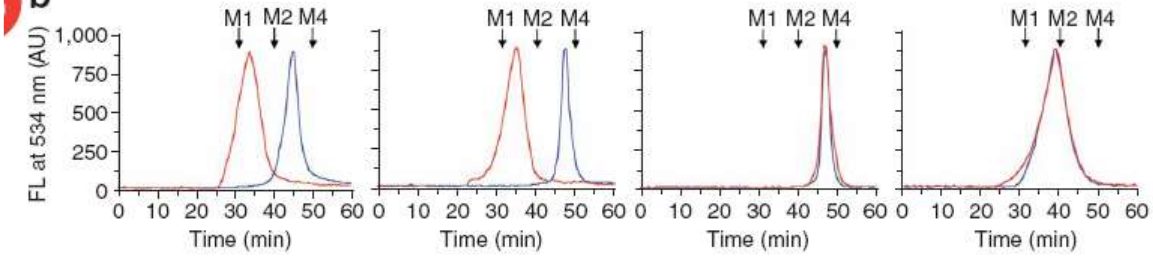

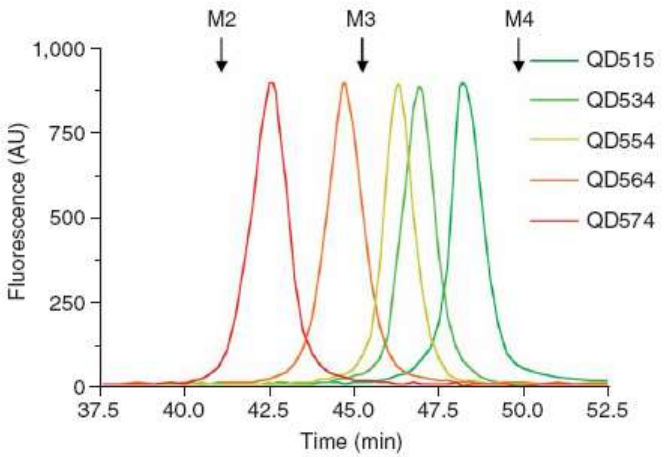

QD-Cys	Em Max (nm)	TEM Diameter (nm)	DLS		GFC
			HD (nm)	%PD	HD (nm)
QD515	515	2.85 ± 0.18	4.64 ± 0.08	20.9	4.36 ± 0.09
QD534	534	3.02 ± 0.20	4.91 ± 0.05	25.9	4.99 ± 0.18
QD554	554	3.30 ± 0.25	5.64 ± 0.01	13.1	5.52 ± 0.14
QD564	574	3.80 ± 0.20	6.40 ± 0.02	24.7	6.70 ± 0.33
QD574	584	4.31 ± 0.46	7.22 ± 0.20	24.8	8.65 ± 0.52

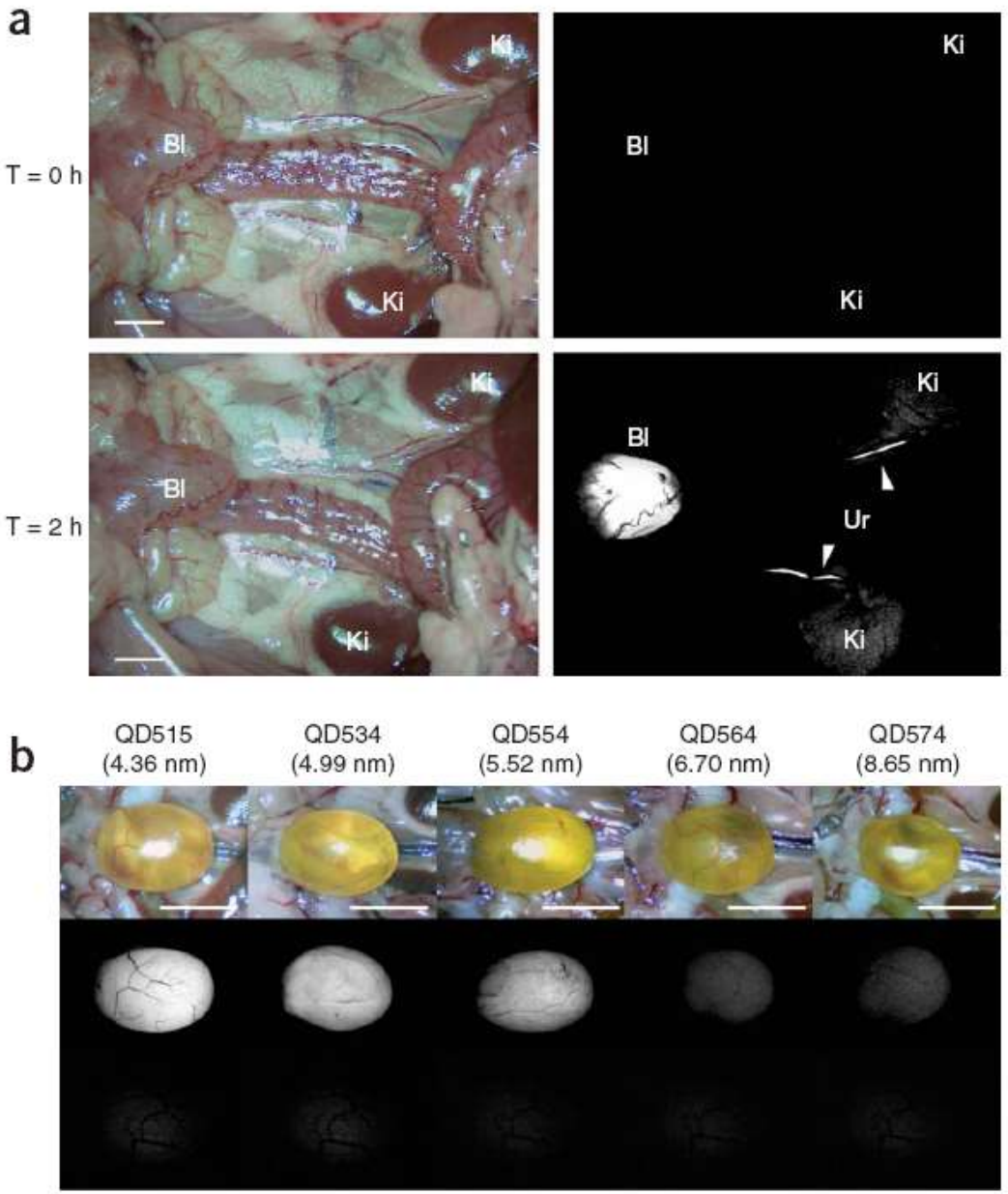

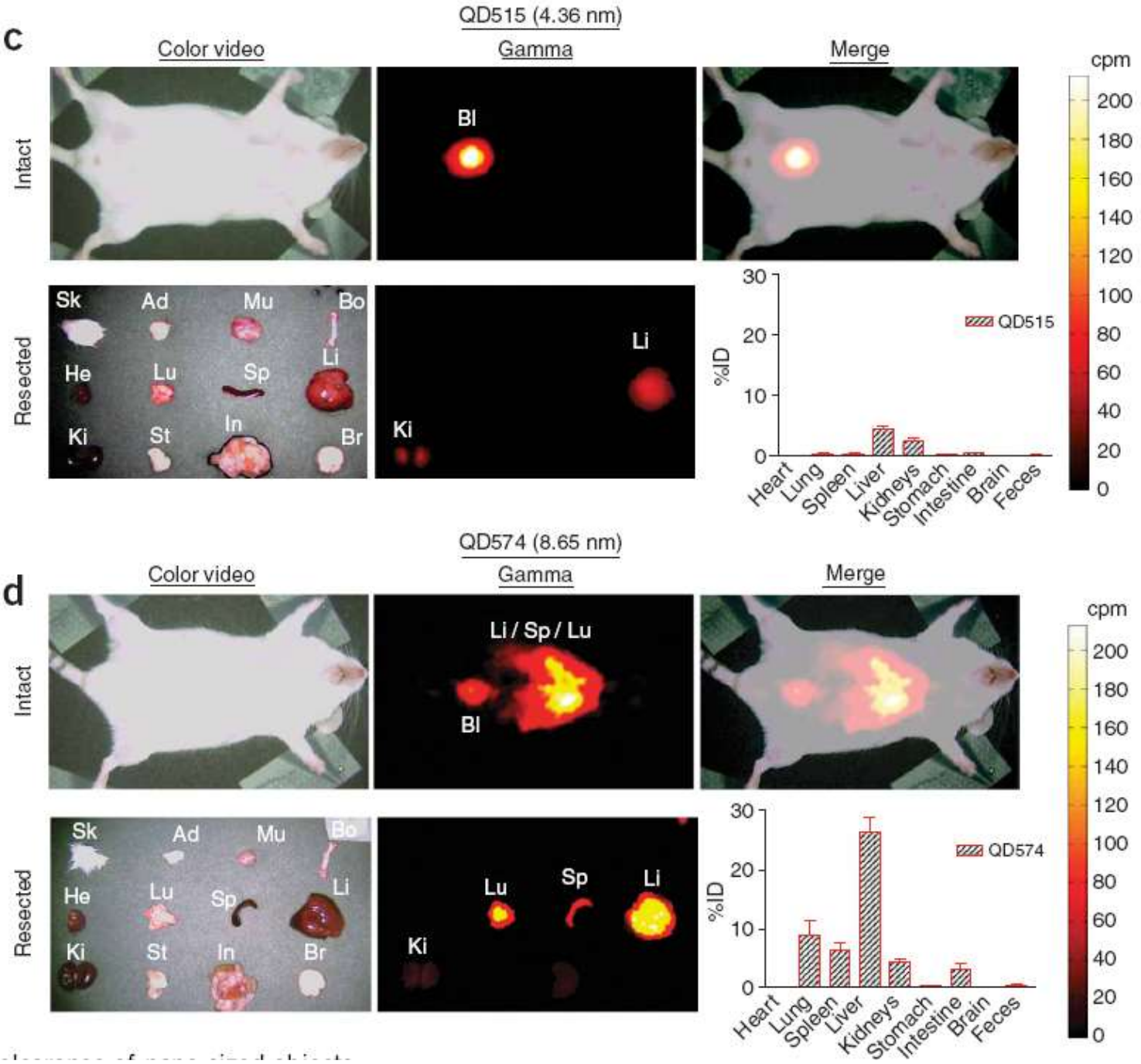
c
QD515 (4.36 nm)
Color video
Gamma
Merge
Intact
Resected
Bl
Sk
Ad
Mu
Bo
He
Lu
Sp
Li
Ki
St
In
Br
cpm
200
180
160
140
120
100
80
60
40
20
0
30
20
10
0
%ID
QD515
Heart
Lung
Spleen
Liver
Kidneys
Stomach
Intestine
Brain
Feces
d
QD574 (8.65 nm)
Color video
Gamma
Merge
Intact
Resected
Li / Sp / Lu
Bl
Sk
Ad
Mu
Bo
He
Lu
Sp
Li
Ki
St
In
Br
Lu
Sp
Li
Ki
cpm
200
180
160
140
120
100
80
60
40
20
0
30
20
10
0
%ID
QD574
Heart
Lung
Spleen
Liver
Kidneys
Stomach
Intestine
Brain
Feces

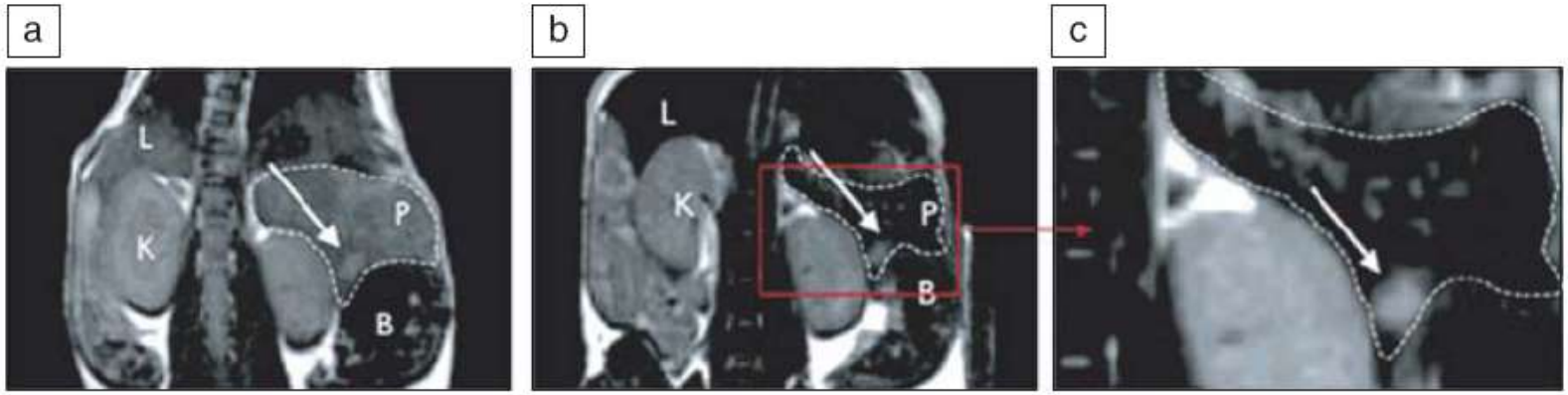

Figure 1. Cross-linked iron oxide (CLIO) nanoparticles for T_2-weighted images of rodent pancreatic cancer: (a) preinjection of CLIO, (b) postinjection of CLIO, and (c) higher magnification of postinjection image with the arrow indicating tumor. L, liver; P, pancreas; K, kidney; B, bowel.[16]

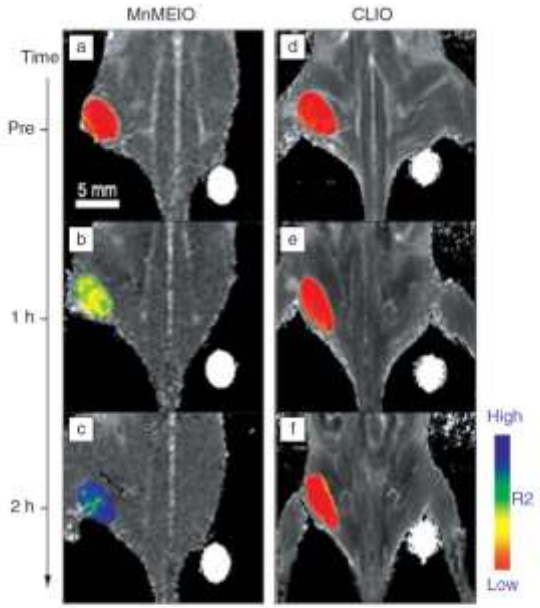

Figure 2. *In vivo* magnetic resonance detection of cancer after administration of magnetic nanoparticles Herceptin conjugates. $MnFe_2O_4$ nanoparticles (MnMEIO) (a–c) show higher signal enhancement than cross-linked iron oxide (CLIO) (d–f).[24] R2, inverse of transverse relaxation time.

Carbon Nanotubes

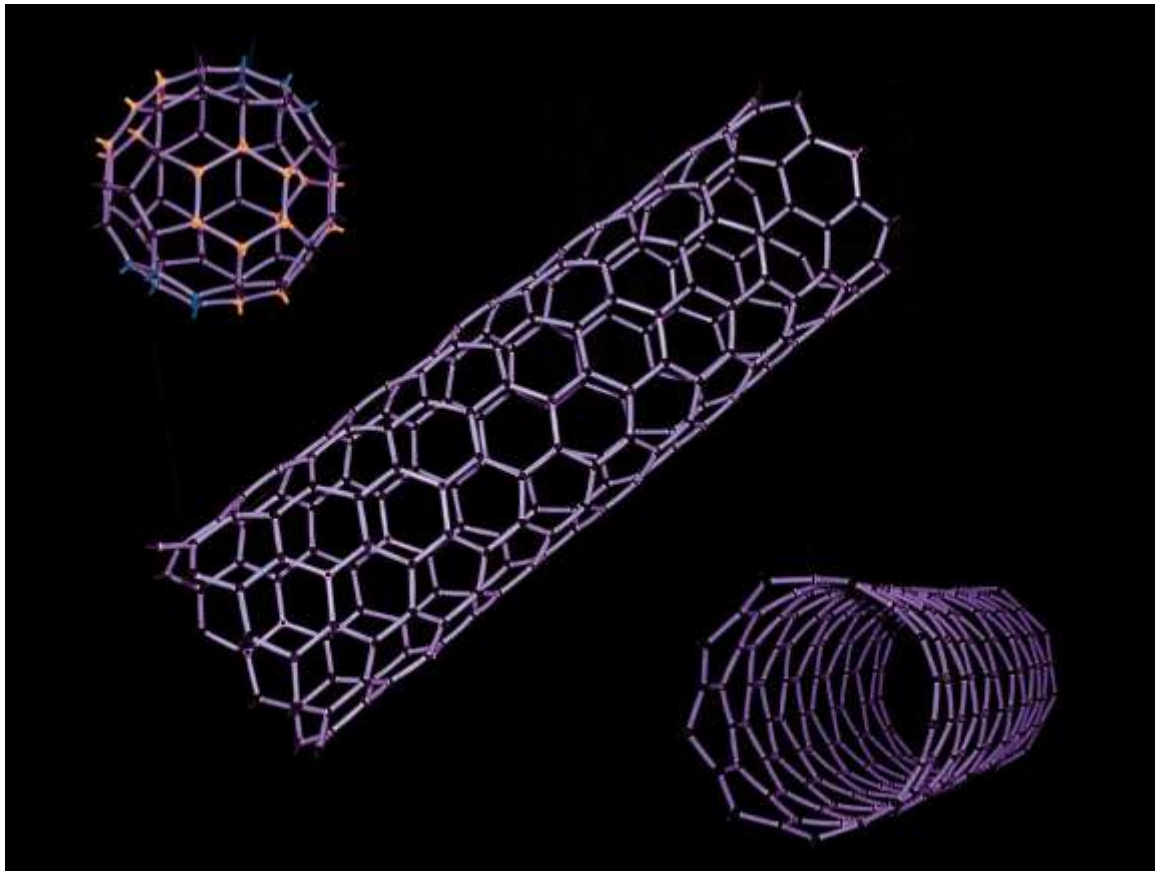

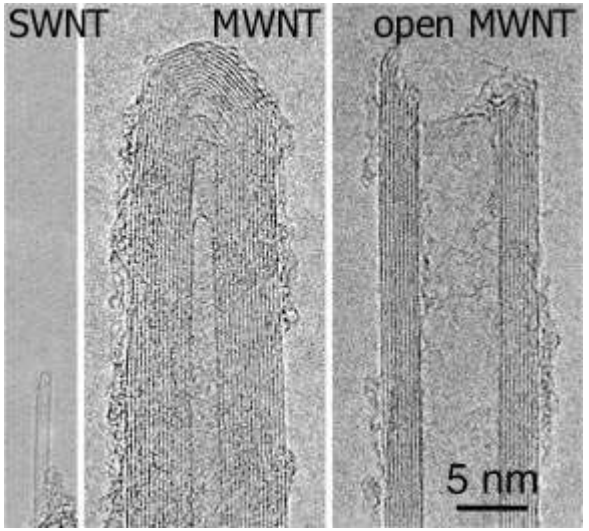

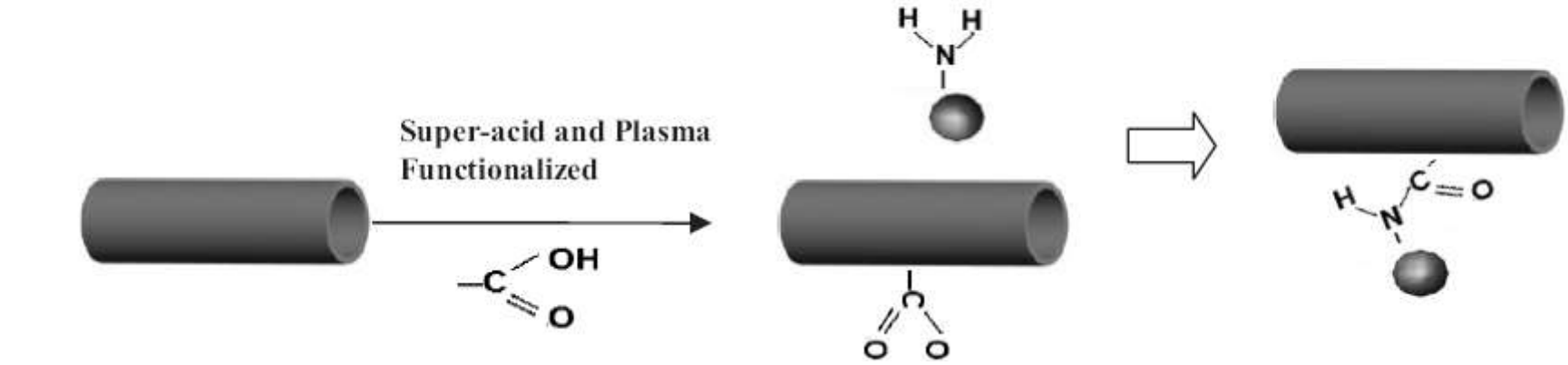

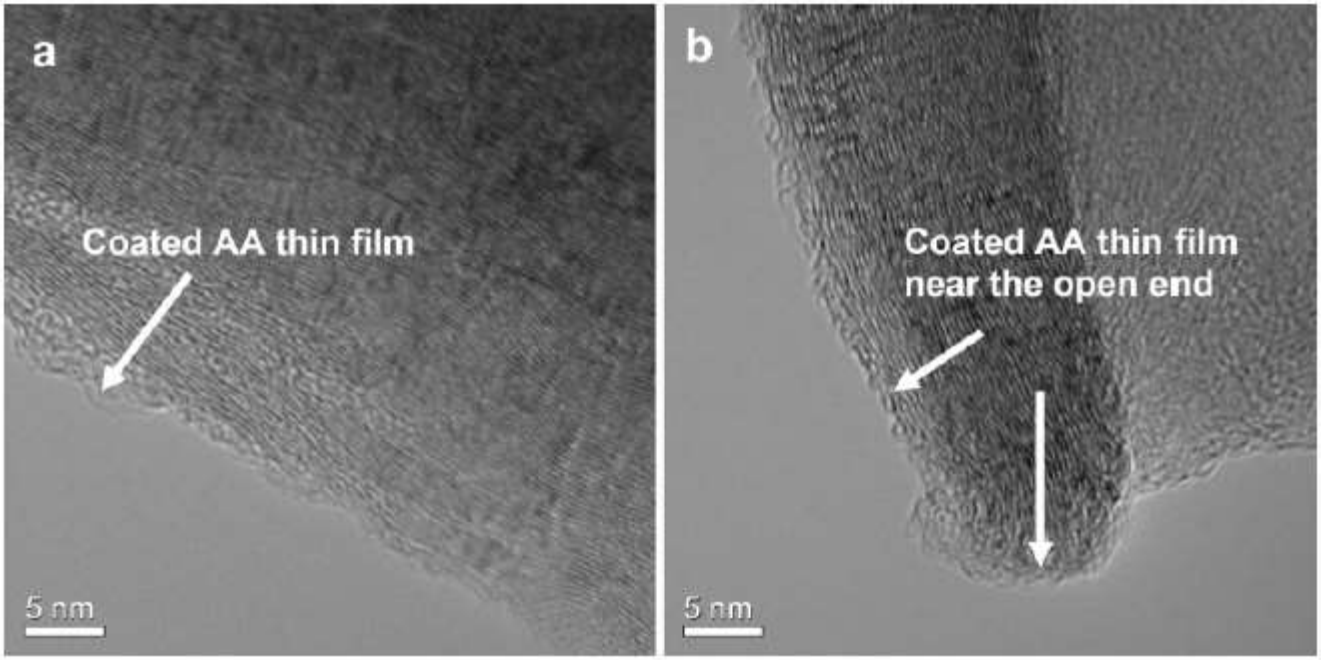

Figure 2. TEM images showing a) the plasma deposited acrylic acid (AA) polymer thin film on the carbon nanotube, the lattice image of carbon nanotube can be clearly seen with an extremely thin layer of polymer film (~ 2 nm); b) the thin film of AA was plasma deposited near the open end of the carbon nanotube.

Adv. Mater. **2007**, *19*, 4033–4037

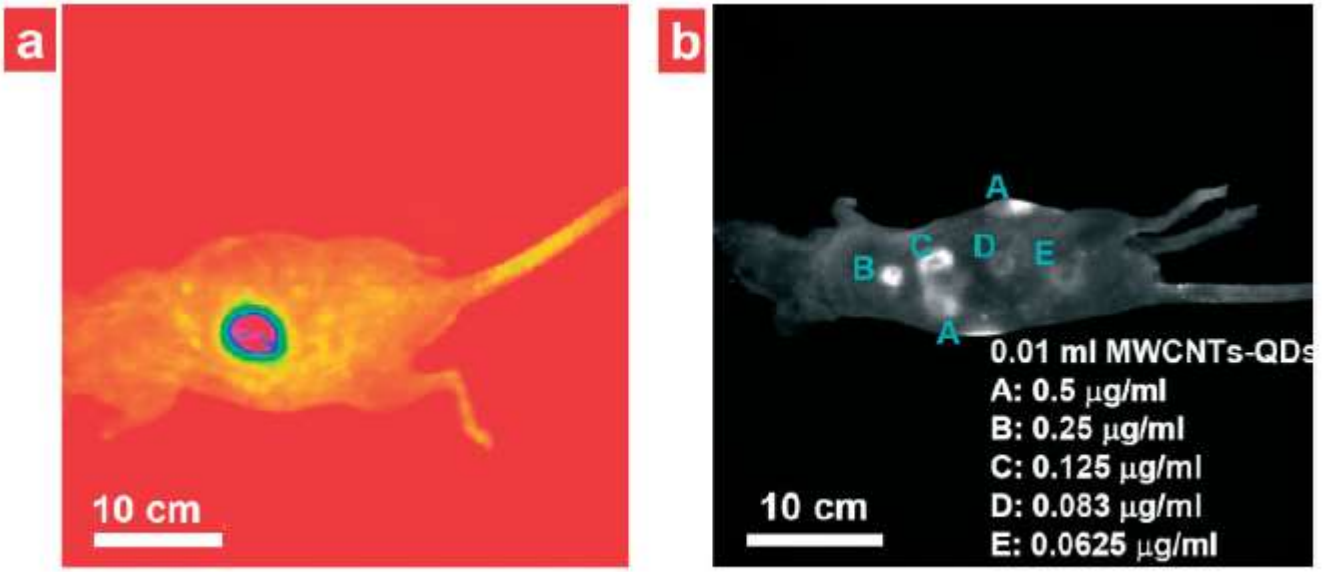

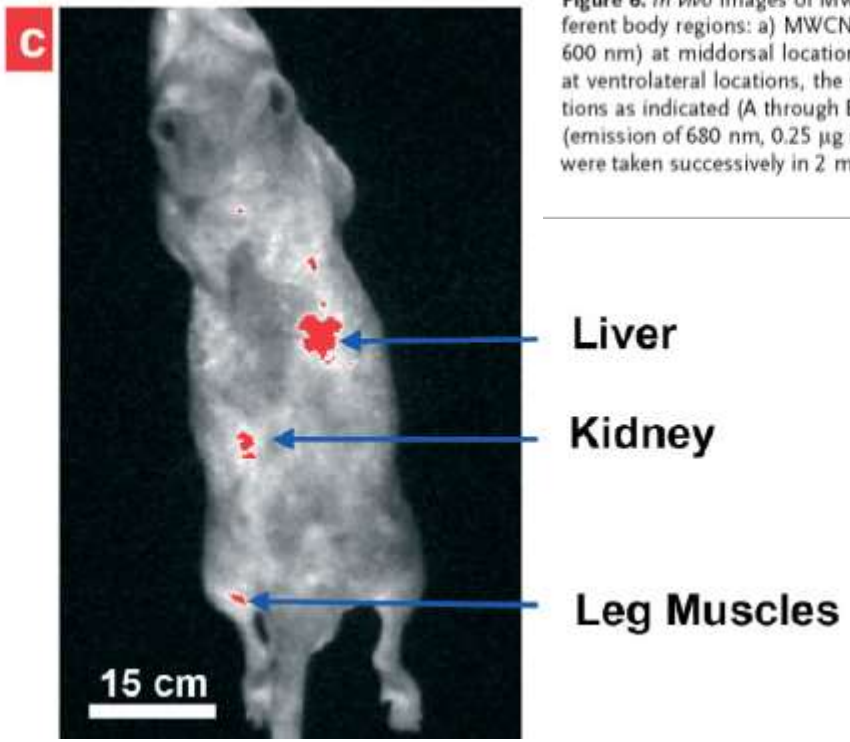

Figure 6. *In vivo* images of MWCNTs-QDs (0.5 μg ml^{-1} in PBS) in mice injected at different body regions: a) MWCNTs attached with CdSe/ZnS quantum dots (emission of 600 nm) at middorsal location; b) MWCNTs attached with CdSe/ZnS quantum dots at ventrolateral locations, the suspensions were diluted by PBS at various concentrations as indicated (A through E); c) MWCNTs attached with InGaP/ZnS quantum dots (emission of 680 nm, 0.25 μg ml^{-1} in PBS) in liver, kidney, and leg muscles. All images were taken successively in 2 min under epi-UV illuminator with excitation of 435 nm.

Polymer

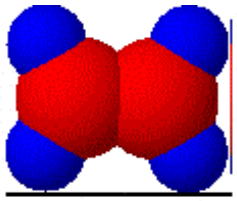

a monomer ethene

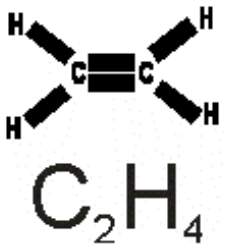

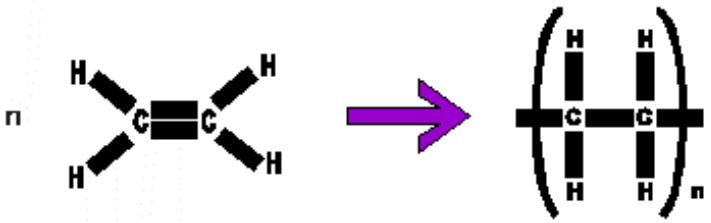

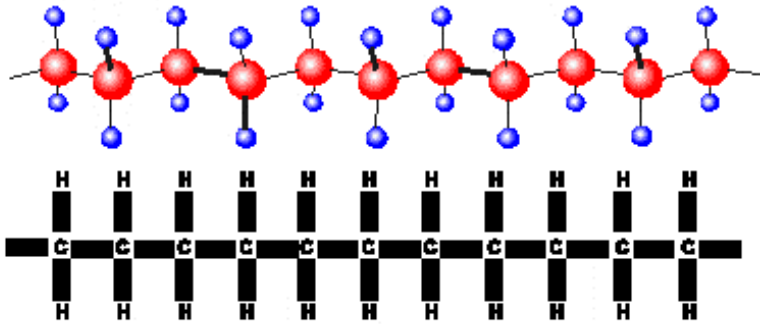

a polymer poly(ethene)

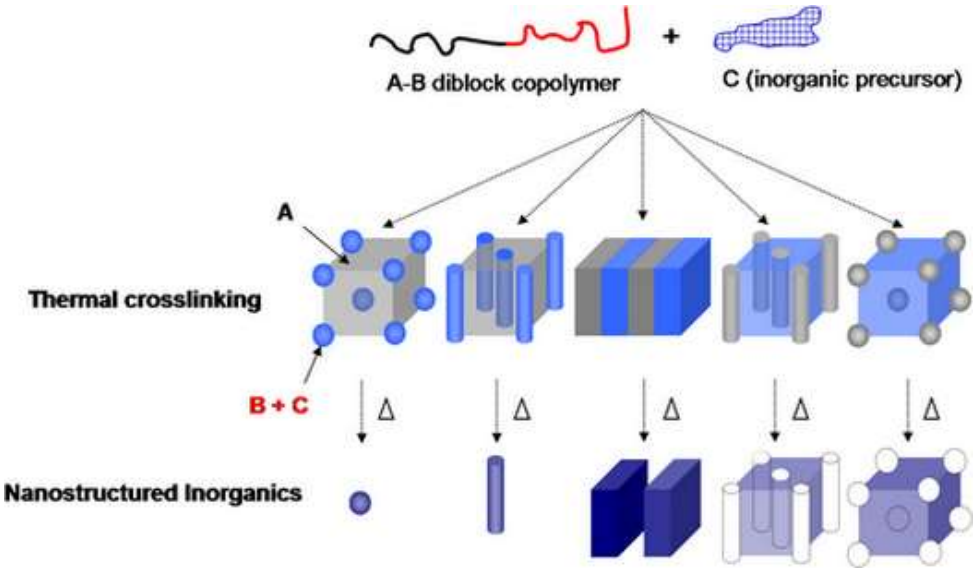

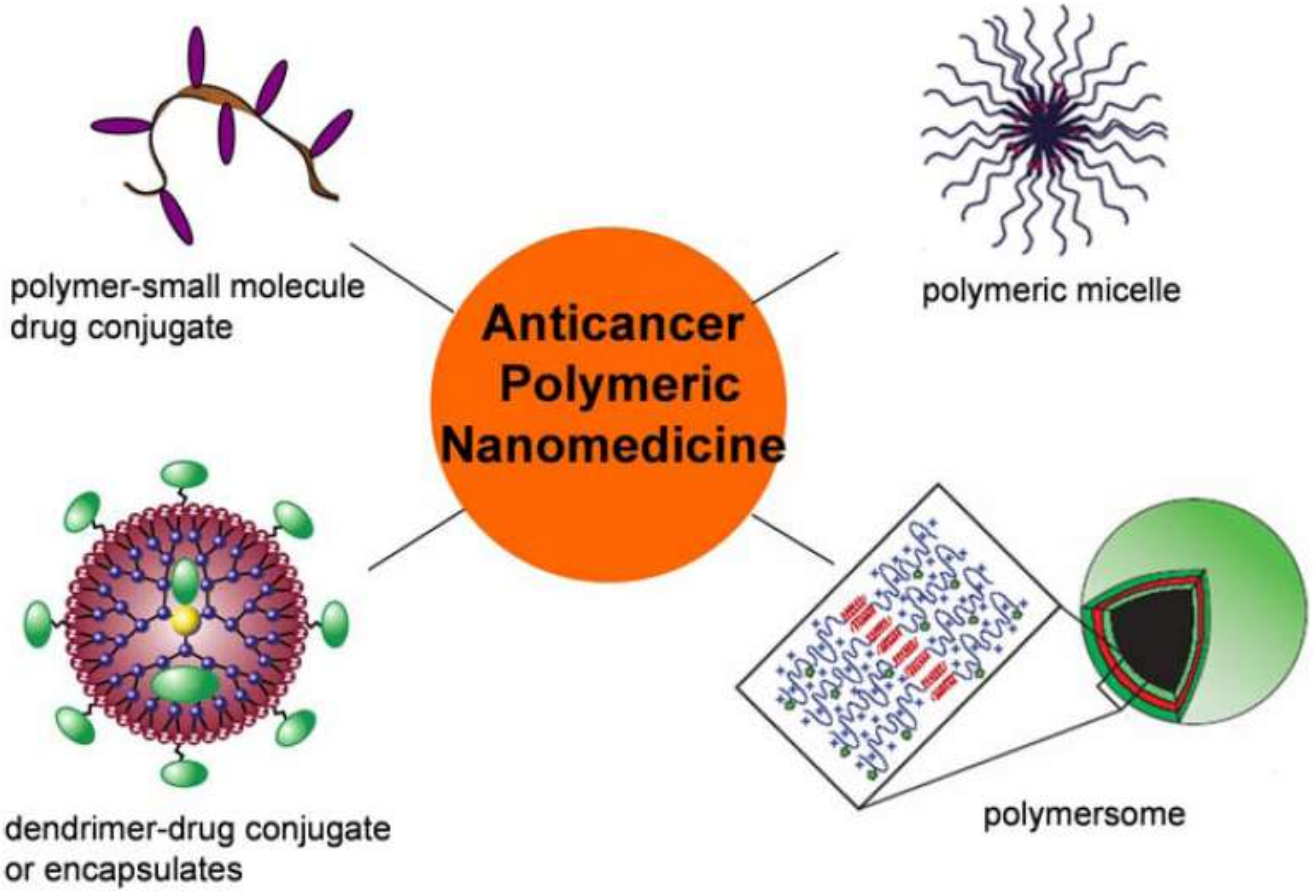

Figure 1. Illustration of various anticancer polymeric nanomedicines that have been developed and are used in cancer drug delivery. Polymer-small molecule drug conjugates are usually hydrophilic (water-soluble) polymers with covalently bound, releasable hydrophobic drug molecules. Polymeric micelles are core-shell micellar nanostructures with a hydrophobic core that can be used for the encapsulation of hydrophobic drug molecules and for the controlled release of hydrophobic therapeutics, and a hydrophilic shell can be used for micelle surface modification (e.g., incorporation of targeting ligands). Polymersomes are a class of hollow spherical nanostructures that enclose a solution and can be used to deliver hydrophilic therapeutics such as DNA and proteins. Dendrimer drug conjugate or encapsulates are a class of drug delivery systems with drugs conjugated to the periphery or encapsulated inside of monodisperse macromolecules with highly branched, symmetric, three-dimensional architectures.

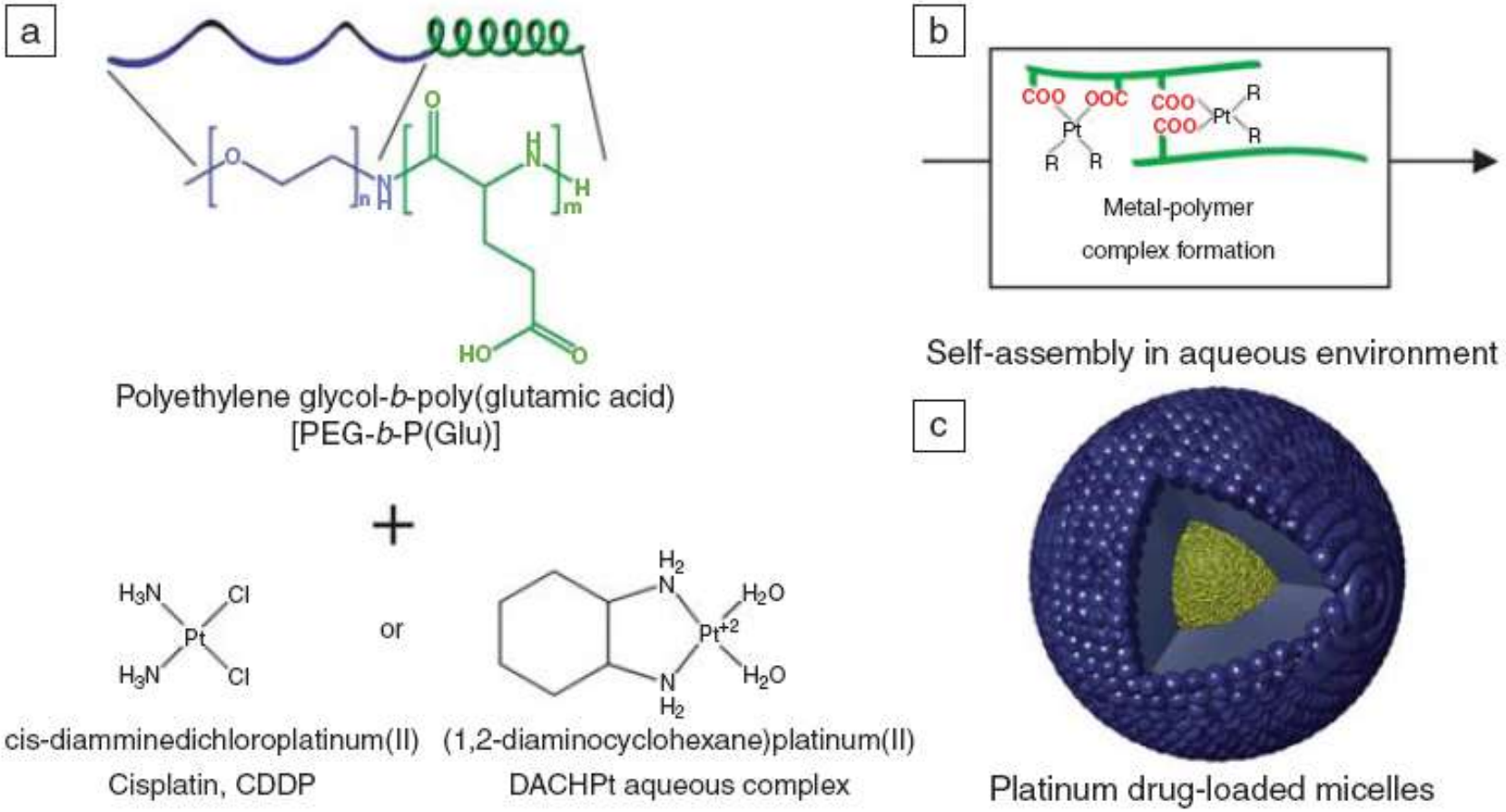

Figure 2. (a) Schematic diagram of proposed self-assembly of platinum drug-loaded polymeric micelles.[101,102] (b) The self-assembly is mediated by the coordination of the platinum (II) and the carboxylate groups (COO) of the poly(glutamic acid) segments. (c) Narrowly distributed polymeric micelles with dense drug-loaded cores are formed.

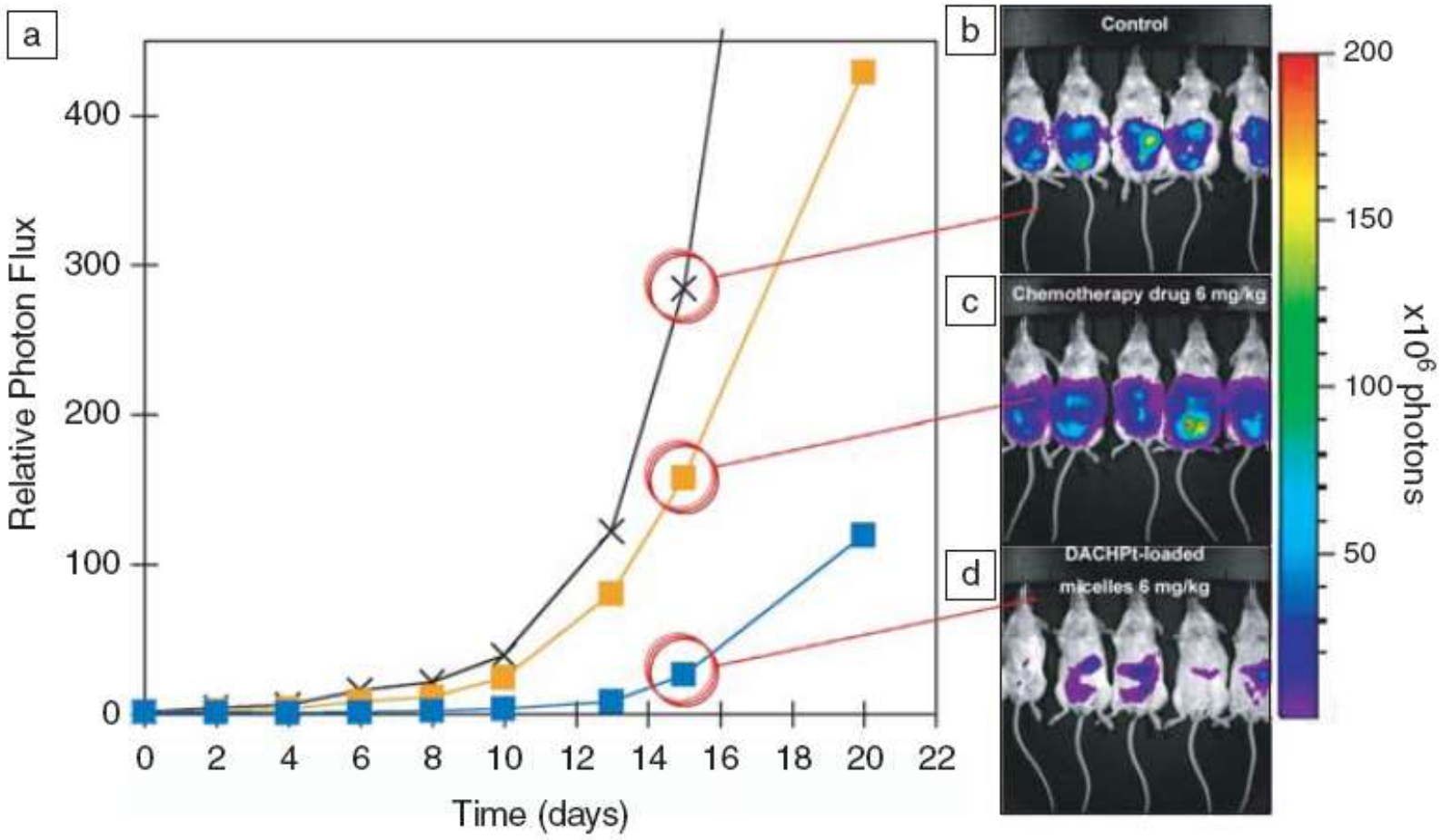

Figure 3. Platinum drug-loaded polymeric micelles.[103] (a) Antitumor activity measured as the relative photon flux, which is the ratio between the photon flux (photons/second) and the initial photon flux, from bioluminescent intraperitoneal (within the abdominal cavity) metastasis and the *in vivo* bioluminescent images corresponding to day 10. (b) Control (crosses), (c) the clinically used DACHPt derivative, oxaliplatin, 6 mg/kg (orange squares), (d) (1,2-diaminocycloheance) platinum (II) (DACHPt)-loaded micelle (blue squares).

Polymer conjugates as anticancer nanomedicines

At a glance

- Water-soluble polymers conjugated to proteins and anticancer drugs are in routine clinical use and clinical development as both single agents and components of combination therapy. This is establishing polymer therapeutics as one of the first classes of anticancer nanomedicine. There is growing optimism about the use of ever more sophisticated polymer-based vectors for cancer therapy.
- The covalent conjugation of synthetic polymers, particularly poly(ethyleneglycol) (PEG), to protein drugs increases their plasma residence, reduces protein immunogenicity and can increase their therapeutic index. Several PEGylated enzymes (such as L-asparaginase) and cytokines (including interferon-α and granulocyte colony-stimulating factor) have now entered routine clinical use.
- Polymer conjugation alters the biodistribution of low-molecular-weight drugs, enabling tumour-specific targeting with reduced access to sites of toxicity. More than ten polymer–anti-tumour conjugates have been transferred into clinical development. They have been designed for lysosomotropic delivery following passive tumour targeting by the enhanced permeability and retention effect (EPR effect) or, in one case, for receptor-mediated targeting by the introduction of a cell-specific ligand. Polyglutamic acid–paclitaxel is showing particular promise in phase III trials in women with non-small-cell lung cancer.
- New strategies are making polymer conjugates active against new molecular targets (for example, anti-angiogenics), and the combination of polymer conjugates with low-molecular-weight drugs (which are routinely used in chemotherapy), radiotherapy or tailor-made prodrugs is showing promise. Moreover, the polymer platform provides an ideal opportunity to deliver a drug combination from a single carrier, and combined endocrine therapy and chemotherapy is showing preclincal potential as a breast cancer therapy.
- The polymers that have been used clinically so far have a linear polymer architecture. The principles for the design of polymer therapeutics are now being applied to new hyperbranched dendrimers and dendritic polymer architectures. Before clinical evaluation it is essential to establish the safety of new polymers, particularly in respect of general toxicity, immunogenicity and metabolic fate.

Box 1 | **Rationale for design of PEG–protein conjugates**

Recombinant DNA and monoclonal antibody technology has created a growing number of peptide, protein and antibody-based drugs. The conjugation of poly(ethyleneglycol) (PEG) to proteins (PEGylation) is proving a useful tool to:

- Increase protein solubility and stability, and also to reduce protein immunogenicity[29,30].
- Prevent the rapid renal clearance of small proteins and receptor-mediated protein uptake by cells of the reticuloendothelial (RES) system.
- Prolong plasma half-life — leading to the need for less frequent dosing, which is of great patient benefit.

Although several water-soluble polymers have been successfully used for protein conjugation, PEG is particularly attractive because:

- PEG is used as a pharmaceutical excipient and is known to be non-toxic and non-immunogenic.
- PEG has a flexible, highly water-soluble chain that extends to give a hydrodynamic radius some 5–10 times greater than that of a globular protein of equivalent molecular weight. Its high degree of hydration means the polymer chain effectively has a 'water shell', and this helps to mask the protein to which it is bound.
- PEG can be prepared with a single reactive group at one terminal end, and this aids site-specific conjugation to a protein and avoids protein crosslinking during conjugation.

Although first generation protein conjugates were synthesized using linear monomethoxyPEGs (molecular weight (Mw) of ~5,000 g mol^{-1}), with many polymer chains randomly attached to each protein molecule, various sophisticated conjugation chemistries have now emerged that use linear or branched PEGs of Mw ~5,000–40,000 g mol^{-1}. Several techniques, most recently including phage display, enable site-specific peptide and protein modification. The specific linking chemistries and synthetic strategies being used are described in more detail elsewhere[29,30,44,45].

Box 2 | **Rationale for the design of polymer–drug conjugates**

Ringsdorf's vision of the idealized polymer chemistry for drug conjugation[67] and Trouet and De Duve's realization that the endocytic pathway might be useful for lysosomotropic drug delivery[156] led to the concept of targetable anticancer polymer–drug conjugates. Low-molecular-weight anticancer agents typically distribute randomly throughout the body, and this often leads to side effects. The attachment of drugs to polymeric carriers can:

- Limit cellular uptake to the endocytic route.
- Produce long-circulating conjugates. Most of the dose of low-molecular-weight drug typically leaves the circulation within minutes, whereas a polymer conjugate will ideally circulate for several hours to facilitate passive tumour targeting caused by the leakiness of angiogenic tumour blood vessels by the enhanced permeability and retention effect (EPR effect)[39]. Conjugates have also been synthesized to contain targeting ligands (such as antibodies, peptides and sugars) with the aim of further promoting increased (building on the EPR effect) tumour targeting by receptor-mediated delivery[26,28].

Several features are needed for the effective design of polymer–drug conjugates:

- The polymer must be non-toxic and non-immunogenic. It must also be suitable for industrial-scale manufacture. Polymer molecular weight should be high enough to ensure long circulation, but for non-biodegradable polymeric carriers this molecular weight (Mw) must be less than 40,000 g mol^{-1} to enable the renal elimination of the carrier following drug delivery. Therefore, the optimum (usually Mw 30,000–100,000 g mol^{-1}) must be tailored to suit the particular polymer being used.
- The poymer must be able to carry an adequate drug payload in relation to its potency.
- The polymer–drug linker must be stable during transport to the tumour, but able to release the drug at an optimum rate on arrival within tumour cells.
- If the drug exerts its effects through an intracellular pharmacological receptor, access to the correct intracellular compartment is essential. Peptidyl and ester polymer–drug linkers have been widely used. In particular, peptide sequences designed for cleavage by the lysosomal thiol-dependent protease cathepsin B[81,82], but pH-sensitive *cis*-aconityl, hydrazone and acetal linkages have also been used[157]. They are hydrolysed within endosomal and lysosomal vesicles because of the local acidic pH (6.5–4.0). The ideal rate of release will vary according to the mechanism of action of the drug being delivered. Typically, conjugates containing doxorubicin linked by Gly-Phe-Leu-Gly release the drug payload over 24–48 h.
- The intracellular delivery and transfer of a drug out of the endosomal or lysosomal compartment is in many cases not only essential for therapeutic activity[158], it also provides the opportunity to bypass mechanisms of drug resistance that are reliant on membrane efflux pumps such as p-glycoprotein[159]. The limitation of polymer Mw to <100,000 g mol^{-1} ensures that the conjugate will be small enough to extravasate easily into the tumour, and will enable endocytic internalization by all types of tumour cell.

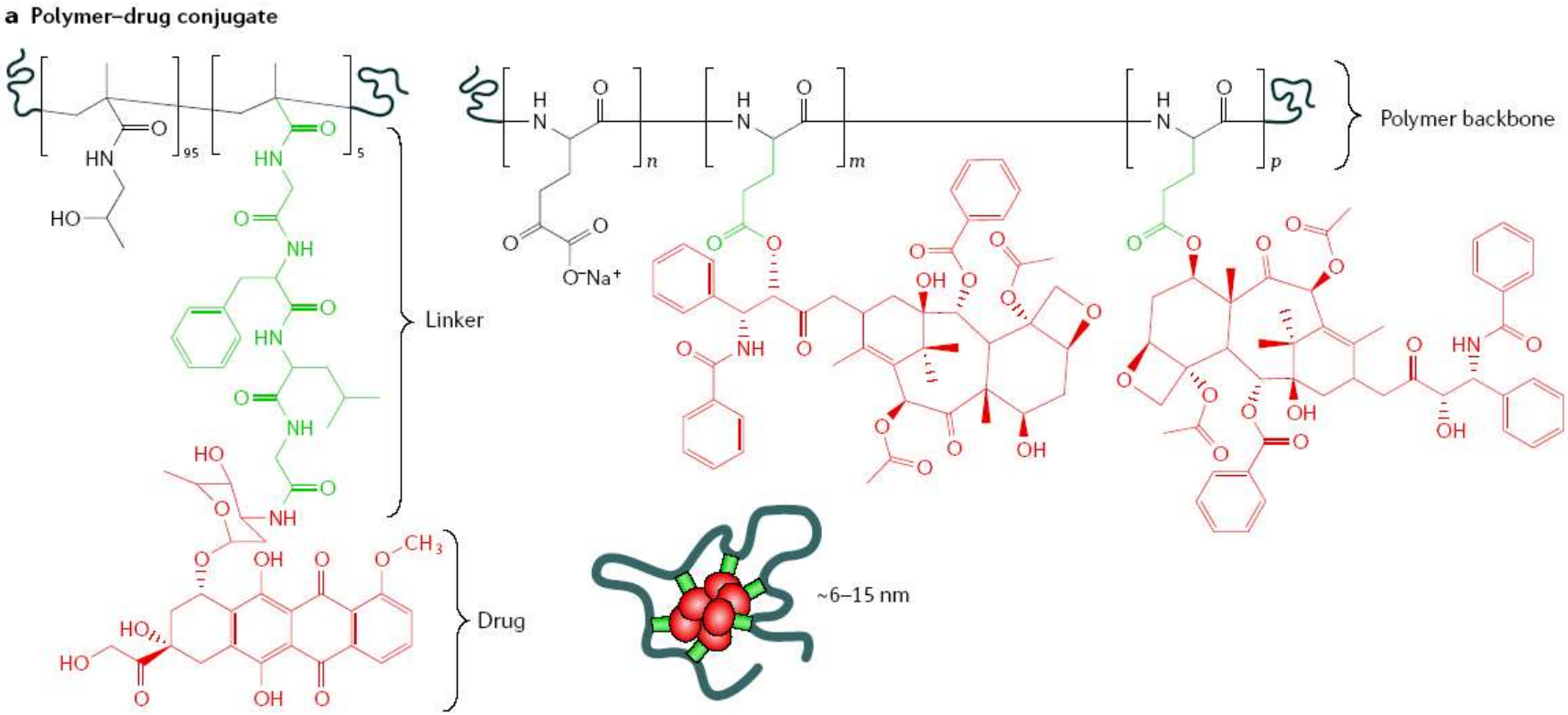
a Polymer–drug conjugate
Linker
Drug
Polymer backbone
~6–15 nm

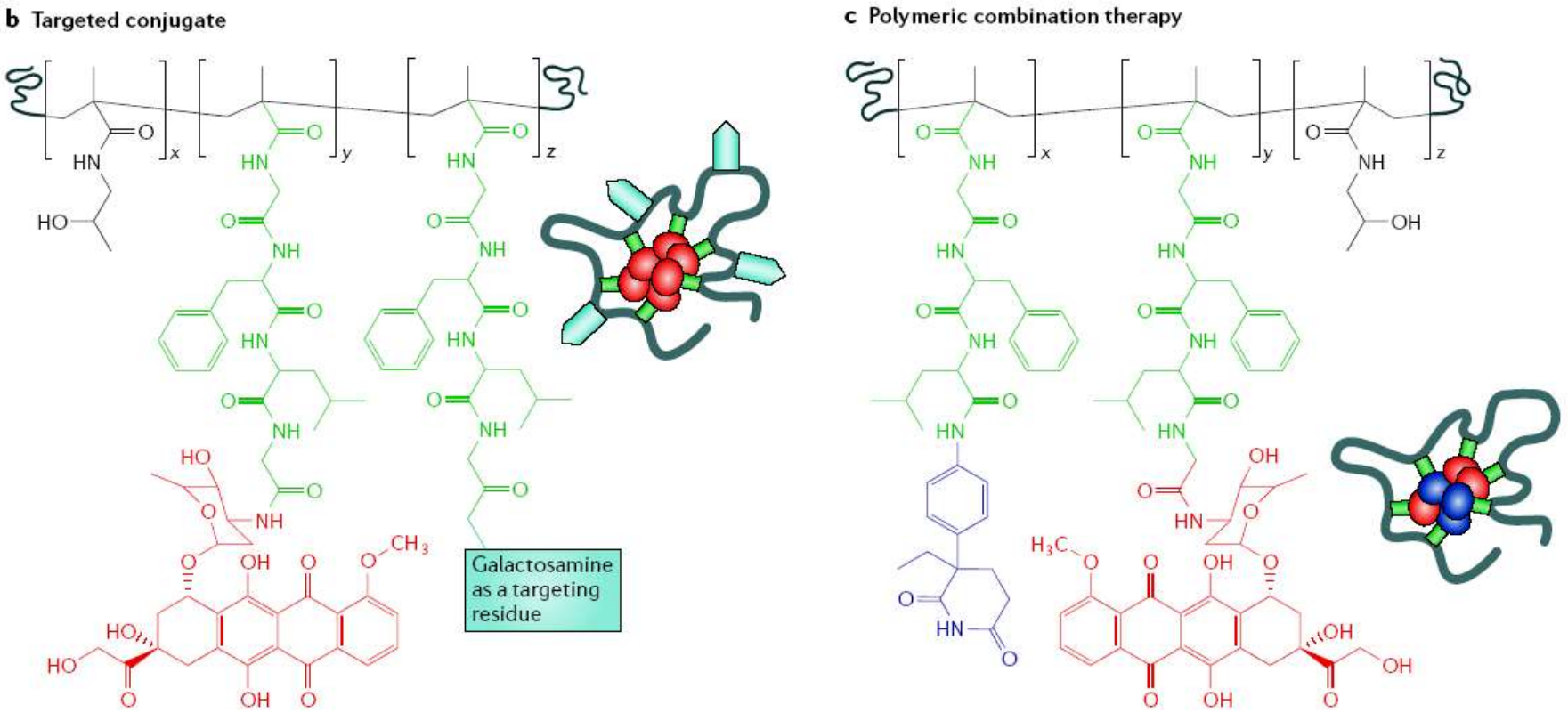

Figure 1 | **Polymer–anticancer drug conjugates.** Each panel shows both the detailed chemical structure and a cartoon of the general structure. The polymer backbone is shown in black, linker region in green, drug in red and additional components (for example, a targeting residue) in blue. **a** | Two examples of more 'simple' polymer–drug conjugates containing doxorubicin (left) and paclitaxel (right) that have progressed to clinical trial. **b** | A multivalent receptor-targeted conjugate containing galactosamine (light blue) to promote liver targeting. **c** | Polymer combination therapy containing the aromatase inhibitor aminogluthethimide (red) and doxorubicin (blue).

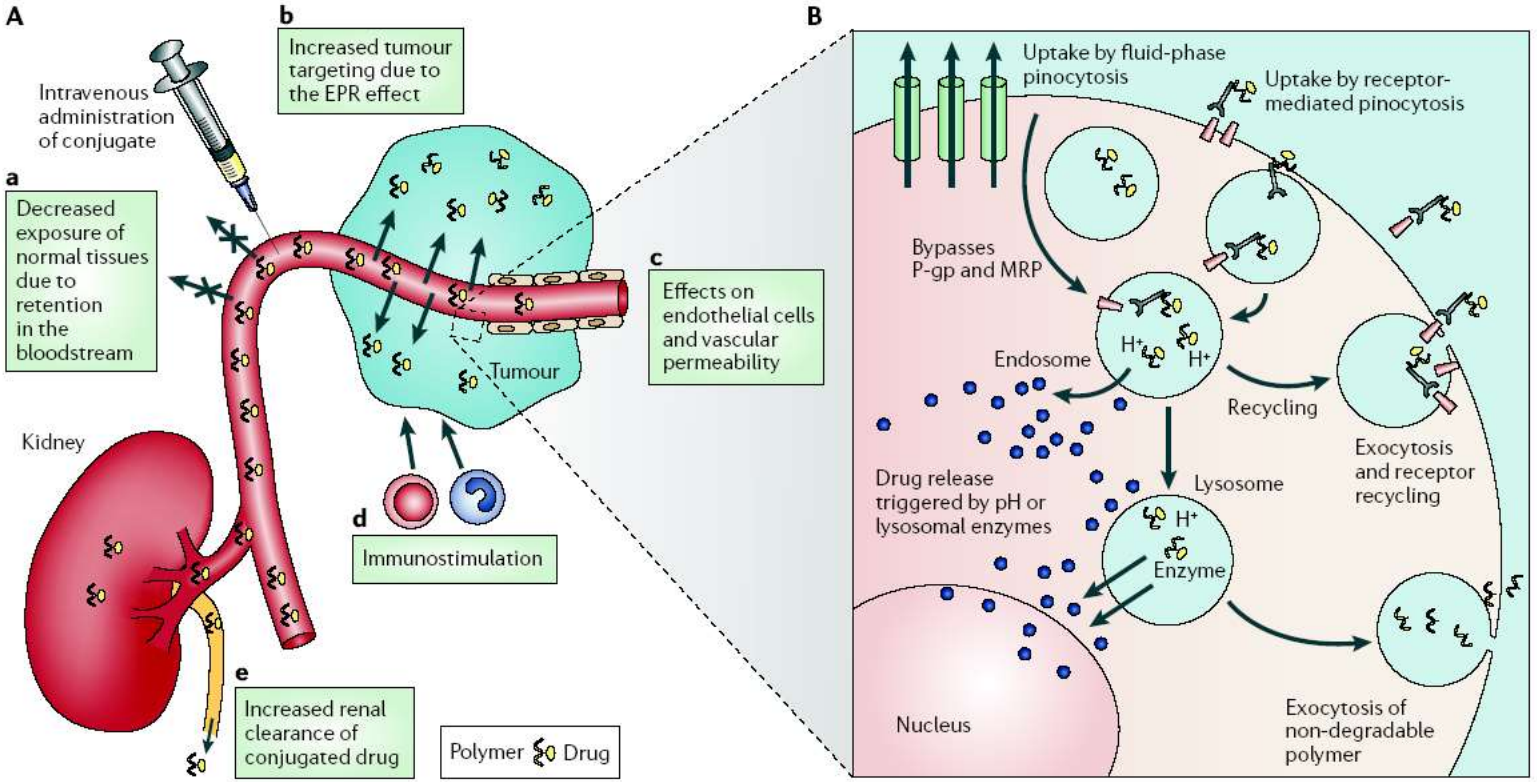

Figure 2 | **Current understanding of the mechanism of action of polymer–drug conjugates. A** | Hydrophilic polymer–drug conjugates administered intravenously can be designed to remain in the circulation — their clearance rate depends on conjugate molecular weight, which governs the rate of renal elimination. **a** | Drug that is covalently bound by a linker that is stable in the circulation is largely prevented fom accessing normal tissues (including sites of potential toxicity), and biodistribution is initially limited to the blood pool. **b** | The blood concentration of drug conjugate drives tumour targeting due to the increased permeability of angiogenic tumour vasculature (compared with normal vessels), providing the opportunity for passive targeting due to the enhanced permeability and retention effect (EPR effect). **c** | Through the incorporation of cell-specific recognition ligands it is possible to bring about the added benefit of receptor-mediated targeting of tumour cells. **d** | It has also been suggested that circulating low levels of conjugate (slow drug release) might additonally lead to immunostimulation. **e** | If the polymer–drug linker is stable in the circulation, for example, *N*-(2-hydroxypropyl)methacrylamide (HPMA) copolymer–Gly-Phe-Leu-Gly–doxorubicin, the relatively high level of renal elimination (whole body $t_{1/2}$ clearance >50% in 24 h) compared with free drug ($t_{1/2}$ clearance ~50% in 4 days) can increase the elimination rate. **B** | On arrival in the tumour interstitium, polymer-conjugated drug is internalized by tumour cells through either fluid-phase pinocytosis (in solution), receptor-mediated pinocytosis following non-specific membrane binding (due to hydrophobic or charge interactions) or ligand–receptor docking. Depending on the linkers used, the drug will usually be released intracellularly on exposure to lysosomal enzymes (for example, Gly-Phe-Leu-Gly and polyglutamic acid (PGA) are cleaved by cathepsin B) or lower pH (for example, a hydrazone linker degrades in endosomes and lysosomes (pH 6.5–<4.0). The active or passive transport of drugs such as doxorubicin and paciltaxel out of these vesicular compartments ensures exposure to their pharmacological targets. Intracellular delivery can bypass mechanisms of resistance associated with membrane efflux pumps such as p-glycoprotein. If >10-fold, EPR-mediated targeting will also enable the circumvention of other mechanisms of drug resistance. Non-biodegradable polymeric platforms must eventually be eliminated from the cell by exocytosis. Rapid exocytic elimination of the conjugated drug before release would be detrimental and prevent access to the therapeutic target. In general, polymeric carriers do not access the cytosol. MRP, multidrug resistance protein.

Dendrimer

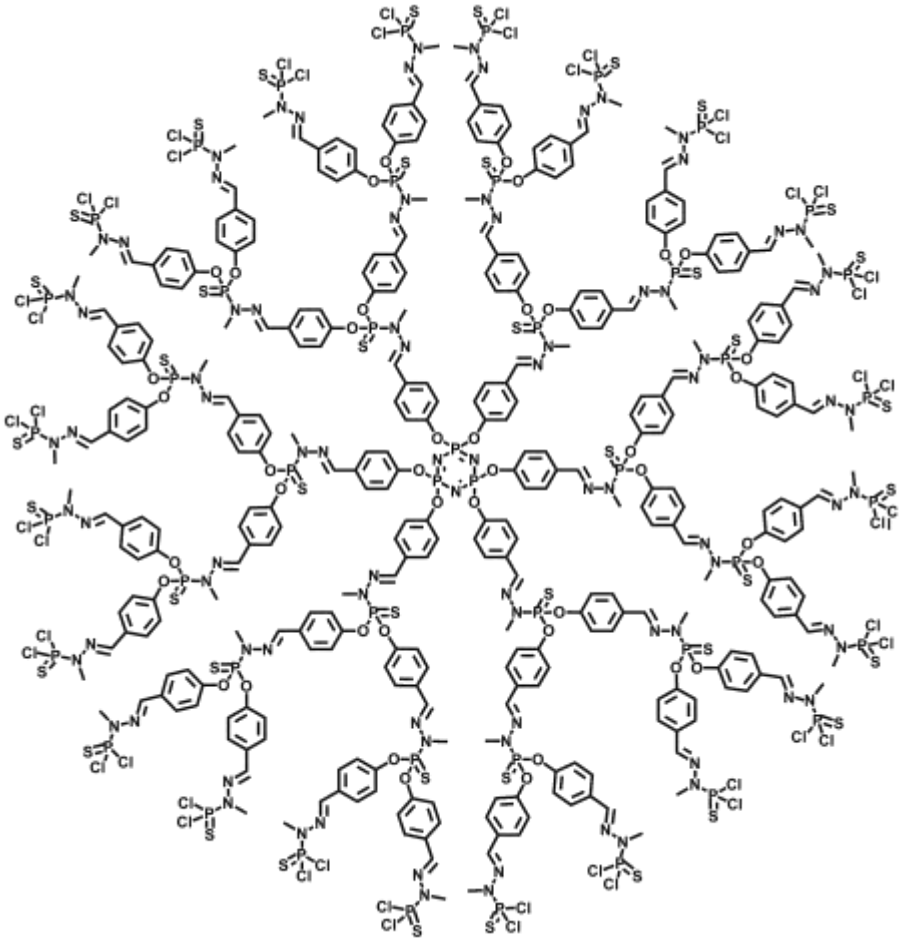

Liposome

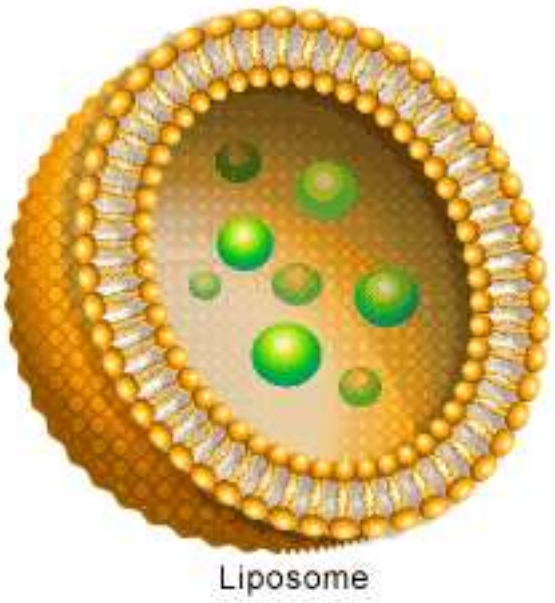

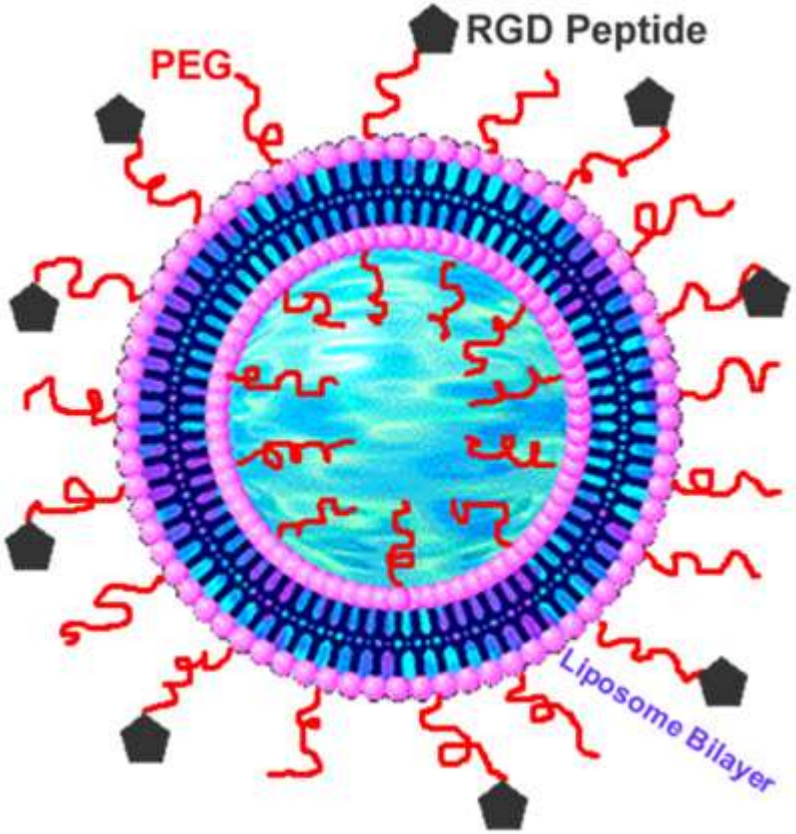

Cationic Lipids

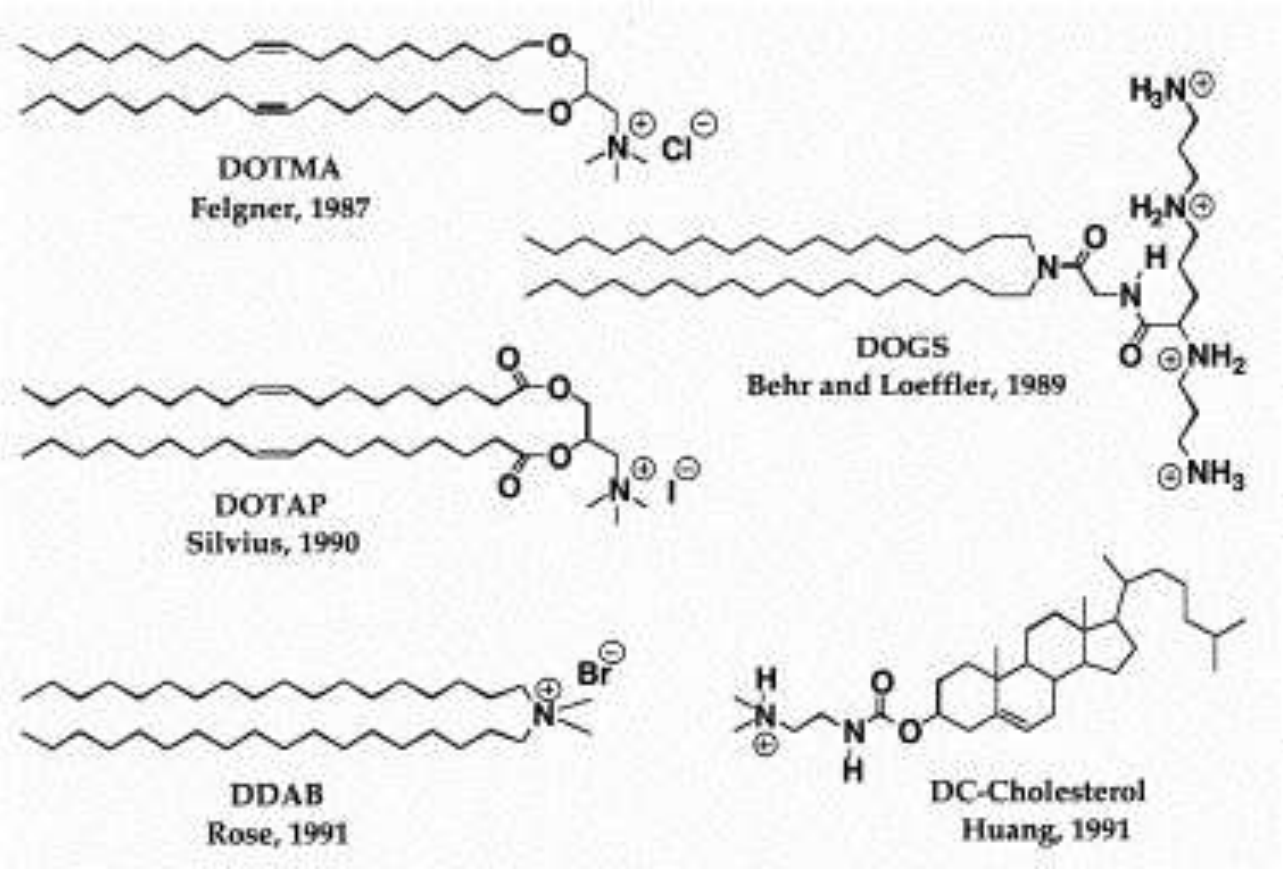

DNA Origami

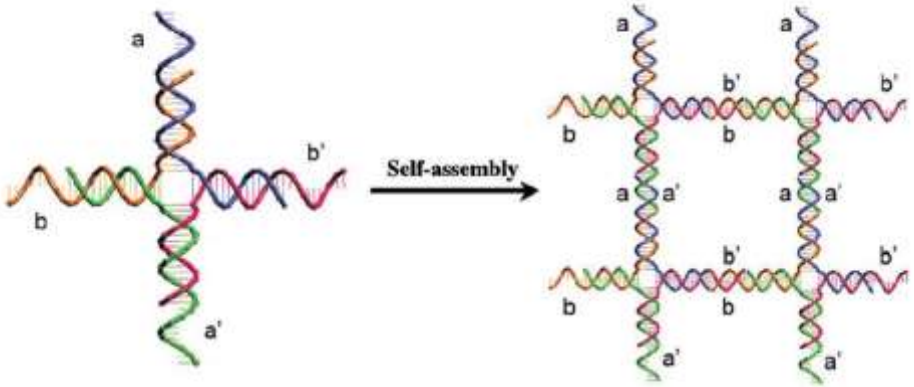

Figure 1. Key concept of DNA tile based self-assembly: combining branched DNA junction with sticky-end associations (e.g. a–a' and b–b' pairings) to self-assemble 2D lattices (adapted from ref. [1]). The DNA model was rendered using the Strata program (www.strata.com).

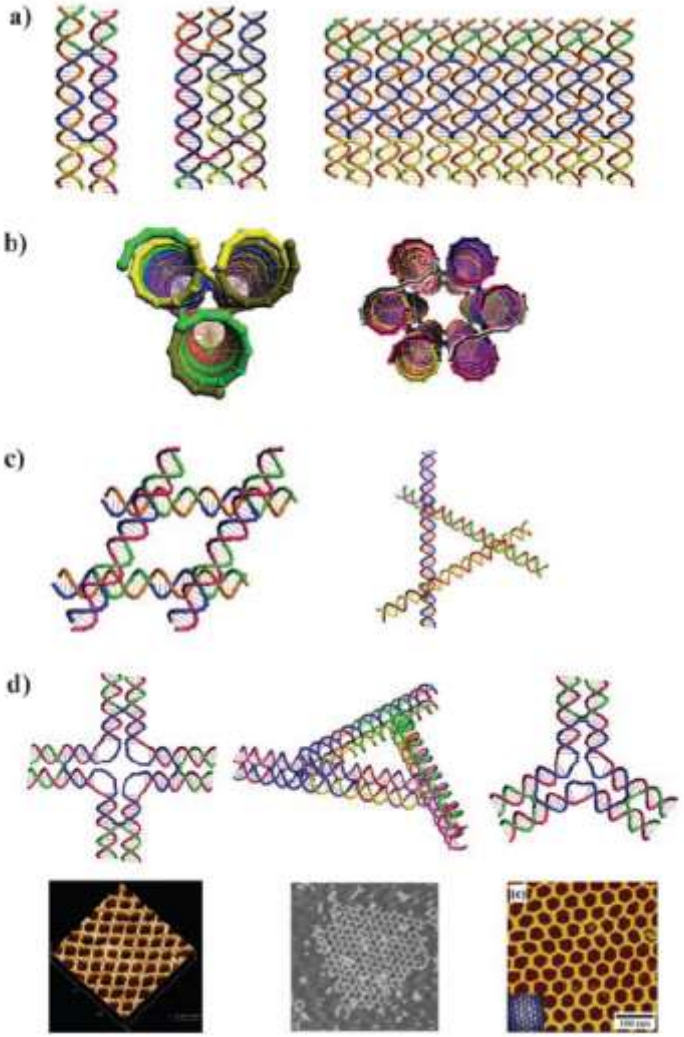

Synthesis from DNA of a molecule with the connectivity of a cube

Junghuei Chen & Nadrian C. Seeman

NATURE · VOL 350 · 18 APRIL 1991

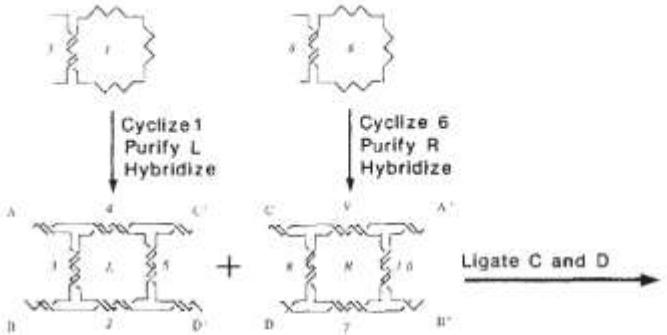

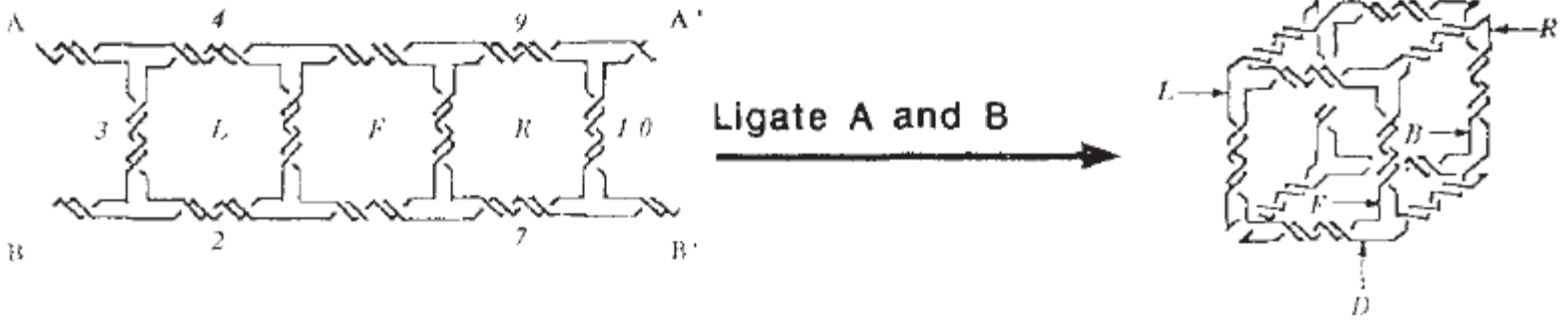

Folding DNA to create nanoscale shapes and patterns

NATURE|Vol 440|16 March 2006

Paul W. K. Rothemund[1]

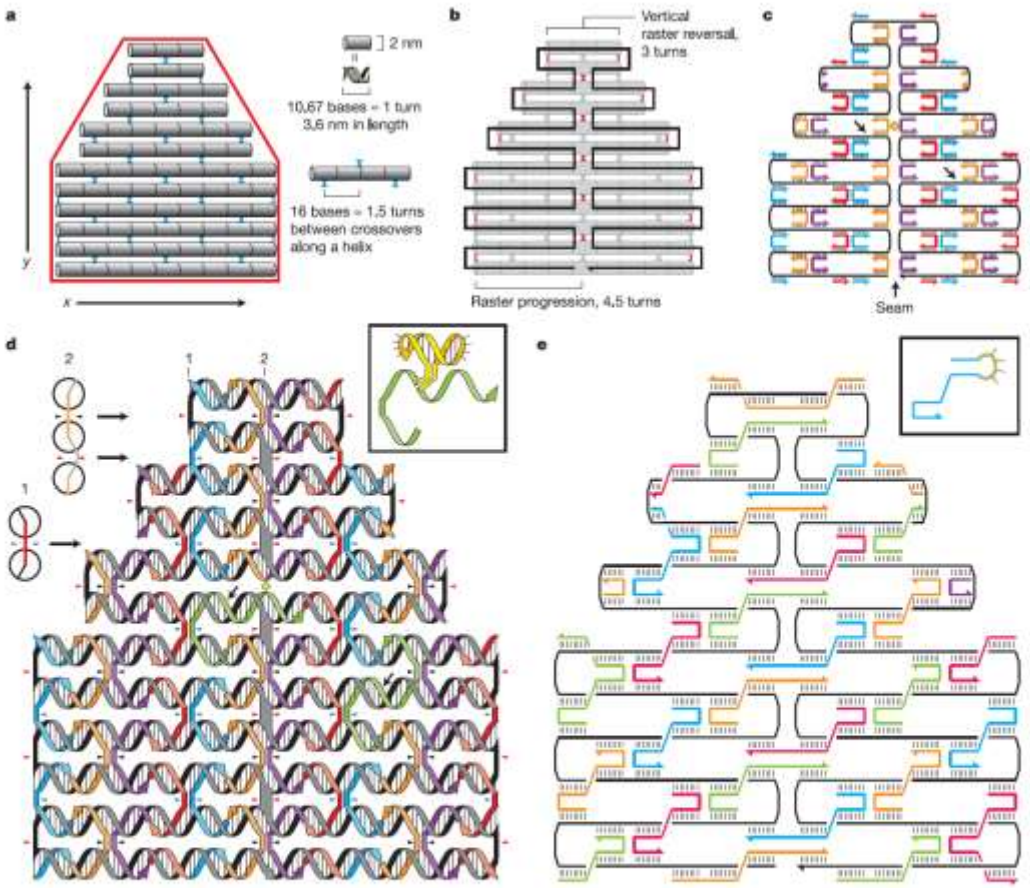

Figure 1 | Design of DNA origami. **a**, A shape (red) approximated by parallel double helices joined by periodic crossovers (blue). **b**, A scaffold (black) runs through every helix and forms more crossovers (red). **c**, As first designed, most staples bind two helices and are 16-mers. **d**, Similar to **c** with strands drawn as helices. Red triangles point to scaffold crossovers, black triangles to periodic crossovers with minor grooves on the top face of the shape, blue triangles to periodic crossovers with minor grooves on bottom. Cross-sections of crossovers (1, 2, viewed from left) indicate backbone positions with coloured lines, and major/minor grooves by large/small angles between them. Arrows in **c** point to nicks sealed to create green strands in **d**. Yellow diamonds in **c** and **d** indicate a position at which staples may be cut and resealed to bridge the seam. **e**, A finished design after merges and rearrangements along the seam. Most staples are 32-mers spanning three helices. Insets show a dumbbell hairpin (**d**) and a 4-T loop (**e**), modifications used in Fig. 3.

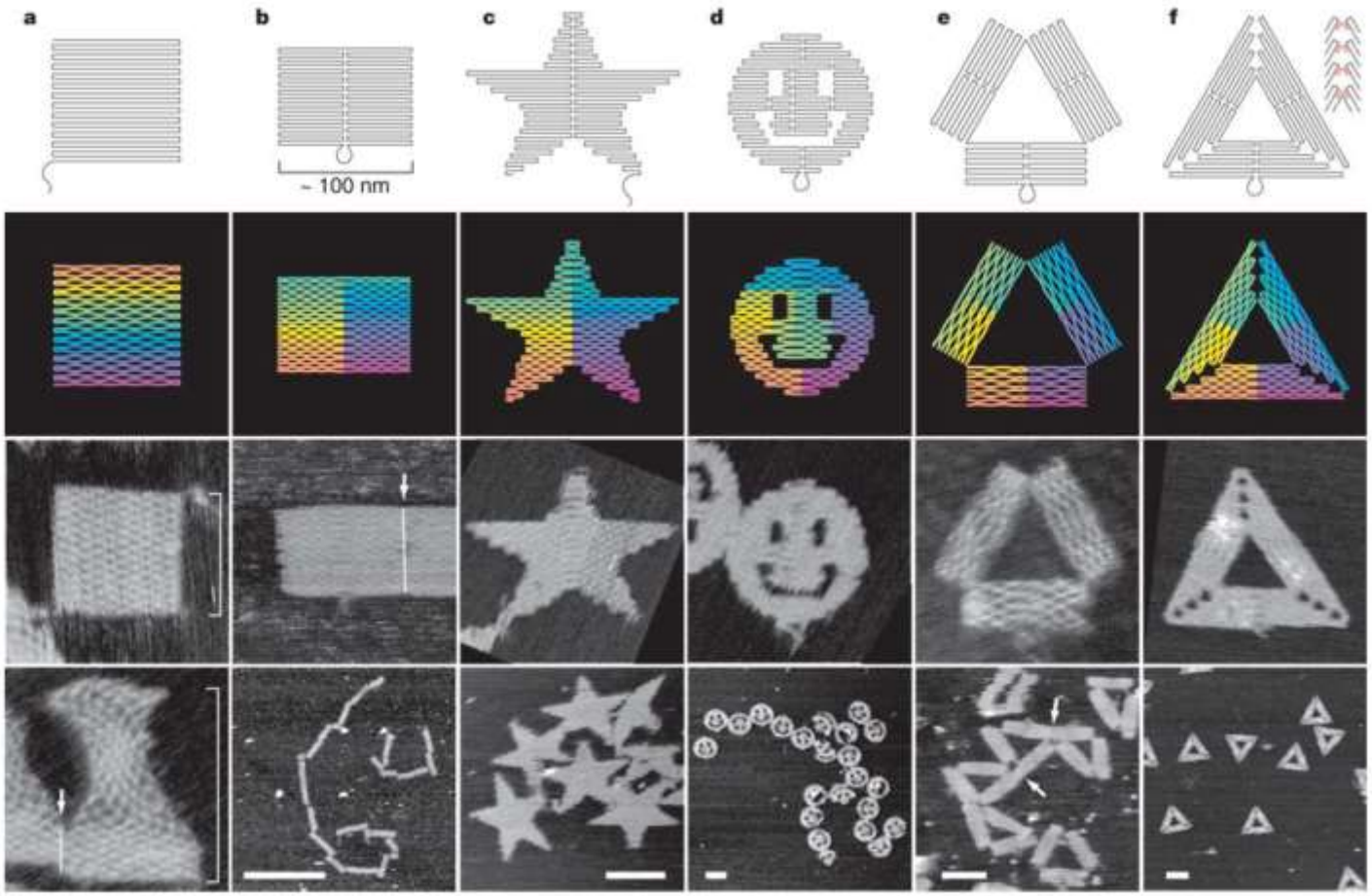
a
b
c
d
e
f
~ 100 nm

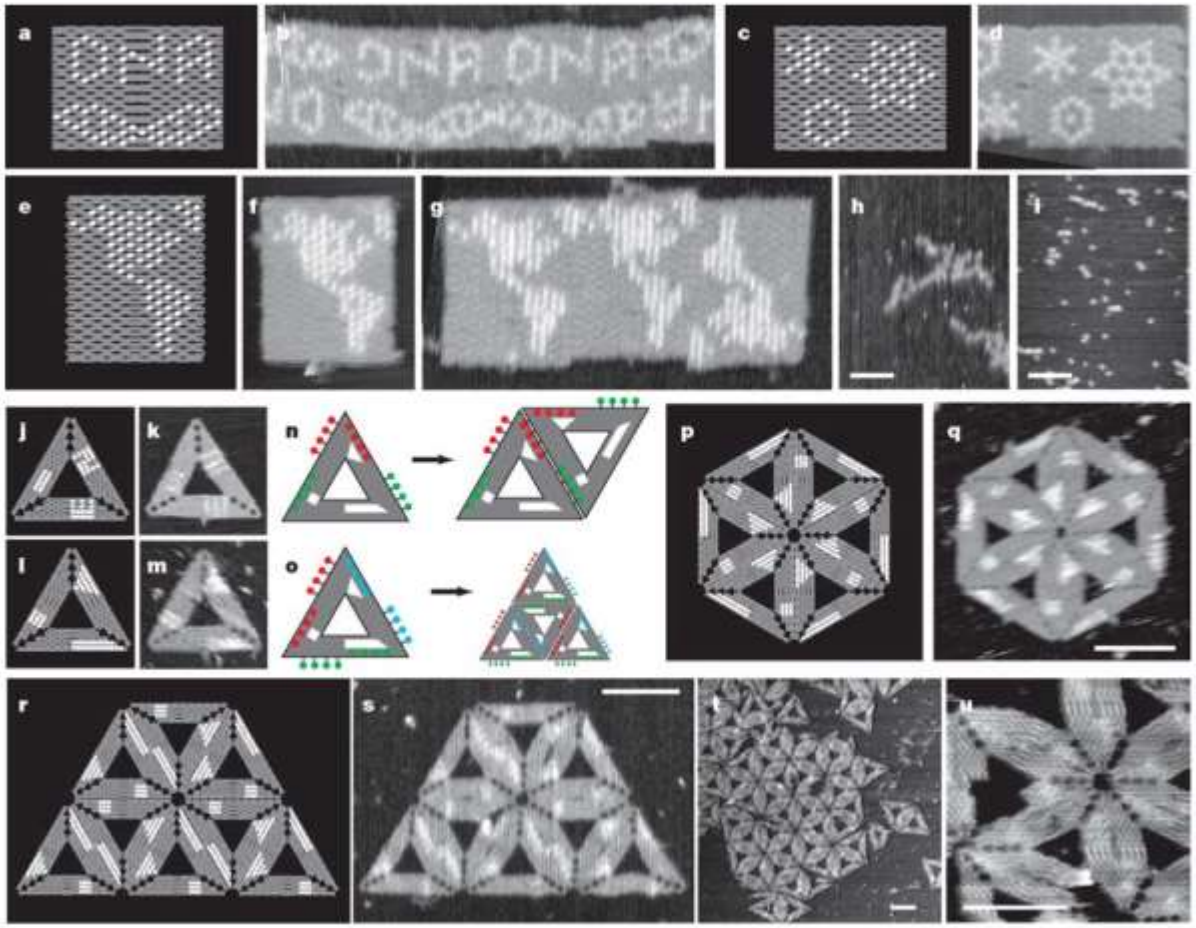
a
b
c
d
e
f
g
h
i
j
k
l
m
n
o
p
q
r
s
t
u

Rapid Folding of DNA into Nanoscale Shapes at Constant Temperature

Jean-Philippe J. Sobczak *et al.*

Science **338**, 1458 (2012);
DOI: 10.1126/science.1229919

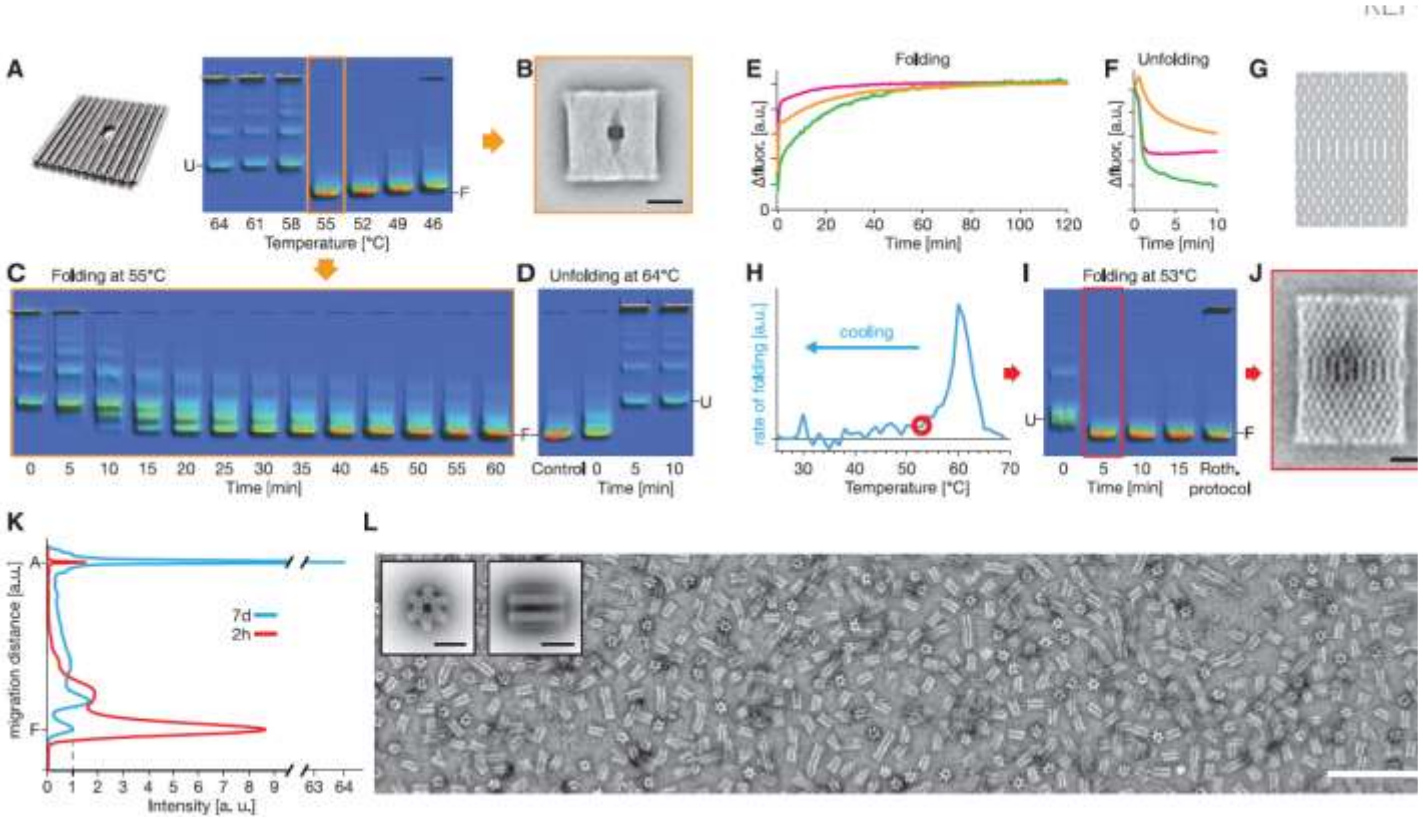

DNA Origami as a Carrier for Circumvention of Drug Resistance

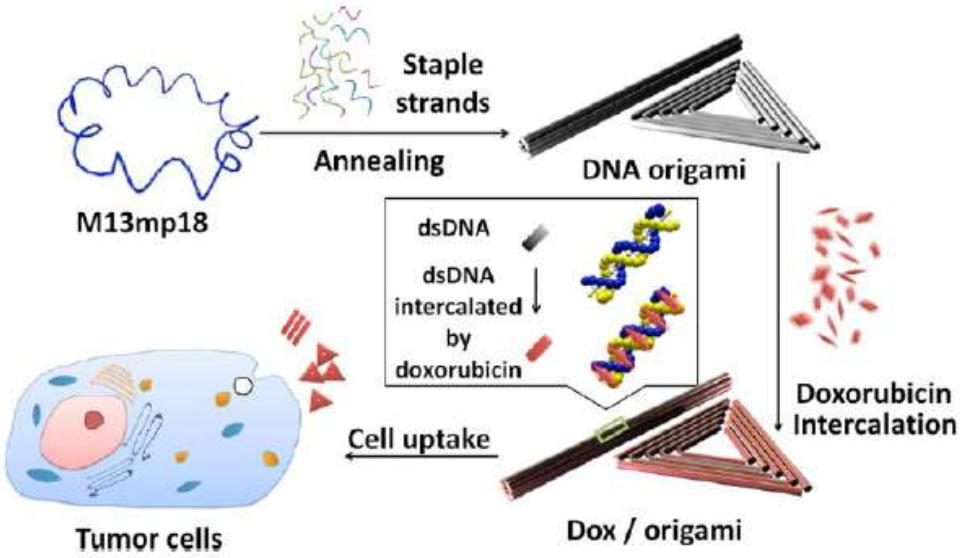

Figure 1. DNA origami and doxorubicin origami delivery system assembly. The long single-strand M13mp18 genomic DNA scaffold strand (blue) is folded into the triangle and tube structures through the hybridization of rationally designed staple strands. Watson–Crick base pairs in the double helices serve as docking sites for doxorubicin intercalation. After incubation with doxorubicin, the drug-loaded DNA nanostructure delivery vessels were administered to MCF 7 cells, and the effects were investigated.

dx.doi.org/10.1021/ja304263n | *J. Am. Chem. Soc.* 2012, 134, 13396–13403

Construction of a 4 Zeptoliters Switchable 3D DNA Box Origami

ABSTRACT The DNA origami technique is a recently developed self-assembly method that allows construction of 3D objects at the nanoscale for various applications. In the current study we report the production of a 18 × 18 × 24 nm^3 hollow DNA box origami structure with a switchable lid. The structure was efficiently produced and characterized by atomic force microscopy, transmission electron microscopy, and Förster resonance energy transfer spectroscopy. The DNA box has a unique reclosing mechanism, which enables it to repeatedly open and close in response to a unique set of DNA keys. This DNA device can potentially be used for a broad range of applications such as controlling the function of single molecules, controlled drug delivery, and molecular computing.

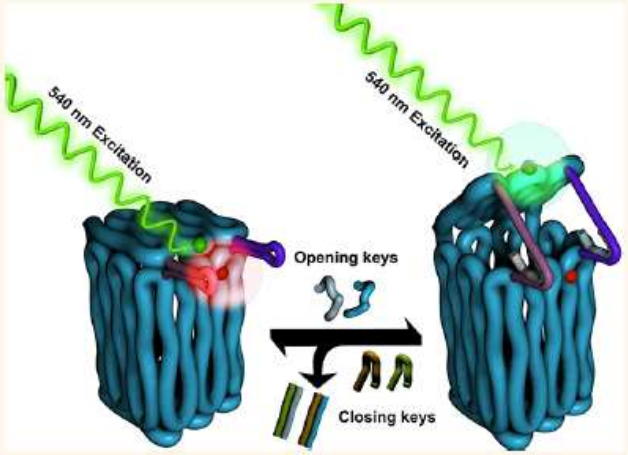

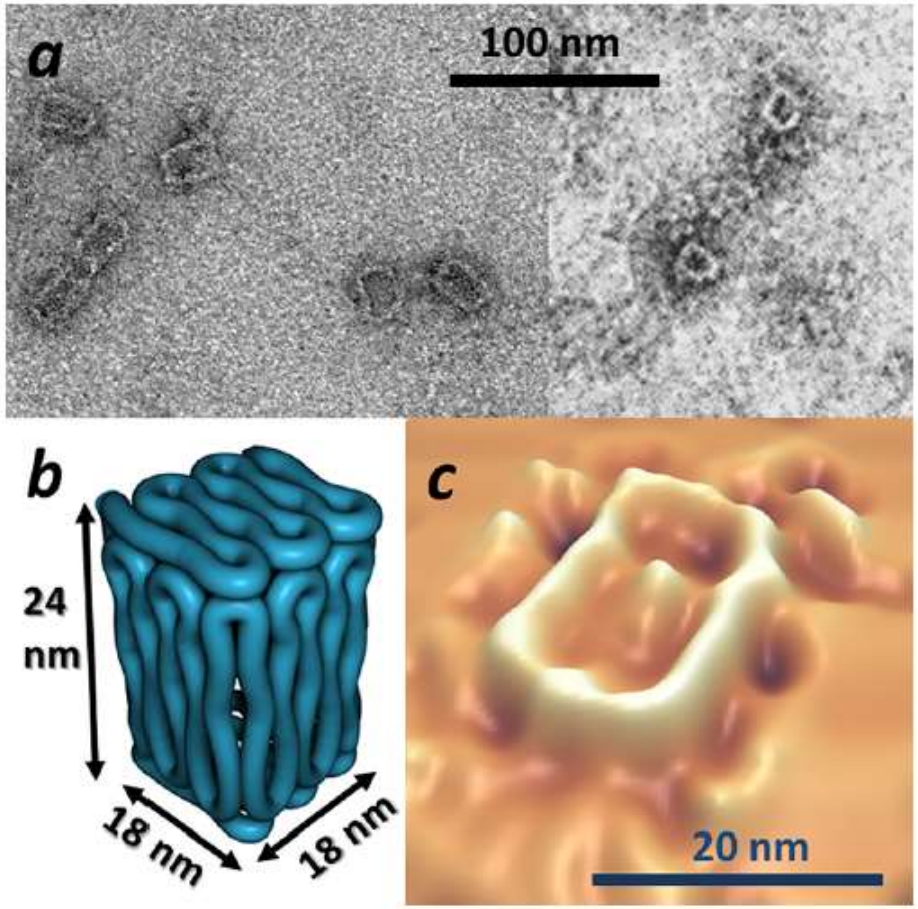
a
100 nm
b
24
nm
18 nm
18 nm
c
20 nm

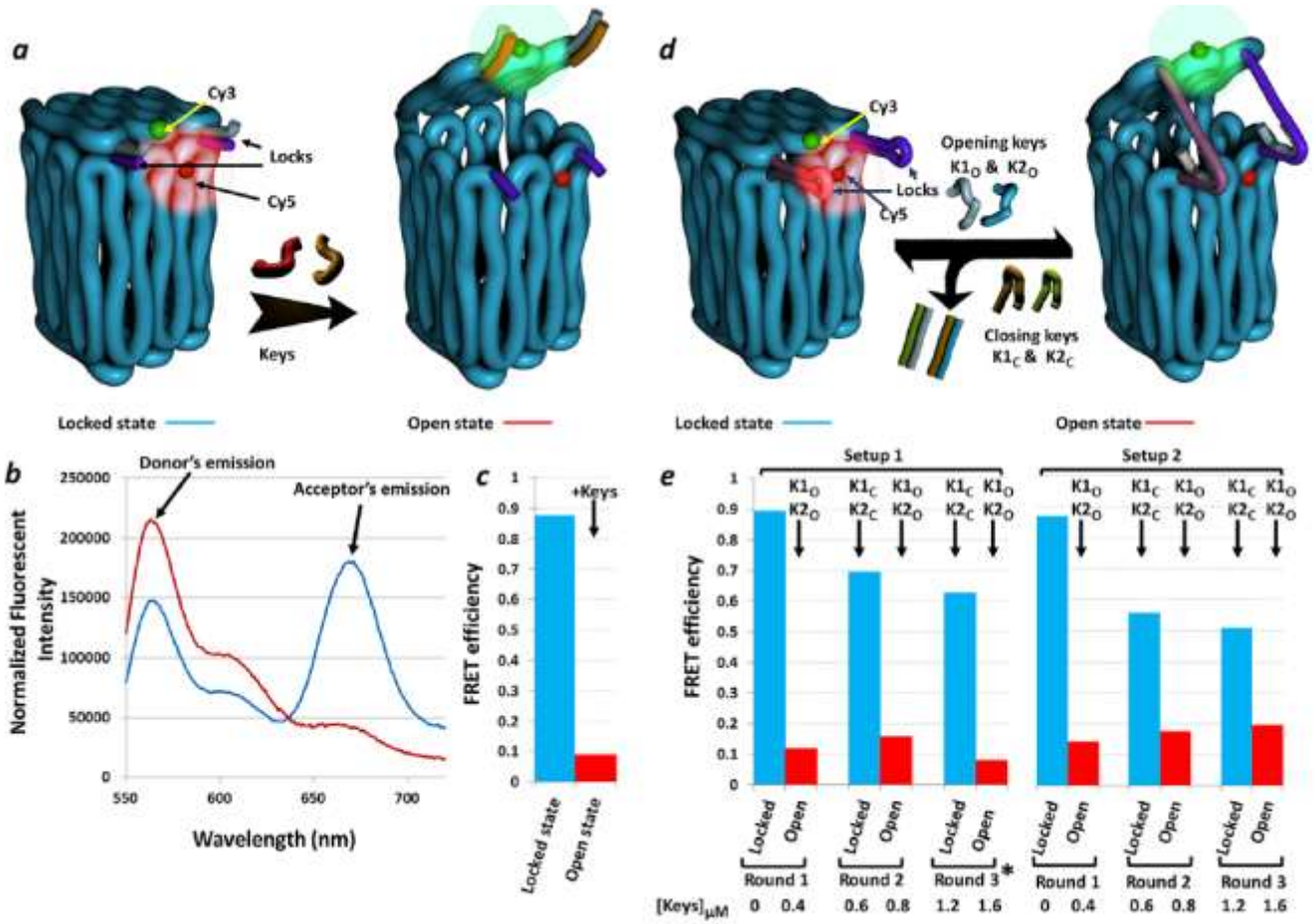
a
Cy3
Locks
Cy5
Keys
Locked state
Open state
d
Cy3
Locks
Cy5
Opening keys
K1O & K2O
Closing keys
K1C & K2C
Locked state
Open state
b
Donor's emission
Acceptor's emission
Normalized Fluorescent Intensity
250000
200000
150000
100000
50000
0
550
600
650
700
Wavelength (nm)
c
+Keys
FRET efficiency
1
0.9
0.8
0.7
0.6
0.5
0.4
0.3
0.2
0.1
0
Locked state
Open state
e
Setup 1
Setup 2
K1O K2O
K1C K2C
K1O K2O
K1C K2C
K1O K2O
K1C K2C
K1O K2O
FRET efficiency
Locked
Open
Round 1
Round 2
Round 3
*
[Keys]μM
0 0.4 0.6 0.8 1.2 1.6
0 0.4 0.6 0.8 1.2 1.6

A Logic-Gated Nanorobot for Targeted Transport of Molecular Payloads

Shawn M. Douglas,* Ido Bachelet,* George M. Church†

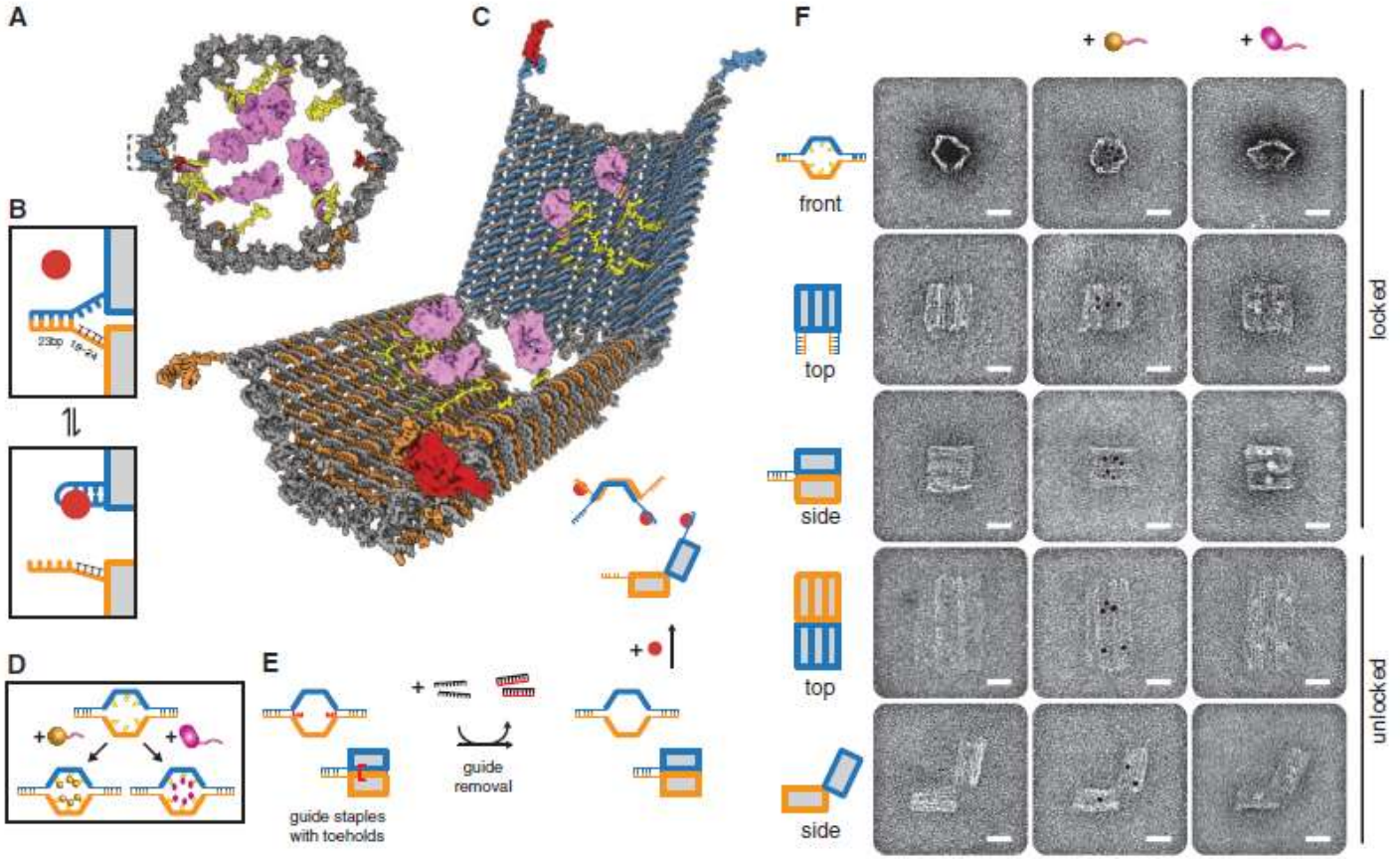

Nanoparticle-mediated cellular response is size-dependent

nature nanotechnology | VOL 3 | MARCH 2008 |

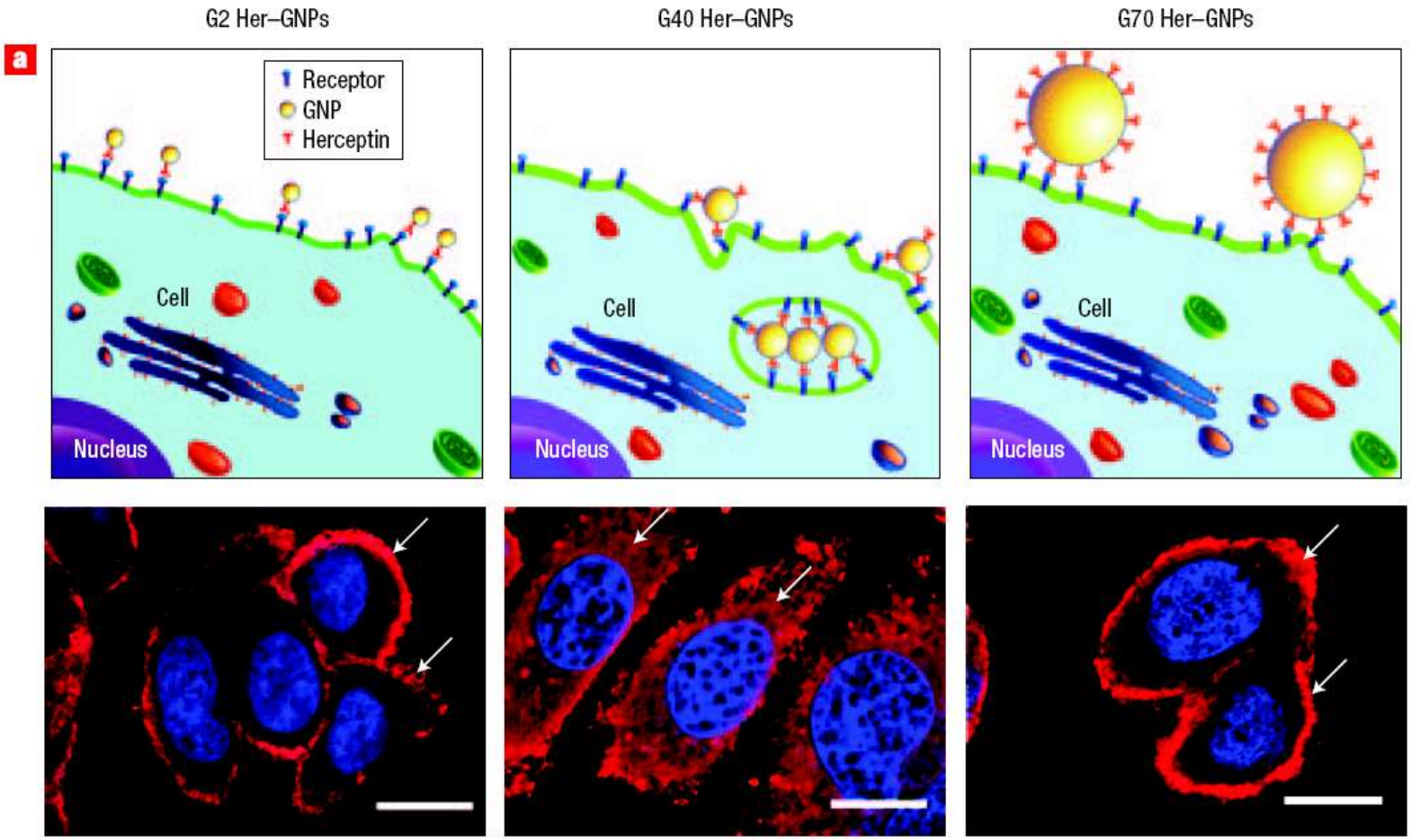

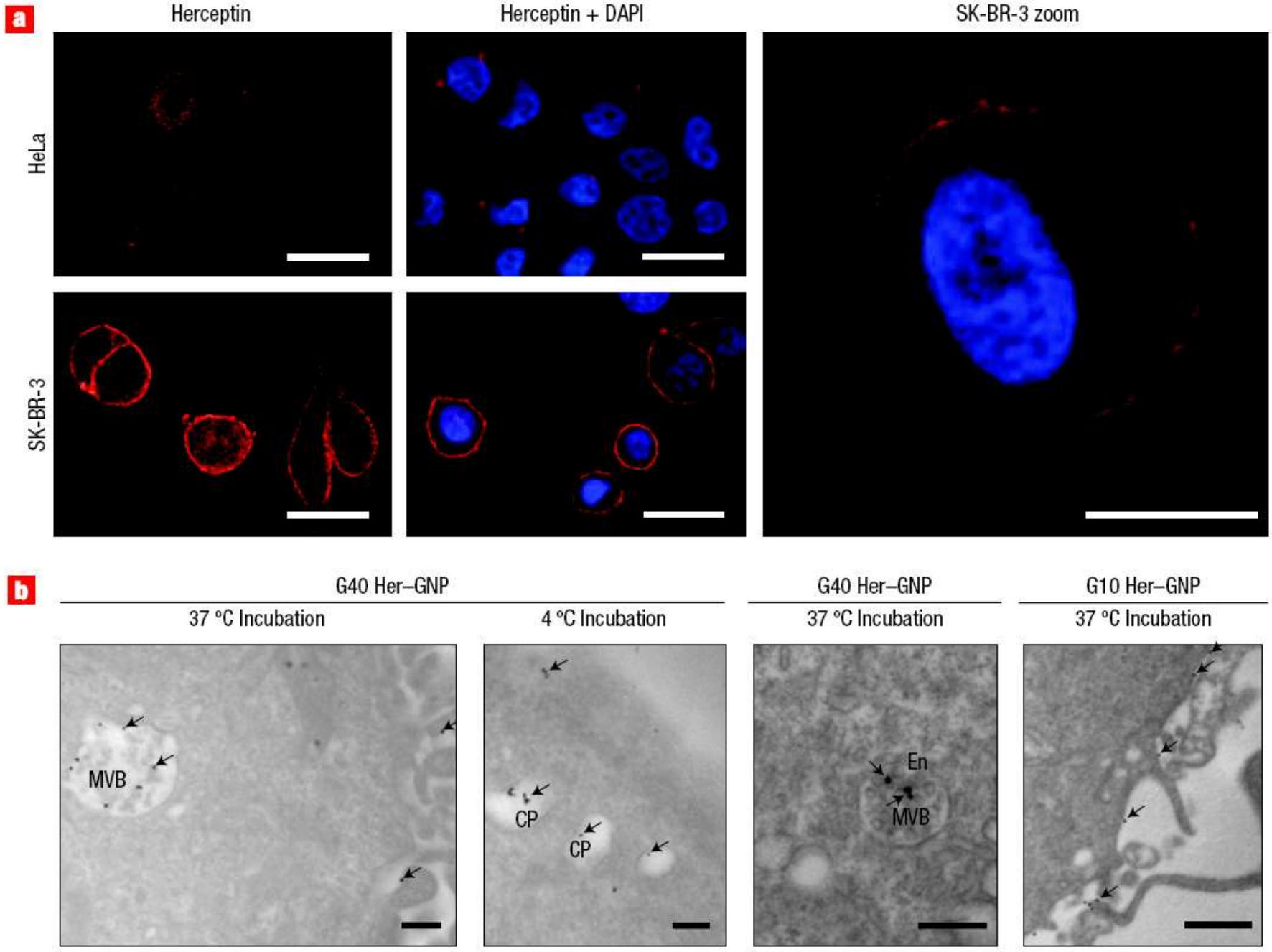
a
Herceptin
Herceptin + DAPI
SK-BR-3 zoom
HeLa
SK-BR-3
b
G40 Her–GNP
37 °C Incubation
4 °C Incubation
G40 Her–GNP
37 °C Incubation
G10 Her–GNP
37 °C Incubation
MVB
CP
CP
En
MVB

Immune Cells

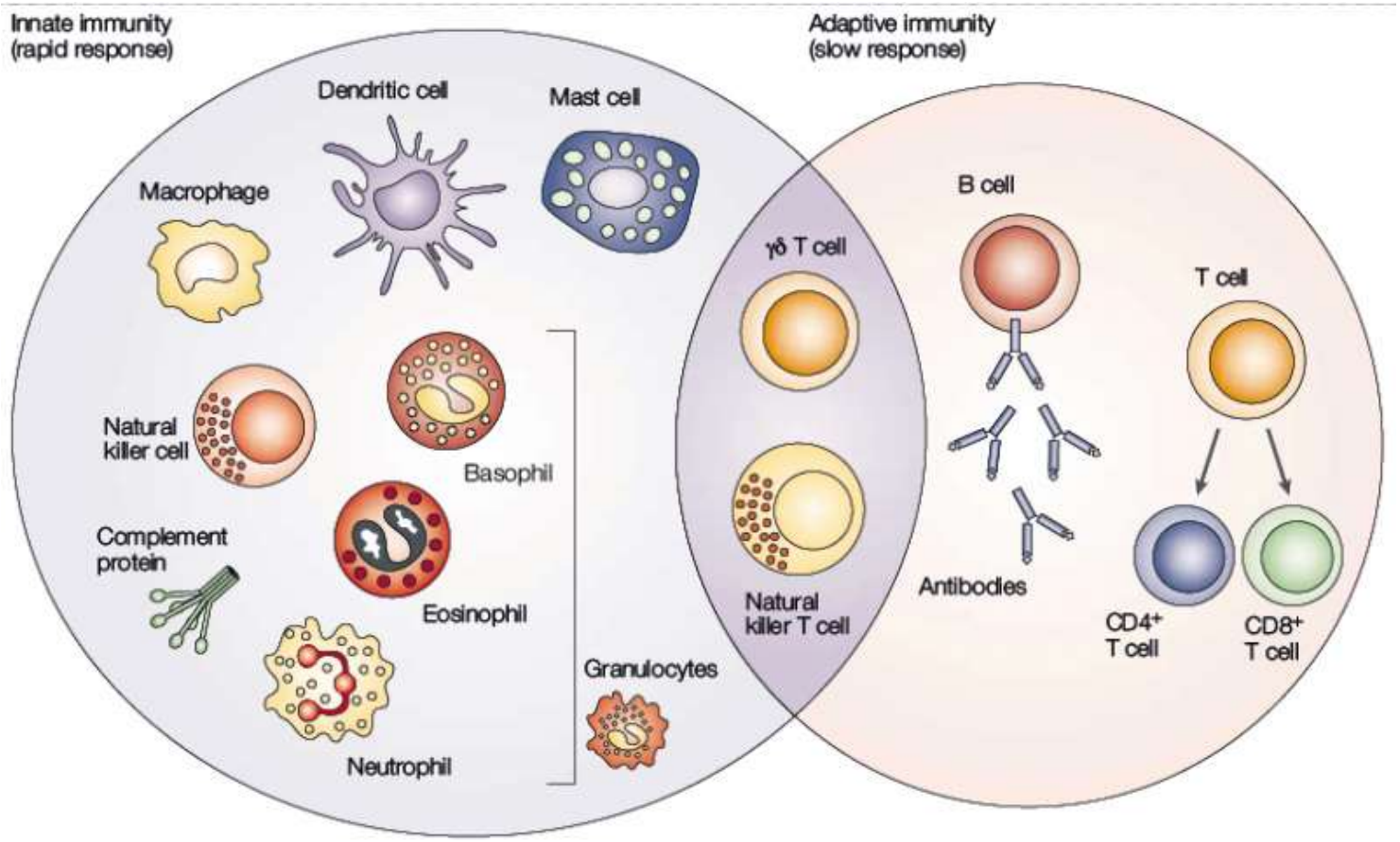

APC

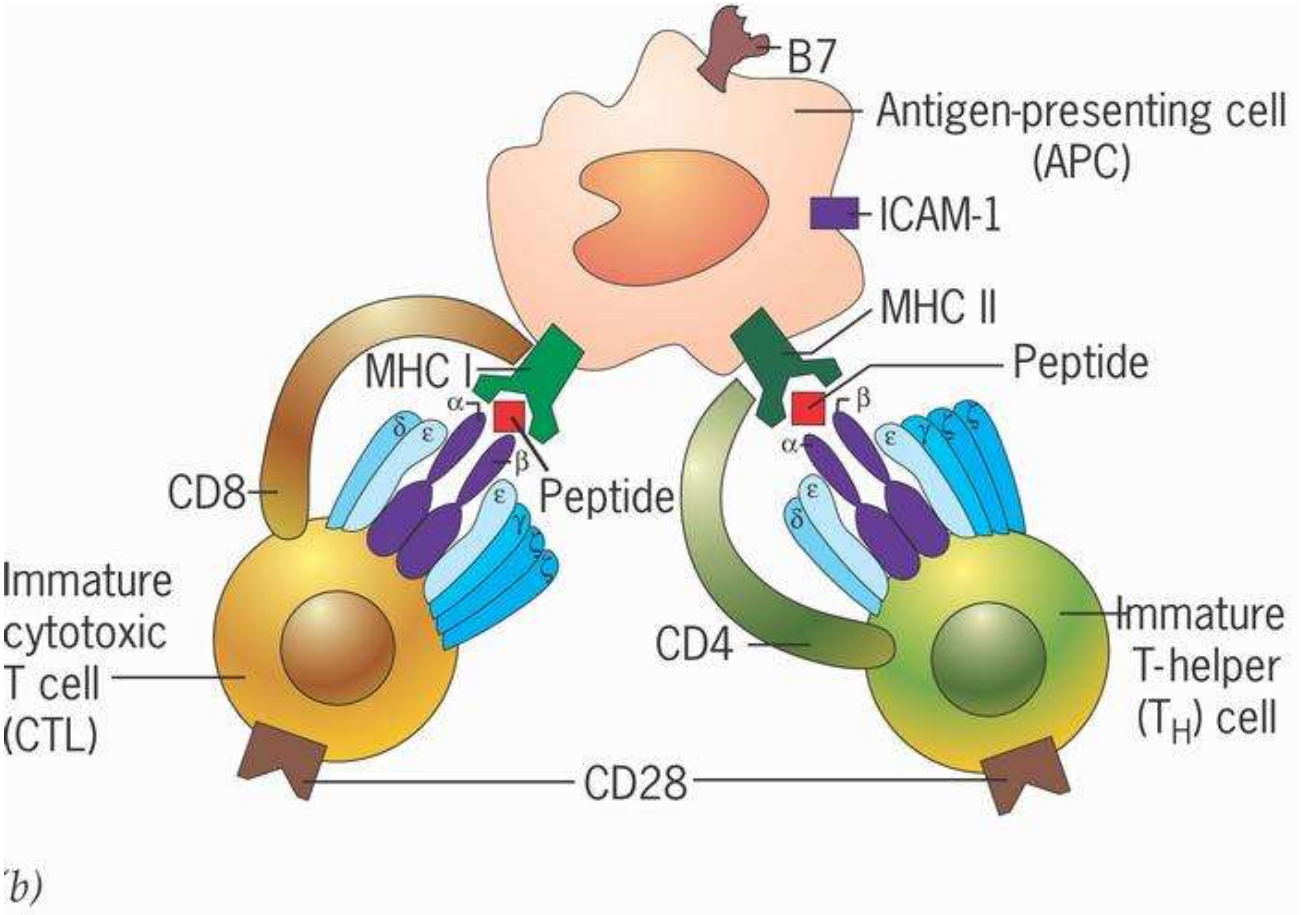
B7
Antigen-presenting cell
(APC)
ICAM-1
MHC II
Peptide
MHC I
α
β
δ
ε
ε
γ
ζ
CD8
Peptide
Immature
cytotoxic
T cell
(CTL)
CD4
Immature
T-helper
(T_H) cell
CD28
(b)

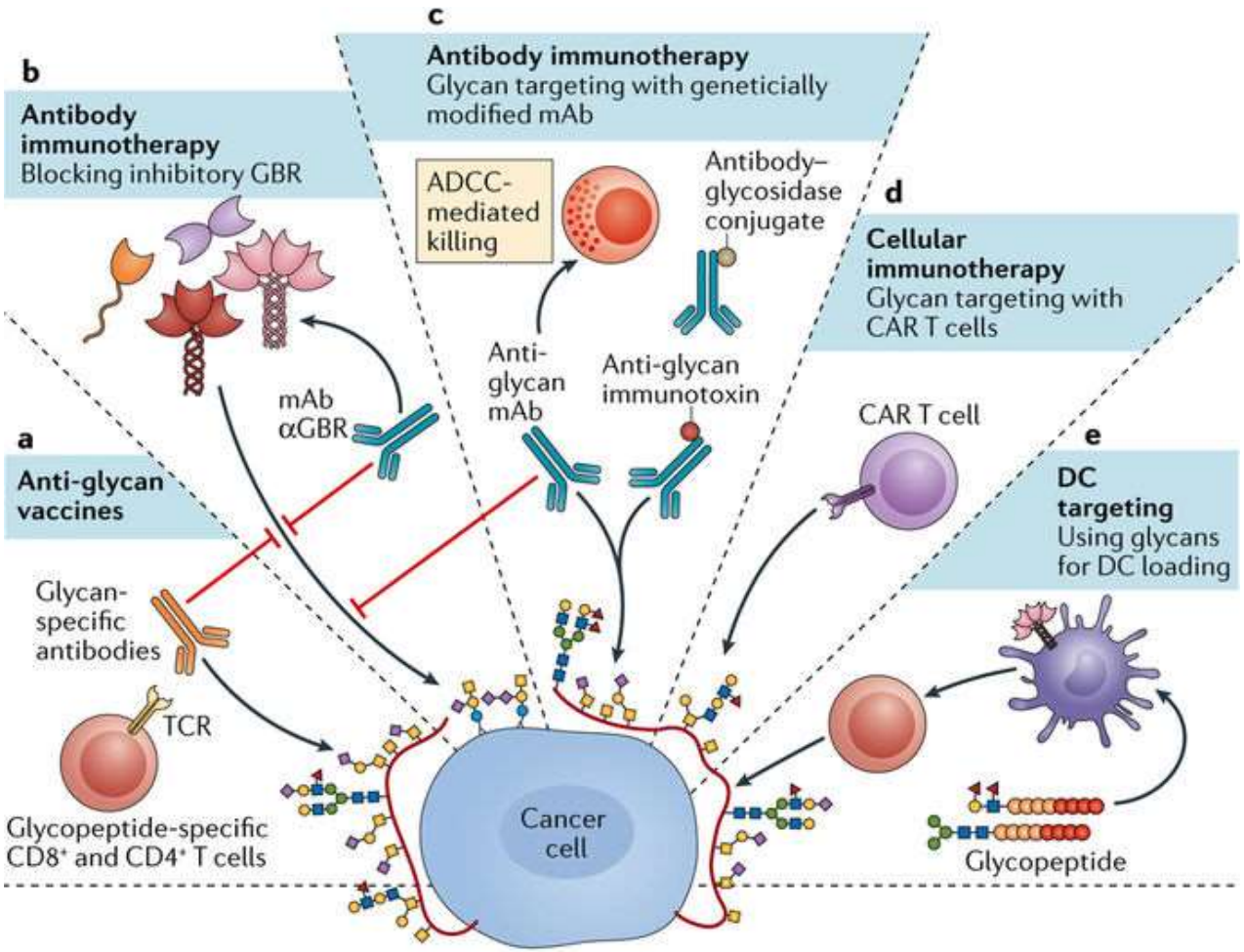
a
Anti-glycan vaccines
Glycan-specific antibodies
TCR
Glycopeptide-specific CD8+ and CD4+ T cells
b
Antibody immunotherapy
Blocking inhibitory GBR
mAb αGBR
c
Antibody immunotherapy
Glycan targeting with geneticially modified mAb
ADCC-mediated killing
Anti-glycan mAb
Antibody–glycosidase conjugate
Anti-glycan immunotoxin
d
Cellular immunotherapy
Glycan targeting with CAR T cells
CAR T cell
e
DC targeting
Using glycans for DC loading
Glycopeptide
Cancer cell

Immune Checkpoint Blockade

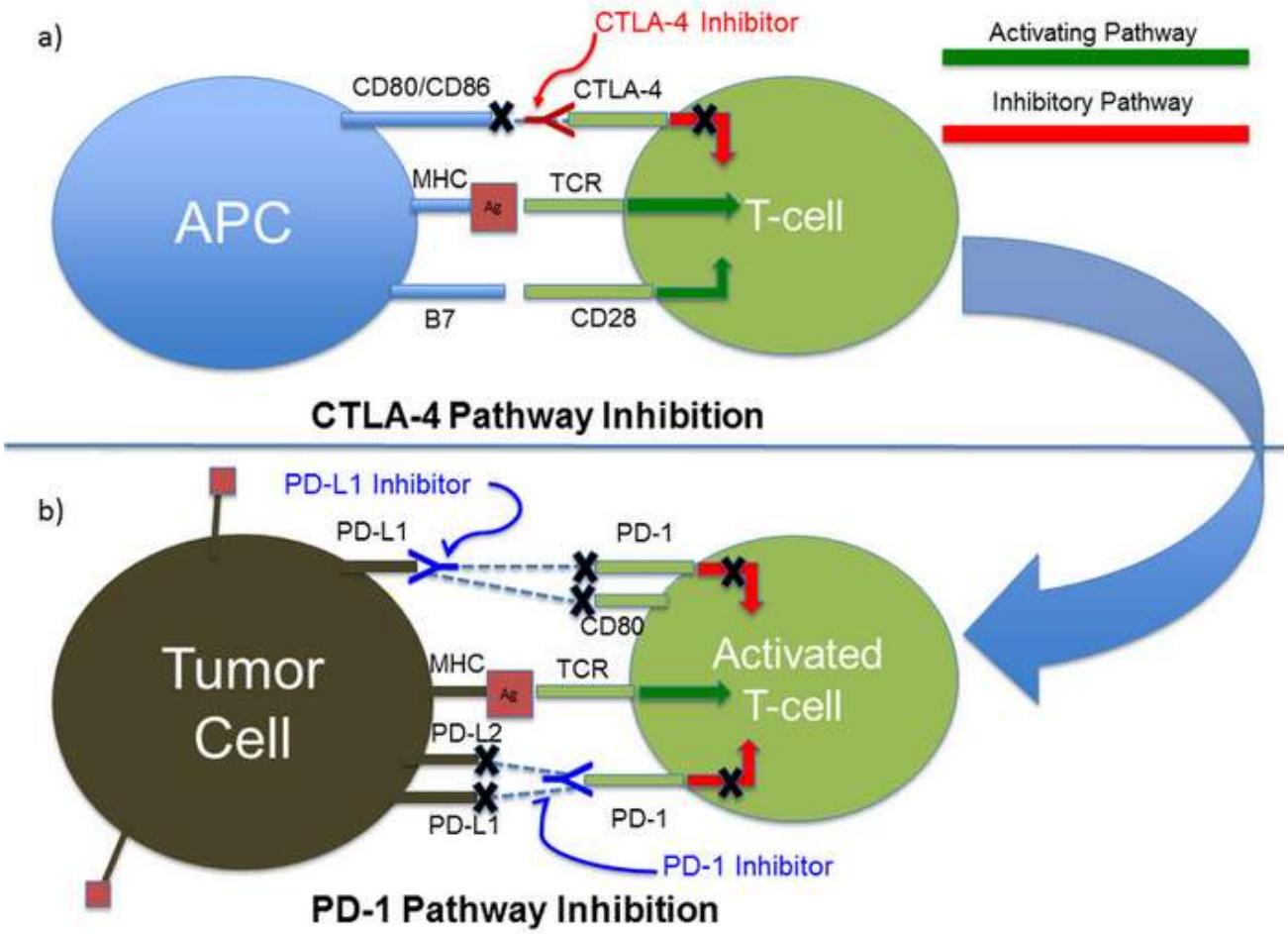

Partners in Immune System Signaling

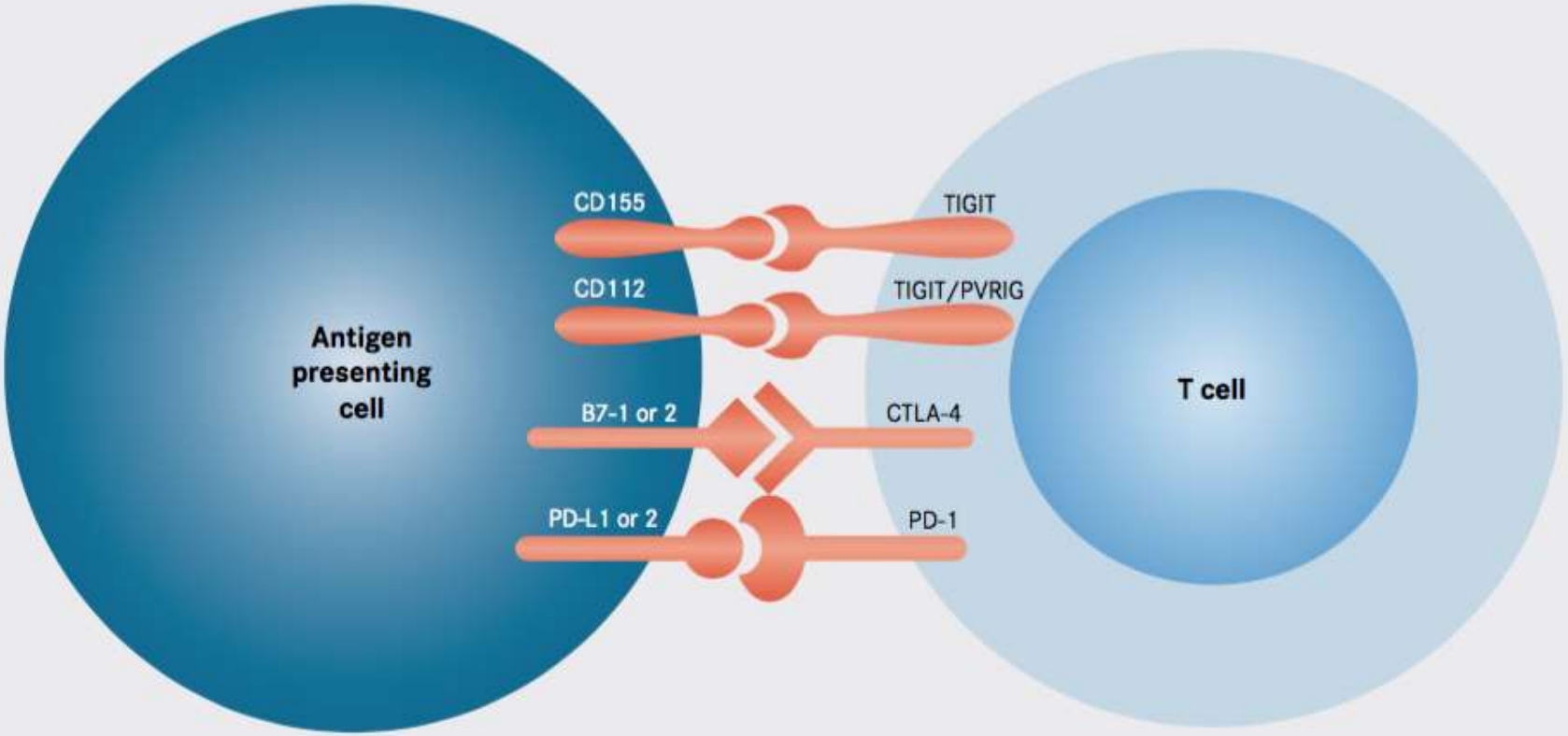

TIGIT is among the T-cell receptors that interact with proteins expressed by antigen presenting cells to send inhibitory signals to the immune system. Dysregulated interaction between TIGIT and its ligands serves to suppress immunity when under attack from cancer cells, similar to the activity of the PD-1 and CTLA-4 pathways.

Overall Survival

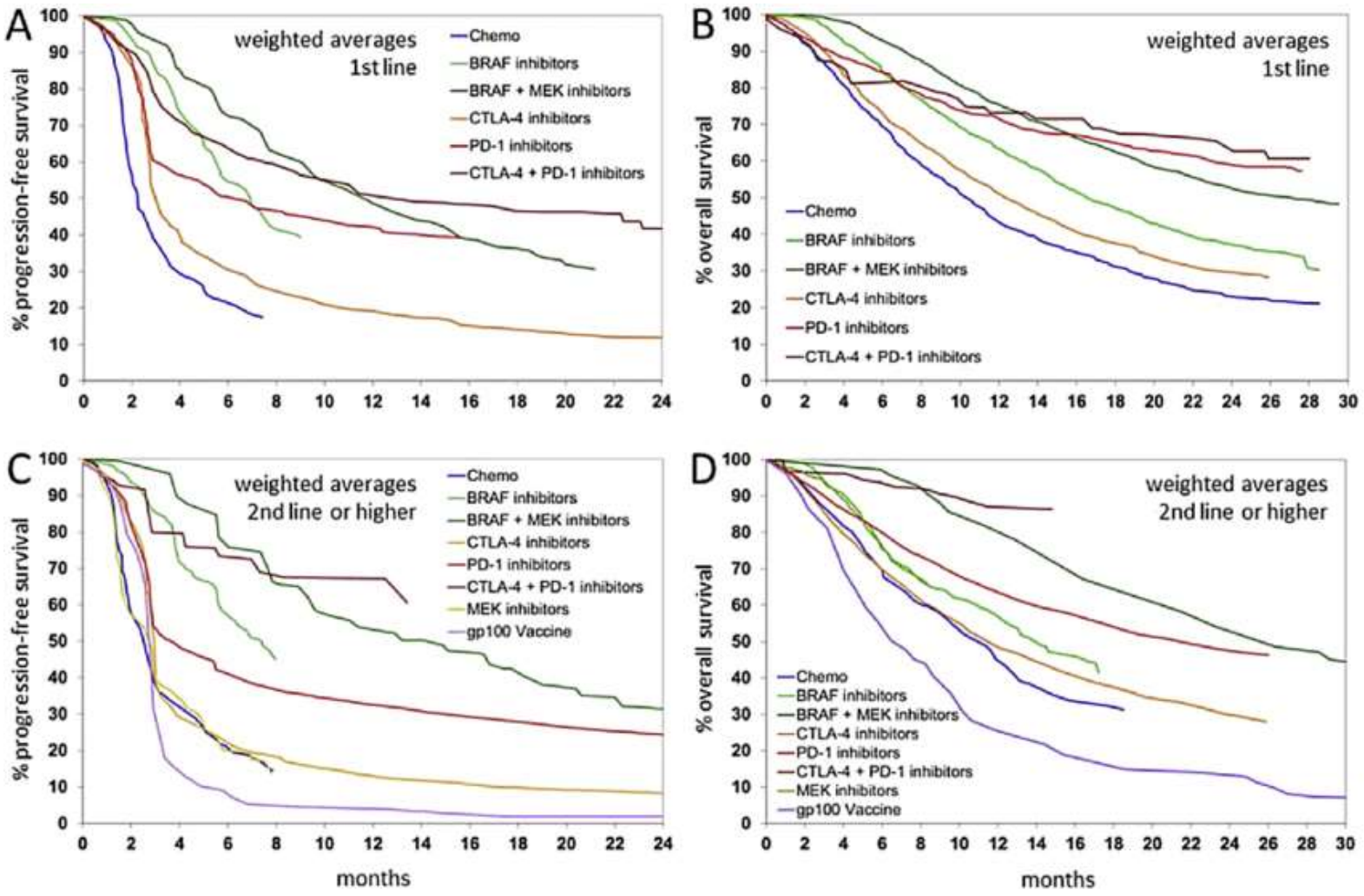

Long Term Survival

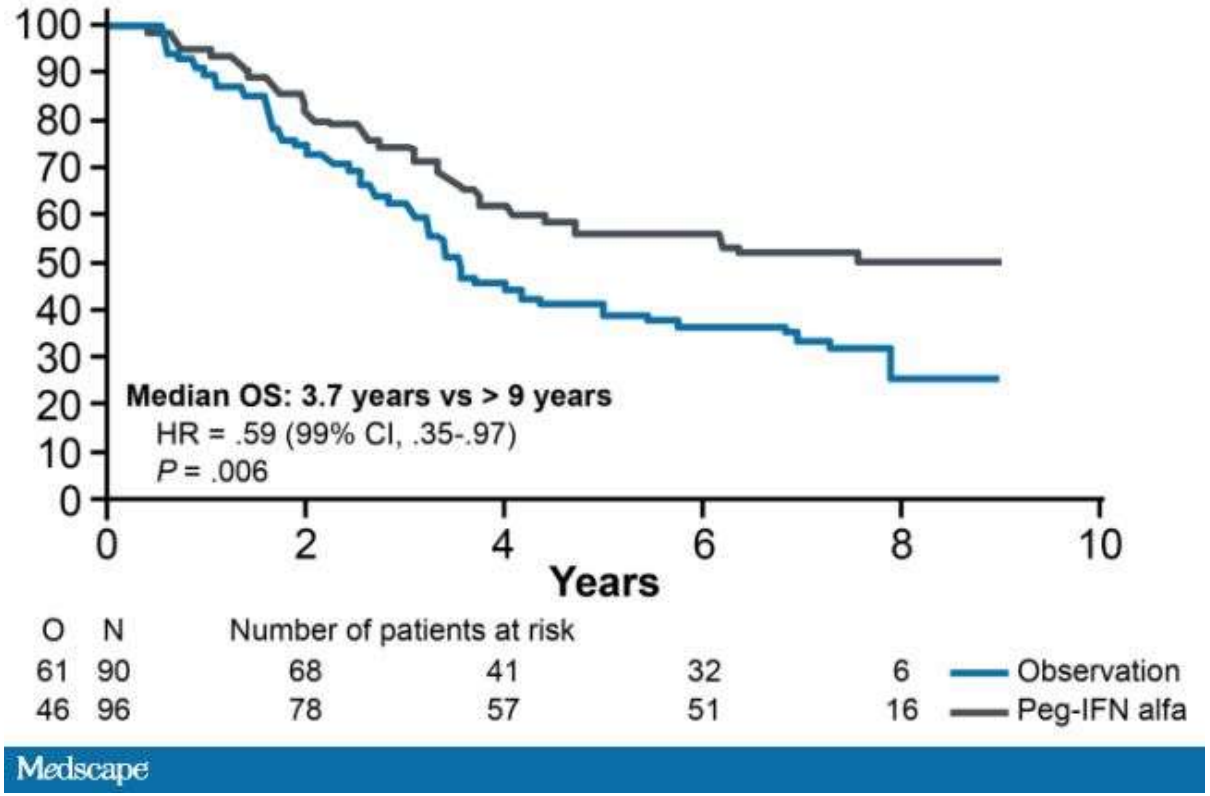

Circulating Tumor Cells

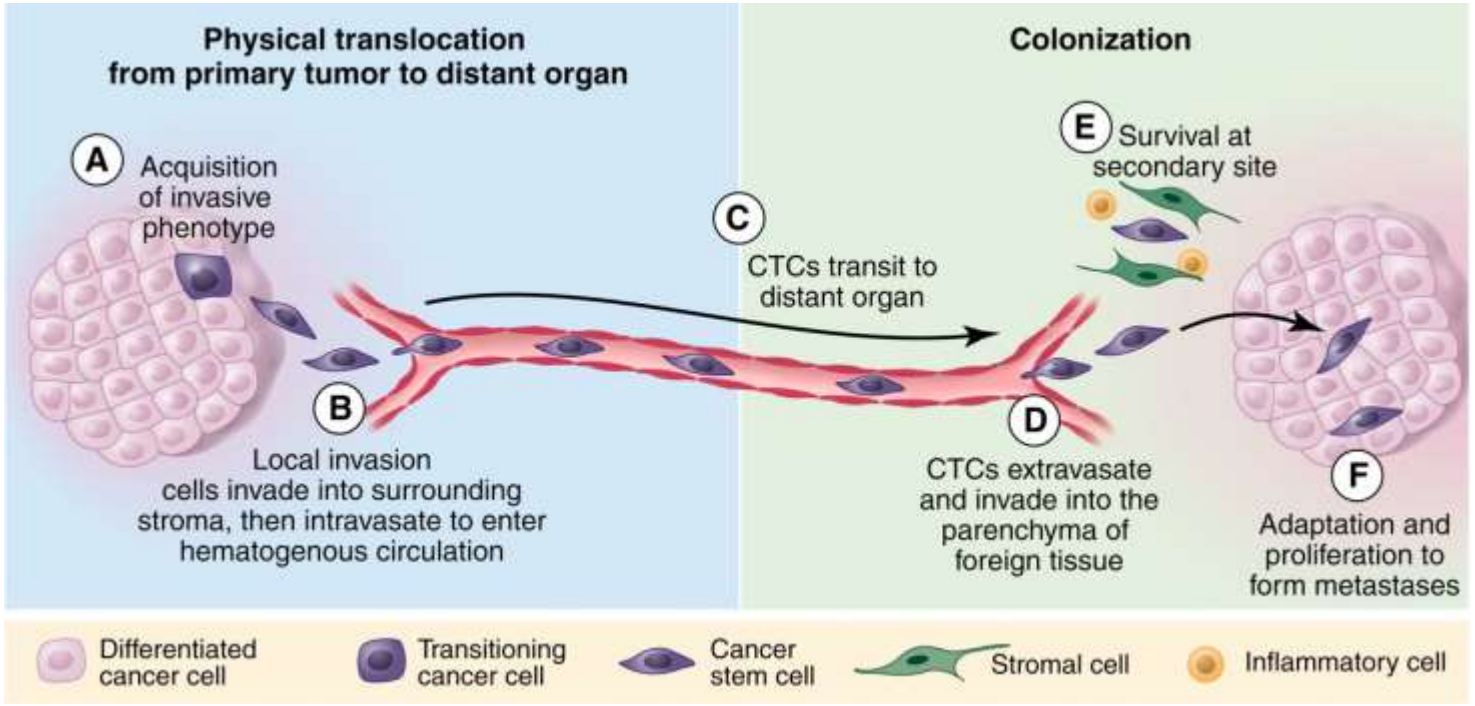

Liquid Biopsy

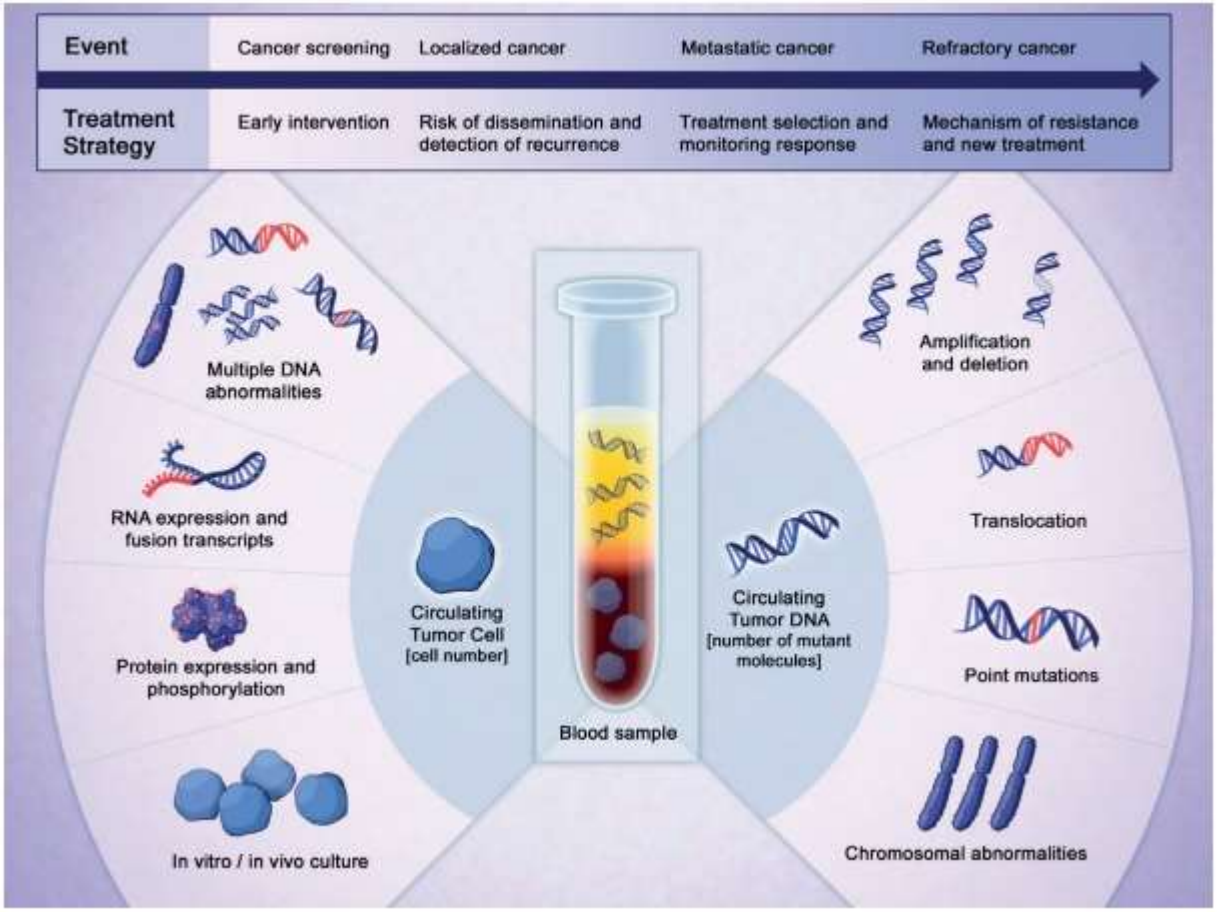

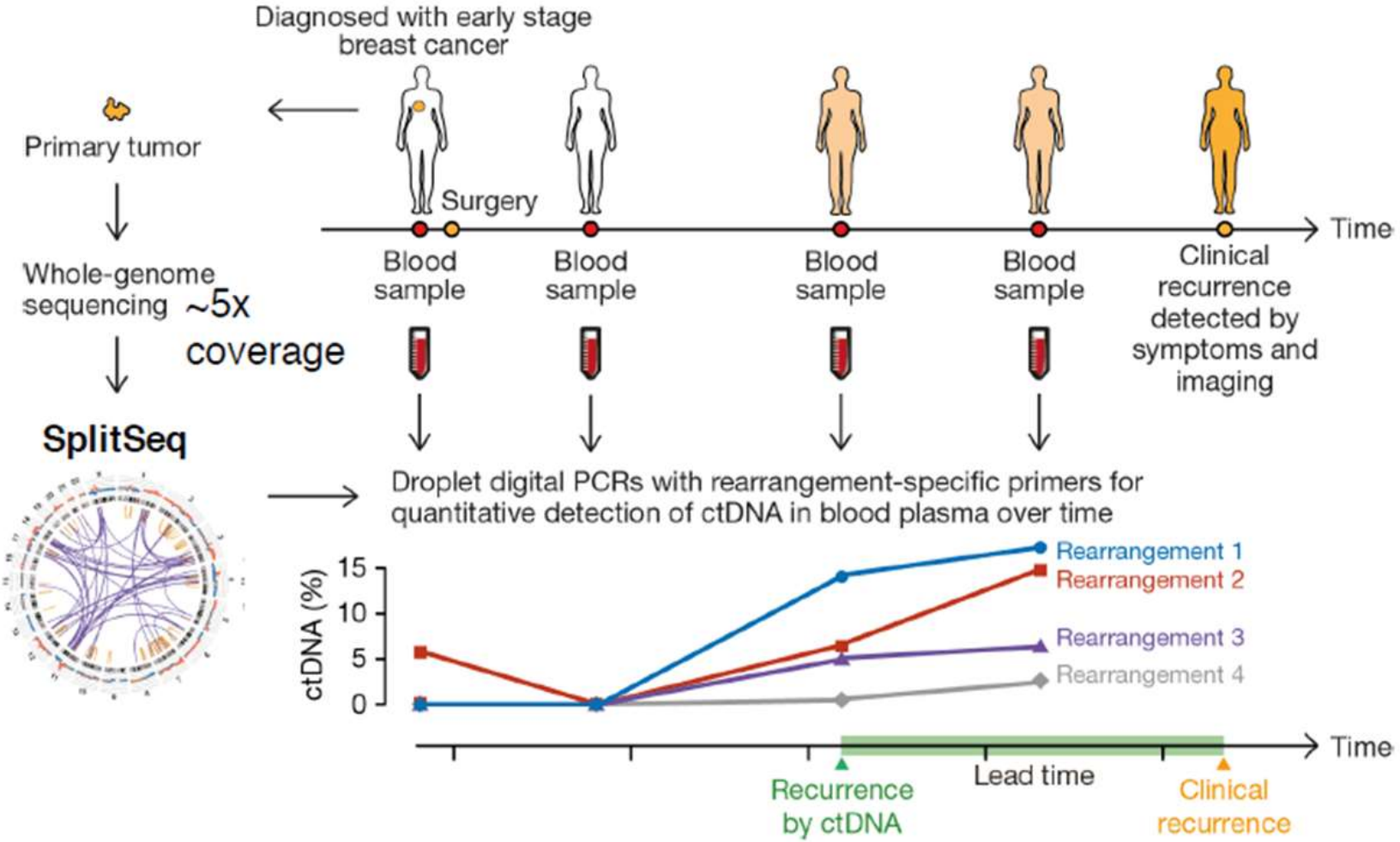
Diagnosed with early stage breast cancer
Primary tumor
Surgery
Time
Whole-genome sequencing
~5x coverage
Blood sample
Blood sample
Blood sample
Blood sample
Clinical recurrence detected by symptoms and imaging
SplitSeq
Droplet digital PCRs with rearrangement-specific primers for quantitative detection of ctDNA in blood plasma over time
ctDNA (%)
15
10
5
0
Rearrangement 1
Rearrangement 2
Rearrangement 3
Rearrangement 4
Time
Lead time
Recurrence by ctDNA
Clinical recurrence

Digital PCR

Droplet digital PCR

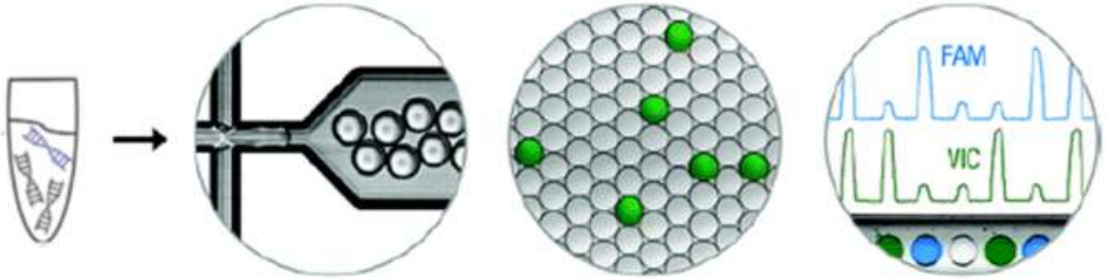

Bio-Rad QX100

1. MAKE	2. CYCLE	3. READ	
Sample is partitioned into 20,000 droplets	Run PCR cycles in all droplets simultaneously	Measure fluorescence intensity in each droplet	Calculate concentration from number of positive droplets

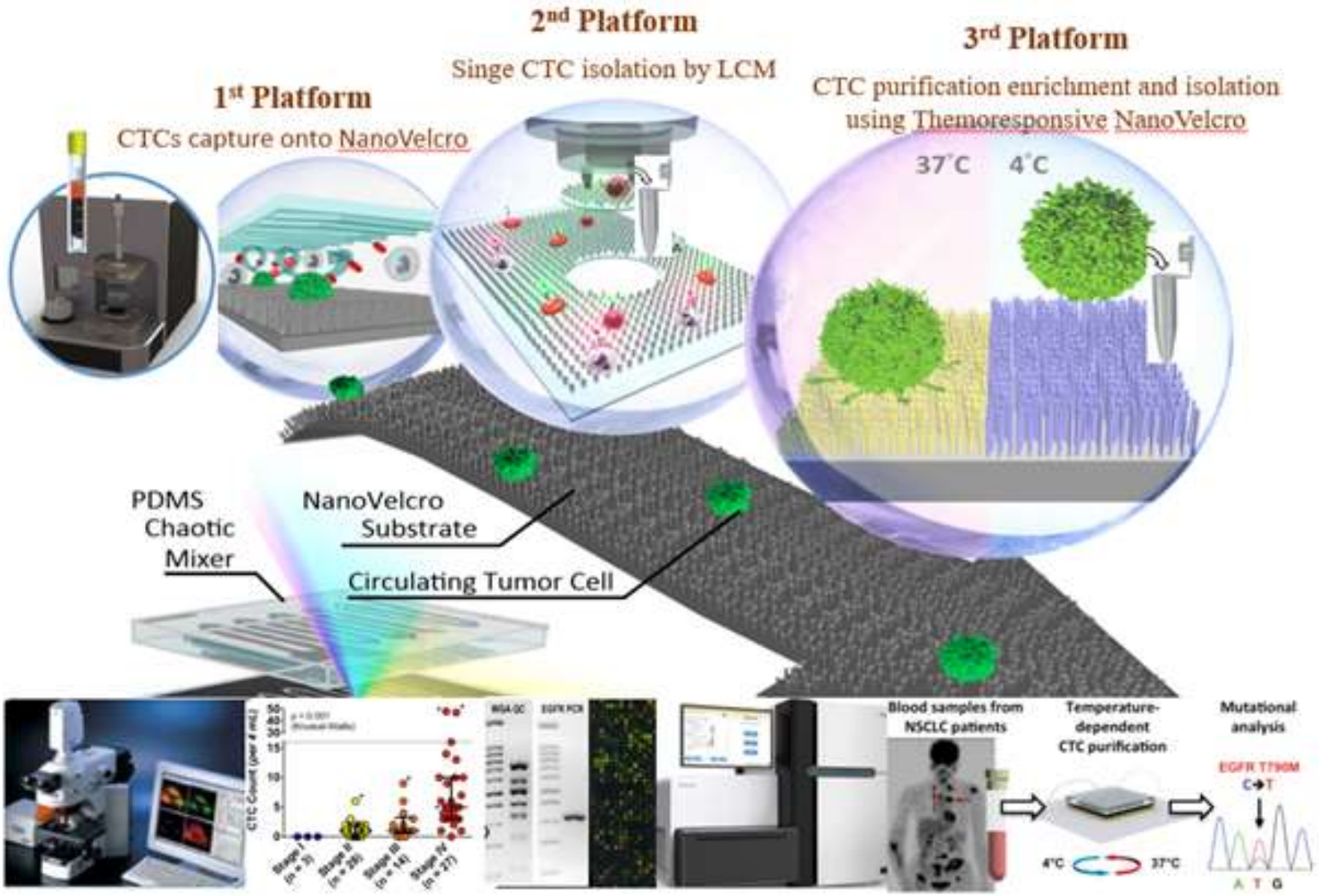
1st Platform
CTCs capture onto NanoVelcro
2nd Platform
Singe CTC isolation by LCM
3rd Platform
CTC purification enrichment and isolation using Themoresponsive NanoVelcro
37°C
4°C
PDMS Chaotic Mixer
NanoVelcro Substrate
Circulating Tumor Cell
Blood samples from NSCLC patients
Temperature-dependent CTC purification
Mutational analysis
EGFR T790M
C→T
4°C
37°C
A T G